ENGINEERING EXPERIMENT STATION
STRUCTURAL RESEARCH SERIES NO. S-12

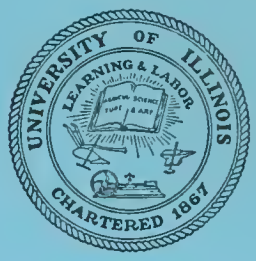

STUDIES OF SLAB AND BEAM HIGHWAY BRIDGES: PART V

TESTS OF CONTINUOUS RIGHT I-BEAM BRIDGES

By
C. P. SIESS and I. M. VIEST

Manuscript for a Proposed Bulletin
of the Engineering Experiment Station
University of Illinois

UNIVERSITY OF ILLINOIS
URBANA, ILLINOIS

STUDIES OF
SLAB AND BEAM HIGHWAY BRIDGES

PART V

TESTS OF CONTINUOUS RIGHT I-BEAM BRIDGES

A REPORT OF AN INVESTIGATION

conducted by

THE ENGINEERING EXPERIMENT STATION
UNIVERSITY OF ILLINOIS

in cooperation with

THE DIVISION OF HIGHWAYS
STATE OF ILLINOIS

and

THE BUREAU OF PUBLIC ROADS
U.S. DEPARTMENT OF COMMERCE

By

CHESTER P. SIESS

and

IVAN M. VIEST

Submitted as a Manuscript for a Proposed Bulletin
of the Engineering Experiment Station
University of Illinois

CONTENTS

APPENDIX: THEORETICAL ANALYSIS OF TWO 2-SPAN CONTINUOUS I-BEAM BRIDGES

FIGURES

FIGURES (Continued)

TABLES

I. INTRODUCTION

1. Object of Tests

Laboratory tests were made on three $\frac{1}{4}$-scale models of continuous I-beam bridges. All three structures were two-span right bridges consisting of five steel beams supporting a reinforced concrete slab. The principal variable studied was the presence or absence of interaction between the beams and the slab, obtained by using or not using shear connectors. All tests were made with pairs of concentrated loads simulating the rear axle loads of one or more trucks.

The primary purposes of the tests were: (1) To compare the action of both beams and slab in positive moment region with that previously determined from tests and analyses of simple-span I-beam bridges; (2) to determine the action of the beams and slab in the negative moment region, and to compare the magnitudes and distribution of the strains in the beams and the slab in this region with those observed in the region of positive moment; (3) to determine the effects of composite action on the behavior of a continuous I-beam bridge, and to compare the action of composite bridges with and without shear connectors in the region of negative moment over the center pier.

These tests of continuous bridges are part of a continuing study of slab and beam highway bridges. This study has included: analyses and tests of simple-span right I-beam bridges, both composite and

non-composite;* x tests of simple-span skew I-beam bridges, both composite and non-composite;** and studies of the behavior of composite beams and shear connectors.xx ***

2. Outline of Test Program

The tests may be divided into two groups:

(1) The first group included the tests of one non-composite bridge, N30. These tests were performed in 1945-46.

(2) The second group included the tests of two composite bridges, C30 and X30. In bridge C30, channel shear connectors were welded to the top flanges of the I-beams at regular intervals throughout the full length of the bridge. In bridge X30, channel shear connectors

* N. M. Newmark and C. P. Siess, "Moments in I-beam Bridges," Univ. of Ill. Eng. Exp. Sta. Bul. 336, 1942.

x N. M. Newmark, C. P. Siess and R. R. Penman, "Studies of Slab and Beam Highway Bridges, Part I: Tests of Simple-Span Right I-beam Bridges," Univ. of Ill. Eng. Exp. Sta. Bul. 363, 1946.

** N. M. Newmark, C. P. Siess and W. M. Peckham, "Studies of Slab and Beam Highway Bridges, Part II: Tests of Simple-Span Skew I-beam Bridges," Univ. of Ill. Eng. Exp. Sta. Bul. 375, 1948.

xx C. P. Siess, I. M. Viest and N. M. Newmark, "Studies of Slab and Beam Highway Bridges, Part III: Small-Scale Tests of Shear Connectors and Composite T-beams," Univ. of Ill. Eng. Exp. Sta. Bul. 396, 1952.

*** I. M. Viest, C. P. Siess, J. H. Appleton and N. M. Newmark, "Studies of Slab and Beam Highway Bridges, Part IV: Full-Scale Tests of Channel Shear Connectors and Composite T-beams," Univ. of Ill. Eng. Exp. Sta. Bul. , 195 .

were omitted in the negative moment region in the vicinity of the center pier. The tests of bridges C30 and X30 were made in 1946-47 and 1947-48, respectively.

The first step in the tests of all three bridges was to produce thorough cracking of the slab. Three principal types of tests were then made:

(1) Influence line tests were made with a pair of concentrated loads. The purpose of these tests was to determine the location of loads required to produce maximum positive and negative moments in the beams.

(2) Slab and beam strain tests were made with one or more pairs of concentrated loads for the purpose of determining the distribution and magnitude of strains in the slab and the beams.

(3) Tests to failure were made with one or more pairs of concentrated loads. The objectives of these tests were the determination of the loads at first yielding of various components of the bridge, the loads at final failure, and the manner of failure.

3. Acknowledgments

The tests reported in this bulletin were made as a part of an investigation of slab and beam highway bridges conducted at Talbot Laboratory by the Engineering Experiment Station of the University of Illinois in cooperation with the Illinois Division of Highways and the Bureau of Public Roads of the U. S. Department of Commerce.

The program of the investigation during the period covered by the tests reported herein was guided by an Advisory Committee having the following personnel.

Representing the Illinois Division of Highways:

G. F. Burch, then Bridge Engineer

W. J. Mackay, then Engineer of Railroad Crossings

L. E. Philbrook, then Assistant Bridge Engineer

Representing the Bureau of Public Roads:

R. Archibald, Chairman, Bridge Committee, American Association of State Highway Officials

E. L. Erickson, Chief, Bridge Branch

E. F. Kelley, Chief, Physical Research Branch

Representing the University of Illinois:

N. M. Newmark, Research Professor of Structural Engineering

F. E. Richart,* Research Professor of Engineering Materials

C. P. Siess, Research Assoc. Professor of Civil Engineering

General direction of the investigation was provided by F. E. Richart and N. M. Newmark. The investigations reported in this bulletin were carried out under the supervision of C. P. Siess. The tests were conducted by C. B. Clarke, then Special Research Associate in Theoretical and Applied Mechanics, L. W. Jones, and E. J. Ward, then Special Research Graduate Assistants.

The results of the tests were correlated and interpreted, and this bulletin prepared by I. M. Viest.

The steel I-beams were annealed by the Chicago Bridge and Iron Company.

* Deceased.

II. FUNDAMENTAL CONSIDERATIONS

4. Scale relations

All specimens were 1/4-scale models. In order to obtain stresses in the model which correspond to those in the full-size structure, or prototype, the loads on the two structures must be related as follows:

(a) Concentrated loads should be 1/16 as large for the model as for the prototype.

(b) Loads distributed over a length, such as weight of a beam per foot of length, should be 1/4 as large for the model as for the prototype.

(c) Loads distributed over an area, such as the weight of the slab per square foot of area, should have the same magnitude per unit of area for the model as for the prototype.

For loads related as above, deflections will be 1/4 as large in the model as in the prototype.

5. Definition of Terms

The following terms are used frequently throughout this bulletin and are, therefore, defined and explained here.

The transverse reinforcement of the slab is in the direction perpendicular to the beams.

The longitudinal reinforcement of the slab is in the direction parallel to the beams.

The equivalent simple span is the distance from the end of the bridge to the nearest point of contraflexure. The length of the equivalent simple span is denoted by a. The equivalent simple-span bridge is a

simple-span bridge having a span length equal to the equivalent simple span and a cross section identical to that of the continuous bridge.

The relative stiffness of the beam and slab is denoted by H and is defined by the equation $H = \frac{E_b I_b}{aEI}$ where $E_b I_b$ and EI are the products of the modulus of elasticity and the moment of inertia of a beam and of a unit width of the slab respectively.

The term midspan refers to a section of the bridge at which maximum positive moments are produced in the beams by moving loads. The location of the midspan section is at W5 and E5 in Figures 4 and 19.

A shear connector is a device for the transfer of horizontal shear from the slab to the beam. In these tests, the shear connectors consisted of short lengths of bar channel with the web transverse to the web of the beam, and with one flange welded to the top of the beam and the other imbedded in the slab.

Composite action is the interaction between the beam and slab which results from the transfer of shear between these two elements. Complete composite action or full interaction exists when the amount of shear transferred is equal to the shear computed for the beam and slab considered as a homogeneous member.

6. Theoretical Analysis

Theoretical moments and deflections of a two-span continuous right I-beam bridge may be computed by the method of analysis described in Bulletin 304,* in the manner outlined in the Appendix. Slab and beam

* N. M. Newmark, "A Distribution Procedure for the Analysis of Slabs Continuous Over Flexible Beams," Univ. of Ill. Eng. Exp. Sta. Bul. 304, 1938.

moments were computed for two continuous two-span bridges having b/a = 0.2 and relative stiffnesses H = 2 and 4, respectively. The results are given in the Appendix. The moments were compared with the results of the studies of simple-span bridges and it was concluded that for the two particular continuous bridges studied approximately the same proportion of a wheel load was carried by the beams of the continuous bridge as would be carried by the beams of an equivalent simple-span bridge.

The results of the theoretical studies were used in planning these tests. However, as the dimensions of the test models were such that they did not permit the use of the moment and deflection coefficients tabulated in Bulletin 336, it was felt that the time-consuming calculations required for an analysis of these bridges were not warranted. An approximate method of computing the moments and deflections was chosen instead. Total moments and average deflections in the beams at any section of the bridge were computed by the conventional elastic analysis for a two-span continuous beam. For non-composite bridge N30 the beam was considered to be of uniform stiffness throughout its length. For composite bridges C30 and X30 the stiffness in the positive moment regions was taken as that for a composite section consisting of the steel beams and the concrete slab; the stiffness in the negative moment region was taken as that for a composite section consisting of the steel beams and the longitudinal reinforcement in the slab. The distribution of the moments and deflections to the individual beams of the continuous bridges was assumed to be equal to the distribution of maximum moments and deflections of the equivalent simple-span bridge. The coefficients tabulated in Appendix A of Bulletin

336* were used for this purpose.

Transverse moments in the slab were also computed from the tables in Appendix A of Bulletin 336. Moments at midspan were taken as those for the equivalent simple-span bridge and moments over the center pier were taken as those for a continuous slab resting on nondeflecting supports ($H = \infty$).

In all calculations of strains and values of H, the modulus of elasticity of steel was taken equal to 30,000,000 psi, and the modulus of elasticity of concrete was taken as 3,150,000 psi for bridge N30 and 3,000,000 psi for bridges C30 and X30.

* N. M. Newmark and C. P. Siess, "Moments in I-beam Bridges," Univ. of Ill. Eng. Exp. Sta. Bul. 336, 1942.

III. DESCRIPTION OF TEST SPECIMENS AND APPARATUS

7. Description of Bridges

The test specimens were 1/4-scale models of full-size I-beam bridges from which certain details were omitted in order to facilitate the interpretation of the test results. The usual sidewalks, curbs, and handrails were omitted, and the roadway was built without a crown, or wearing surface. The beams were equally spaced and the outside beams were placed at the edge of the slab.

The test bridges were two-span continuous structures with two spans of 15 ft, each consisting of five steel I-beams spaced at 1.5-ft intervals and supporting a reinforced mortar slab 1 3/4 in. thick. These dimensions were dictated by several requirements, the most important of which was the necessity for making the bridges as similar as possible to the simple-span bridges previously tested, so that the results for the two types of structures could be easily compared. The two-span layout was recognized as not being typical of current practice. Its choice, however, was dictated by space requirements since the maximum total length of bridge which could be constructed in Talbot Laboratory at the time of these tests was about 40 ft. It was considered undesirable to reduce the scale of the model. It was also recognized that to get a continuous bridge strictly comparable to the simple-span bridges N15 and C15 (Bulletin 363), the span length of the continuous bridges should have been such as to have an equivalent simple span 15 ft long. However, this would have required a structure over 40 ft long and thus could not be used on account of the space limitations.

The sizes of beams were determined by the design of prototype structures as continuous bridges with two spans of 60 ft, each consisting of five steel I-beams spaced at 6 ft and supporting a reinforced concrete slab 7 in. thick. Bridges N30 and C30 were designed for H-20 lane loading* using a procedure proposed by N. M. Newmark and C. P. Siess.[x] An allowable stress of 18,000 psi was used for the steel beams. The beam sections chosen were 33 WF 125 for the non-composite bridge N30 and 27 WF 91 for the composite bridge C30. Bridge X30 did not require any additional designing; except for the omission of shear connectors over the support, it was identical with bridge C30. The dimensions of the bridges and the sizes of the beams were scaled down from those for the prototypes. The dimensions of the model bridges are given in Table 1 and the various sections of the bridges are shown in Fig. 1.

Preliminary designs of the slab indicated that the amount of reinforcement required for the continuous model bridges would not differ appreciably from that used in the simple-span bridges N15 and C15. This amount of reinforcement was therefore selected to correspond to that for the simple-span bridges. All reinforcement was made of 1/8-in. square bars; its amount is tabulated in Table 1. The spacing of the transverse reinforcement throughout the entire length of the bridge was the same as in the corresponding simple-span bridges. The spacing of the bottom longitudinal reinforcement throughout the entire length of the bridge and of

* "Standard Specifications for Highway Bridges," The American Association of State Highway Officials, Washington, D.C., 1944, p. 131, Article 3.2.8 (c).

[x] N. M. Newmark and C. P. Siess, "Design of Slab and Stringer Highway Bridges," Public Roads, Jan.- March 1943, Vol. 23, No. 7, pp. 157- 164.

the top longitudinal reinforcement in the positive moment region was equal to the spacing of the corresponding reinforcement in bridge C15. The spacing of the top longitudinal reinforcement in the region of the negative moment was half of the spacing of the corresponding reinforcement in the remaining parts of the bridge. This was achieved by inserting additional longitudinal bars extending a few inches beyond the points of contraflexure. The additional bars were 5 ft long in bridges N30 and C30, and 6 ft 8 in. long in bridge X30; they were staggered 6 in. to prevent formation of a plane of weakness. The four corners of the slab were reinforced with additional diagonal bars in order to prevent excessive cracking at these locations.

Diaphragms between the beams were located over each support. The end diaphragms consisted of beams having the same cross section as the main beams. The diaphragm over the center pier consisted of a 4-in. standard channel welded to the beam webs at a level near the bottom flange; this diaphragm did not bear against the underside of the slab. No intermediate diaphragms were used.

In composite bridges C30 and X30 the shear connection consisted of 1 x 3/8 x 1/8-in. channels with one flange welded to the beam and the other imbedded in the slab. The layout of shear connectors is shown in Fig. 1. The spacing of the connectors was uniform at 6 1/4 in. In bridge C30, shear connectors were provided throughout the entire length of the beams. In bridge X30, no shear connectors were provided for a distance of 28 in. on each side of the center pier.

8. Materials

The physical properties of the steel in the beams were obtained

from tension tests of coupons cut from the flanges. The results of the tests are given in Table 2. The yield point of the beams themselves depends not only on the yield point of the coupons but also on the magnitude of residual stresses relieved during the cutting of the coupons. The magnitude of the residual stresses and of the apparent yield point of beams is discussed in Section 9.

The slab reinforcement consisted of 1/8-in. square cold-rolled bars of SAE 1112 steel. These bars were normalized to lower their strength and rusted to improve their bond, in the manner described in Section 8 of Bulletin 363. The physical properties of the bars obtained from tension tests are summarized in Table 3.

The slabs were made from a sand-cement mortar consisting of a standard brand of Type I Portland cement and an artificially graded mixture of Wabash River Valley torpedo sand and fine Lake Michigan beach sand. The gradation of the sand mixture was identical with that described in Section 8 of Bulletin 363. The proportions of cement to sand were 1:5.7 by weight for bridge N30 and 1:4.9 for bridges C30 and X30. The water-cement ratio by weight was 0.77 for bridge N30 and 0.69 for bridges C30 and X30.

The mortar for bridges N30 and C30 was mixed in a tilting drum mixer of 3.5-cu ft capacity and for bridge X30 in a non-tilting drum mixer of 6.5-cu ft capacity. From 50 to 66 control cylinders 2 x 4 in., several from each batch, and from 10 to 16 control beams 2 x 1 3/4 x 17 in. were made for each bridge. The control specimens were cured under wet burlap for 28 days and then painted with a white enamel paint and stored in the laboratory until the time of test. The cylinders were tested at the beginning, in the middle, and at the conclusion of the tests.

The results of the tests of control cylinders and beams are given in Table 4. The modulus of elasticity was determined from stress-strain curves obtained with an averaging compressometer having a 2-in. gage length. The modulus of rupture was obtained from tests with third-point loading on a span of 15 in.

9. Residual Stresses

Measurements on the steel I-beams showed the presence of residual stresses. These stresses were caused by unequal cooling of the I-beams after rolling and by welding of shear connectors. The measurements of the residual stresses due to rolling and due to welding of shear connectors are described in the following paragraphs and their magnitudes are given in Table 5. A check on these measurements was provided by the observed strains at first yielding of the bridges; the yield point strains of coupons, corrected for the residual strains, are compared with the strains at first yielding of the beams in Table 6.

The residual strains in the I-beams of the non-composite bridge N30 could result only from the rolling. Their magnitude was determined on a section 5 ft 10 in. long cut from the same stock of beams as those for the bridge. Strain gage lines for a 2-in. Berry gage were placed at the center of this section. After an initial set of readings was taken, a 12-in. section containing the gage lines was cut out; the flanges were then cut from the beam and the strain readings were again taken. The differences between the original and final readings represent the residual strains. The average residual stress for the top and bottom flanges was a tension of 19,000 psi (Table 5). It may be seen from Table 6 that there

was good agreement between the coupon strains corrected for the residual strains and the strains at first yielding measured on bridge N30.

Because of the large residual stresses in the beams of bridge N30, it was decided that the 7-in. beams for bridges C30 and X30 should be stress-relieved before using. This was done by heating the beams to a temperature of approximately 1100 deg F and holding them at that temperature for about four hours. The residual stresses remaining in the beams after this heat treatment were determined in the manner described for bridge N30. The average residual tension in the flanges was 2500 psi.

Additional residual stresses were produced in the beams of C30 and X30 as a result of welding the shear connectors to the top flanges. Tensile stresses were produced in both flanges and in the lower part of the web, while balancing compressive stresses were produced in the upper part of the web. Welding of the shear connectors caused the beams to deflect downward with a maximum deflection of 3/4 in. for the beams of bridge C30 and 1 1/2 in. for the beams of bridge X30. An approximate calculation of the magnitude of residual stresses was made on the assumption that the welding of shear connectors produced a uniform curvature along the full lengths covered by the shear connectors, and that the residual stresses were distributed uniformly throughout the entire depth and width of the top flange.

In order to determine the accuracy of this method of computing the residual stresses, the following experiment was carried out: Shear connectors were welded to one flange of a 16-ft length of a 7-in. Junior Beam taken from the same lot as the beams used in bridges C30 and X30. The size and spacing of the shear connectors were the same as those used

in the model bridges. The residual stresses were computed from the measured deflection. The actual residual stresses were then determined by cutting off the flanges and measuring the strains. The stresses thus obtained were corrected for the residual stresses due to rolling equal to a tension of 2500 psi. The ratio of the corrected measured stresses to the computed residual stresses was 0.71 for the top flange and 0.81 for the bottom flange. Ratios 0.71 and 0.81 were then used as correction factors for the residual stresses computed from the deflections of the beams used in the bridges. For bridge C30, the residual stresses were assumed to be the same at all points along the beam, since shear connectors were welded throughout the length. However, for bridge X30 it was assumed that no residual stresses due to welding the shear connectors would occur over the center pier inasmuch as no shear connectors were attached in that region. The magnitudies of the corrected computed residual stresses are given in Table 5. The apparent yield point stresses, equal to the coupon yield point stresses corrected for the residuals, are also given in that table.

The check on the accuracy of the residual strain measurements is provided by the yield point strains found in the bridge tests (Table 6). Unfortunately, for composite bridges this check is obscured by the presence of shrinkage strains. The shrinkage of the slab tends to produce a downward deflection at midspan and therefore induces tension stresses in the bottom flange. Thus the yield point strains found in bridge tests should be smaller than the corrected coupon strains. The test data indicate a difference in the expected direction. On the other hand, the results of the bridge tests indicate large initial compressive strains in the top flange, over the center pier as shown in Table 6, but it seems unlikely

that shrinkage alone could have caused strains of this magnitude. It is possible, however, that some portion of the compressive strains in the top flanges could have resulted from the deflections of the beams over the center pier relative to the end piers, occurring when the beams were first seated in place.

10. Construction of Test Specimens

The five I-beams for each bridge together with the end and intermediate diaphragms were assembled into a single frame by welding. The top of the end diaphragms were level with the top of the I-beams. For the composite bridges, the shear connectors were welded next. Each connector was arc-welded to the upper flange of the beam in the direction at right angles to the axis of the beam, with continuous fillet welds along both edges of the flange of the channel.

The beams were fitted with bearing blocks having a radius of 3 in. and uniform bearing between the beams and the bearing blocks was obtained by means of a bedding of litharge and glycerine cement. The bridge was supported on three concrete piers about 6 ft high; on top of each was placed a length of 1 1/4 x 4-in. cold-rolled steel bar bedded in cement mortar to serve as a bearing plate. These bearing plates were very carefully leveled so that their top surfaces lay in the same plane.

Forms for the slab, consisting of plywood bottom forms and steel side forms, were constructed next. The assembly of beams and forms for bridge X30 is shown in Fig. 2.

All of the reinforcement for the slab of each bridge was assembled into a single mat. One such reinforcing mat is shown on Fig. 2 to

the right of the bridge piers. The reinforcing mats were fabricated as described in Section 9 of Bulletin 363.

The top flanges of the beams for bridge N30 were covered with a liberal coating of wax to prevent bond between the slab and the beams. For bridges C30 and X30 the top surfaces of the beams were left in the as-rolled condition. After the forms were oiled, the reinforcing mat was put in place.

The mortar was placed with the aid of a vibratory screed in one continuous operation. As soon as the consistency of the mortar permitted, the top surface of the slab was struck off and trowelled smooth. The slab was cured under wet burlap for 28 days. It was then painted with two coats of white enamel to prevent excessive shrinkage.

To prevent lifting of the bridges off the end piers, bridges C30 and X30 were tied to the piers by means of four round bars welded to each end diaphragm and fastened to the end piers. The lifting of the ends of bridge N30 was prevented by dead weights placed on the bridge over the end diaphragms.

A view of bridge C30 under test is shown in Fig. 3.

11. Loading Apparatus and Instruments

Load was applied by means of a screw jack bearing against a steel frame which was anchored to the floor of the laboratory. The load was measured with elastic-ring dynamometers of 50,000 or 125,000-lb capacity. From the dynamometer the load was transmitted to the slab through a distributing beam and two loading disks. Loading disks were 3 3/4 in. in diameter and were bedded on a sheet of sponge rubber to insure uniform distribution of the load.

Strains on the beams and on the mortar slab were measured with 1-in. gage length type A-11 SR-4 strain gages. Strains on the reinforcement were measured with 1-in. gage length type A-12 SR-4 strain gages, except for the longitudinal bottom reinforcement where 2-in. gage length Huggenburger extensometers were used on bridge N30 and 1/4-in. gage length type A7 SR-4 strain gages were used on bridges C30 and X30. All gages were attached after the curing of the slab had been completed. Access to the reinforcing bars was provided through holes formed by wooden blocks fastened to the bars and removed after the mortar had hardened. A detailed description of the method used for attaching the gages has been published elsewhere.* A total of 325 SR-4 gages were used on bridge N30 and 335 gages were used on each of the other two bridges. Strains were read with a Baldwin-Forboro Portable Strain Indicator, Type K. The reading was facilitated by use of a 100-point switching unit. The instruments may be seen in Fig. 3 to the right of the bridge.

Deflections of the steel beams were measured with deflectometers bearing against the floor of the laboratory and equipped with 0.001-in. dial indicators.

* E. Hognestad and I. M. Viest, "Some Applications of Electric SR-4 Gages in Reinforced Concrete Research," Journal of the American Concrete Institute, Feb. 1950, Vol. 21, No. 6, Proceedings Vol. 46, pp. 445-454.

IV. TESTS OF NON-COMPOSITE BRIDGE N30

12. Description of Tests

All tests were made with one, two, or four pairs of loads applied at midpanels or over the beams in increments of 250-1000 lb per loading disk. The two loads of each pair were 18 in. apart. Loads were applied at the sections denoted in Fig. 4 as 0, E1 through E6, and W1 through W6. Except in the tests to failure, care was taken that strains in the beams and in the reinforcement would not exceed the yield point. The slab was 119 days old at the beginning of tests and 210 days old at the conclusion of tests.

The locations of the strain gages are shown in Fig. 4. In the spans, gages were located on the inside surfaces of the top and bottom flanges of the I-beams, on the top and bottom transverse reinforcing bars, on the bottom longitudinal bars, and on the top surface of the slab.* Over the center pier, gages were located on the inside surfaces of the top flanges of the I-beams, on the top and bottom transverse reinforcement, on the top longitudinal reinforcement and on the top surface of the slab.x

Strains were measured only on gages located at sections pertinent to the aim of the particular test. In the majority of the tests, strains were measured under and in the vicinity of the loads; in some tests strains were recorded on all gages at the loaded section, in others on all gages

* Four type A-11 SR-4 strain gages were attached to the top slab surface at each of the following locations: over beams B and D at Section E3 and over beam C at Section W5.

x Two type A-11 SR-4 strain gages were attached to the top slab surface over beam C at Section 0.

over the center pier. Gages located on the surface of the slab were read in the cracking tests only. Deflections of beams were measured at Sections E3 and W5. Both strains and deflections were measured at each increment of load.

A valuable check on the reliability of the test data was provided by symmetrical locations of gages and loads.

Tests were made in the following order: cracking tests, influence line tests, slab strain tests, maximum beam strain tests, tests to failure of beams by yielding, the tests to failure of the slab by punching, and the test for maximum capacity of the bridge.

Cracking Tests. The slab was first cracked systematically with a pair of loads applied at each of the 44 positions shown in Fig. 5. Loads were applied in increments 250-500 lb. The maximum load per panel was 3500 lb in the spans and 4000 lb ove the center pier. When load was applied at position 1, 2 and 3 (Fig. 5), strains were measured in the bottom transverse reinforcement in the two loaded panels, and in the top transverse reinforcement and on the top surface of the slab over the beam between the two loaded panels. When load was applied at positions 14, 15, 30, 31 and 32, strains were measured in the bottom transverse and longitudinal reinforcement in the two loaded panels, and in the top transverse reinforcement and on the top slab surface over the beam between the two loaded panels. No measurements were taken when load was applied at the remaining 36 positions.

Influence Line Tests. These tests were made with two pairs of loads. First, loads placed at B, C, CD and DE were applied at Sections W2 through W5 and beam strains were measured at Sections W1 through W6,

O, E1 and E3 for each position of the loads. Strains in the transverse reinforcement were read at Section W5, over beam D and in panels CD and DE. Strains in the longitudinal reinforcement were read at Section O over all five beams and in all four panels. Next, loads placed at AB, BC, C and D were applied at Sections E2 through E5 and beam strains were measured at Sections E1 through E6, O, W1 and W3. Strains in the transverse reinforcement were read at Section E3, over beam B and in panels AB and BC. Strains in the longitudinal reinforcement were read at Section O over all five beams and in all four panels. Loads were applied in four increments of 500 lb.

Slab Strain Tests. One pair of loads was applied successively at AB-BC, BC-CD, and CD-DE. The loads were applied first at Section W5, then at Section E3 and finally at Section O. For each loading, strains were measured in the transverse bottom reinforcement under the load and in the transverse top reinforcement over the beam between the loads. In addition, in tests with loads at Section W5 and E3, strains were measured in the bottom longitudinal reinforcement under the load and on all beam gages at Sections W5 or E3, W1, E1 and O. The loads were applied in increments of 250-500 lb; the maximum load was 4000 lb.

To determine the maximum strains in the longitudinal reinforcement, two pairs of loads were applied first at Section W5, and next at Section E3. Loads were applied at AB, BC, CD and DE. Longitudinal strains were measured under the loads, and transverse strains were measured under the loads and over the beams between the loads. Beam strains were measured on all gages at Sections W5, W1, E1 and O. In addition, deflections were read at the loaded section. The maximum load was reached in 250- and 500-lb increments.

Maximum Beam Strain Tests. Maximum beam strains in the span were determined from the results of the influence line tests. For maximum beam strains over the center pier, four pairs of loads were applied at Sections W3 and E3, two pairs at each section. Loads were placed at B, C, CD and DE. Strains were read on all beam gages at Sections W3, W1, O, E1 and E3. Strains in the top longitudinal reinforcement were read over the center pier. Load was applied in seven 500-lb increments.

Tests to Failure. These tests may be divided into three parts: first yielding of the beams, punching of slabs, and tests of the maximum capacity of the bridge.

(1) For yielding of the beams at midspan, two pairs of loads (at B, C, CD and DE) were applied at Section W5. Strains were measured on all beam gages at Sections W5, W1, 0, E1; in the transverse reinforcement under the load at DE and over the beams C and D, at Section W5; in the longitudinal reinforcement under the loads at CD and DE; and in the longitudinal reinforcement over the center pier in all panels and over all beams. Deflections were measured at Section W5. Loads were applied in increments of 500 and 1000 lb. The maximum load was 6500 lb.

For yielding of the beams over the center pier, four pairs of loads were applied at Sections E3 and W3, two pairs at each section (at AB, BC, C and D). All strain gages on beams were read at Sections W3, W1, 0, E1 and E3. Strains in the longitudinal reinforcement were measured on all gages over the center pier and under the loads at AB and BC at Section E3. Strains in the transverse reinforcement were measured under the loads at AB and BC and over the beams B and C at Section E3. Deflections were measured at Section E3. Loads were applied in 500- and 1000-lb increments. The maximum load was 7500 lb.

(2) Thirteen tests with one pair of loads were carried up to failure of the slab by punching. The locations of the loads are described in Section 17. Strains were measured in six tests in the transverse and longitudinal reinforcement under the loads and over the beams between the loads. Loads were applied in 500-lb increments until failure occured by punching of the slab.

(3) A test for the maximum capacity of the bridge was made with two pairs of loads, at Section W5, one load located at each midpanel. This test was carried to failure of the beams by buckling.

From the large amount of data collected in the tests of bridge N30 only representative data are presented in the following sections. In general, deformations for symmetrical gages and loads were in good agreement; beam strains and deflections exhibited excellent agreement. There were some differences between corresponding strains in the reinforcement, but even these fell within the range of scatter which might be expected in such tests.

13. Cracking Tests

The first step in the tests was a systematic cracking of the slab made for the purpose of simulating the condition which would exist in an actual structure. The pattern of cracks on the bottom of the slab of bridge N30 resulting from the cracking tests is shown on Fig. 6 for the east span. The crack pattern on the other half of the bridge was similar. As was expected, the cracking was most extensive in the central portion of the slab and decreased toward the center pier.

Load-strain curves for the transverse reinforcement and the surface of the slab are shown in Fig. 7. The open circles represent strains at Section W5 and the solid circles represent strains over the center pier. Some of the stress-strain curves in this figure bend over at strains equal to 10-15 x 10^{-5}. This is especially noticeable in one curve representing the strains on the surface of the slab. This break in the load-strain curve is usually taken as an indication of the occurence

of first cracking. The magnitude of strain at first cracking observed in these tests compares favorably with that observed in the tests of simple-span bridges (Bulletin 363, Section 29).

It can be observed in Fig. 7 that there was a marked difference in the strains measured in the span and over the center pier. In the span (open circles) the transverse strains in panel CD were large and cracking of the slab evidently took place, while over beam C the strains were much smaller than those corresponding to first cracking. A similar behavior was observed in the tests of simple-span bridges (Bulleting 363, Figs. 18 and 34). The behavior at Section 0 over the center pier was somewhat different (solid circles in Fig. 7): larger strains were observed over the beam than in the panels, but all strains were large enough to produce cracking. Thus it may be concluded that in the span cracking took place only in the panels because the deflections of the I-beams caused a substantial decrease of the transverse slab moments over the beams. Over the center pier, where the beams could not deflect, the slab cracked both in panels and over the beams.

Residual strains of the magnitude indicated by the symbols on the zero-load line in Fig. 7 were measured on the release of load. Similar residual strains were observed in the tests of simple-span bridges (Bulletin 363, Fig. 18). Their existence is believed to be due at least in part to the release of compressive shrinkage strains.

14. Influence Line Tests

These tests were made to determine the location of the section at which maximum beam strains occurred in the span and to determine the

location of loads for maximum strains in the beams over the center pier. The results are presented in Figs. 8 and 9.

Maximum strains measured on the bottom flange of beam C at various sections of the bridge are plotted in Fig. 8. Each point in this figure represents strains corresponding to the load applied at the section at which strains were measured. Thus the dotted line drawn through the points represents a curve of maximum strains. The largest of these maximum strains is located approximately at Section 5; this is 8.5 ft from the center pier. If the bridge is considered as a continuous beam of constant cross-section, the theoretical section of maximum moment would be located 8.55 ft from the center pier. Thus the experimentally and theoretically determined critical sections compare favorably.

The experimental influence line for the strains in the top flange of beam C over the center pier is shown in Fig. 9. As the loads moved from Section 6 to Section 4, the strains over the center pier increased. For loads at Sections 2, 3 and 4, the strains over the center pier remained practioally constant. Theoretically, for maximum negative moments loads should be located 6.34 ft from the center pier. Section 3 was located at a distance of 6.5 ft from the center pier.

In the following sections of this bulletin, Section W5 is referred to as the maximum positive moment section or midspan. Accordingly, the maximum beam strains in the span are those measured at Section W5 for loads applied at Section W5. The maximum beam strains over the center pier are those corresponding to loads placed simultaneously at Sections W3 and E3.

15. Beam Strain Tests

Maximum beam strains at midspan were measured in the influence line tests for one pair of loads and in the tests to failure of the beams for two pairs of loads. The results are plotted in Fig. 10. In this figure, strains measured on the bottom flanges are shown as full lines and strains measured on the top flanges are plotted as dash lines. Broken thin lines represent the strains computed as outlined in Section 6.

It can be seen in Fig. 10 that the bottom and top flange strains were practically equal. This indicates that there was no interaction between the slab and the beams. Furthermore, the test data are in excellent agreement with the calculated values. The only noticeable discrepancies are in the strains for the edge beams A and E. Strains measured on the edge beams were smaller than the computed ones. It should be noted, however, that after the application of the first load increment, the experimental and the computed load-strain curves were approximately parallel. It was observed at the beginning of the test that there was no contact between the outside beams and the slab, probably because the slab curled as it shrank. Consequently no load could be transmitted to the edge beams until the contact was restored. After contact was restored, the edge beams carried their share of the load as indicated by the parallelism of the experimental and computed load-strain lines.

Maximum beam strains over the center pier are plotted in Fig. 11 for two pairs of loads in each span. Top flange strains are shown as full lines, theoretical strains as broken thin lines. As at midspan, lifting of the slab at the edges of the bridges is clearly indicated by the test results. The agreement between the theory and the test results is again satisfactory.

The quantitative agreement between the computed and measured load-strain curves shown in Figs. 10 and 11 indicates that the total moments at any section of a continuous I-beam bridge of the type tested may be computed in the same manner as for a continuous beam. It indicates also that the distribution of the total moment to the various beams is the same as that for the maximum moment of an equivalent simple-span bridge; that is, a bridge having the same cross section as the continuous bridge and a span length equal to the distance between the point of contraflexure and the end support of the continuous bridge. The distribution of the strains over the center pier is practically the same as that at midspan.

A better comparison of the distribution of strains at the maximum positive moment section, over the center pier, and at midspan of the equivalent beam is given in Table 7. The values of strains for the individual beams listed in this table are expressed in percent of the total strain on the particular cross section. The comparison was made for four transverse positions of the loads. The measured strains were evaluated from the slopes of the load-strain curves, and the theoretical values were computed from the tables of Bulletin 336 for $H = 3.76$ and $b/a = 0.12$. The test results are in remarkable agreement with the theoretical values.

Measured deflections of the I-beams are compared with the theoretical values in Fig. 12. The agreement is not as good as for strains, but the differences between the theory and the test data are small. A major part of the difference can be attributed to the lifting of the slab from the edge beams.

The distribution of the measured and theoretical deflections is compared in Table 8 for four different transverse positions of the loads. In this table, deflections of the individual beams are expressed in percent of the sum of the deflections of all five beams. The measured deflections were evaluated from the slopes of the load-deflection curves and the theoretical values were computed from the tables in Bulletin 336 for $H = 3.76$ and $b/a = 0.12$. The comparison shows an excellent agreement between the theoretical and test values.

It is apparent from the comparisons of the data in Tables 7 and 8 that for all types of loading the distribution of the deflections was more uniform than the distribution of strains. However, the differences were not too large. This last point is illustrated in Table 9 in which maximum beam strain expressed in percent of the total strain is compared with the maximum beam deflection expressed in percent of the total deflection. The table includes values for four types of loading; all values listed are those computed for the midspan of the equivalent simple-span bridge. It can be seen that the percentage deflection of the critical beam is always smaller than the percentage strain. The magnitude of the difference varies with the type of loading, it is larger for one pair of loads than for two pairs of loads. The maximum difference is 13.8 percent.

16. Slab Strain Tests

Strains in Transverse Reinforcement. In all tests, the transverse strains measured on gage C located directly under the load were smaller than those measured on the adjacent gages 1E and 1W (Fig. 4). A similar phenomenon was observed in the case of some longitudinal strains.

In order to find an explanation of this phenomenon, the distribution of transverse strains in the longitudinal direction was studied for loads located successively over gages 2E, 1E, C and 1W. In each test, strains were measured on all five gages, 2E, 1E, C, 1W and 2W, located under and in the vicinity of the load. The results of one such series of tests are shown in Fig. 13. In this figure, measured strains are plotted against the distance of the particular gage line from the load. Strains measured on the same gage lines are marked with the same symbol for all locations of the load.

In all four tests presented in Fig. 13, the strains measured on gage C were smaller than would be expected, regardless of whether the load was placed over gage C or over some other gage. It is believed that the low strain readings on gage C were caused by local failures of bond. This belief is supported by the fact that the bar with gage C was covered with several other gages resulting in the destruction of bond on a relatively large portion of the bar surface; the other bars on which transverse strains were measured carried only one gage. If the bond of the bar covered with gage C was destroyed, this bar could not carry as much load as it would have carried had the bond not been destroyed; thus a redistribution of load must have taken place when the bond was destroyed and the adjacent bars (with gages 1E and 1W) picked up the major portion of this redistributed load. It seems likely that the strains measured at 1E and 1W were not much smaller than one would have expected to measure at C in the case of perfect bond. For these reasons, the measured transverse strains presented in this section are those measured on gage lines 1E and 1W.

Load-strain curves for the transverse reinforcement for a pair of loads are plotted in Fig. 14. This figure includes strains at Sections W5, E3 and O, in the outside and inside panels under the load and over the first interior beam located between the loads. Measured strains plotted as full curves are those measured on gages 1E, 1W and 2E. Strains computed for cracked and uncracked sections are shown as dotted lines; for loads located at Section W5 strains were computed for $H = 3.76$ and $b/a = 0.12$, and for loads located at Section O strains were computed for $H = \infty$ and $b/a = 0.12$.

It is apparent from this figure that the measured strains did not agree with the computed strains. With the exception of strains over the beam at W5, the measured strains are larger than those computed for the uncracked section and smaller than those computed for the cracked section. This discrepancy could have been caused by at least two factors. It was assumed in the theoretical computations for cracked section that the mortar was not capable of carrying any tension; this condition could not have been satisfied in the tests. Although the slab was cracked, the cracks could not extend up to the neutral axis; thus, the sections were actually stronger than assumed in the theory for cracked section and weaker than assumed in the theory for uncracked section. Furthermore, an equal stiffness was assumed for all sections. This assumption is also incorrect, since some sections were cracked more extensively than others. For example, at midspan, sections over the beam did not crack at all, whereas the sections in the panels were cracked quite thoroughly. As a consequence, the actual distribution of moments between the various sections of the slab must have differed from the theoretical one. These

findings are in qualitative agreement with the results of the tests of simple-span bridges (e.g. compare with Fig. 43, Bulletin 363).

The load-strain curves in Fig. 14 illustrate the effect of beam stiffness on strains in the transverse reinforcement. At midspan, where the beams deflect most, strains in the panels under the loads are large whereas strains over the flexible beams are very small; over the center pier, where the beams cannot deflect, strains in the panels are slightly smaller than those over the beams. Strains over the center pier are somewhat smaller than those in the panels at midspan, but considerably larger than those over the beams at midspan. Strains at Section E3 are intermediate between these two extremes.

All data in Fig. 14 correspond to loading with one pair of loads located in one outside and one interior panel. The load-strain curves resulting from other types of loading were in qualitative agreement with those shown in Fig. 14. A quantitative comparison is presented in Table 10. Strains measured at midspan under the load are presented in percent of the strain measured in panel DE for loads at B, C, CD and DE. Both computed and measured values are included. Although the theory indicates that the largest strains occur in the inside panel, the test data show just the opposite. The test data also show that the differences between the critical strains for the various types of loading were small.

Strains in Longitudinal Reinforcement. Maximum strains in the bottom longitudinal reinforcement at midspan were produced by loading with four loads, one at the center of each panel. These maximum strains are shown in Fig. 15, and were usually of the same order of magnitude as those measured in the transverse reinforcement (Fig. 14).

The distribution of strains in the top longitudinal reinforcement over the center pier is shown in Fig. 16 for two types of loading. Considerable variations of strain may be observed from bar to bar. Since these variations follow a practically identical pattern for both types of loading, it seems probable that the variation was a characteristic of the specimen rather than of the type of loading. The maximum strains in this reinforcement were smaller than the maximum strains in either the longitudinal or transverse reinforcement at midspan.

The strain distribution curves in Fig. 16 may be used for evaluating the contribution of the slab to the moment-carrying capacity of the bridge over the pier. This contribution was approximately one percent of the total load carried by the section over the center pier.

17. Tests to Failure

First yielding of the slab reinforcement occured during the punching tests with one pair of loads at Section W5 and with one pair of loads at Section 0. The load-strain curves obtained from these tests are presented in Fig. 17.

Yielding of Slab Reinforcement. The criterion of yielding adopted for the purposes of this bulletin was a break in the load-strain curve. The yield point strain of 0.00152 indicated in Fig. 17 is that determined from the tests of coupons and is included for purposes of comparison. A sharp break in the load-strain curves in Fig. 17 may be seen for one location at midspan and for one location over the center pier in both cases for the transverse reinforcement. The breaks in the curves were observed at strains of 0.00157 and 0.00165. It seems likely

that the small differences between the coupon yield strain and the yield strain observed in the bridge tests were the result of compressive strains induced by shrinkage of the slabs.

The loads at first yielding of the reinforcement are given in Table 11. The transverse reinforcement at midspan in panel CD yielded at a load of 5000 lb per panel. First yielding over the pier was observed at a load of 5500 lb per panel; this yielding took place in the transverse reinforcement over beam C.

Loads which caused first yielding of slab reinforcement may be converted approximately to live loads corresponding to a standard H-20 truck by dividing by 1300 lb.* If expressed in this way, the reinforcement in bridge N30 yielded at 3.8 LL at midspan and at 4.2 LL over the center pier. In the corresponding simple-span bridge first yielding of reinforcement was produced at 4.93 LL (Bulletin 363, Table 10). The yield point strains of the reinforcement, the thickness of the slabs and the amounts of the transverse reinforcement at midspan were equal in both bridges, the continuous and simple span, but the amount of longitudinal reinforcement was less in the continuous bridge. The ratio of the longitudinal to the transverse bottom reinforcement was 0.87 in bridge N15 and 0.54 in bridge N30. An increase in this ratio results in spreading the load to transverse bars located farther away from the load. Thus it seems possible that the higher load for the first yielding of the reinforcement

* This calculation neglects the dead load moments in the slabs which are negligible in both the prototype and model bridges.

in the slab of the single-span bridge N15 was the result of the higher ratio of the longitudinal to the transverse reinforcement.

Yielding of I-beams. The yield tests of beams were made with two pairs of loads at Section W5 for maximum positive moment, and with two pairs of loads in each span at Section W3 and E3 for maximum negative moment. The load-strain curves for these tests are presented in Figs. 10 and 11.

It is pointed out in Section 9 that residual tension stresses of about 19,000 psi were found in the flanges of the I-beams (Table 5). As a result, the bottom flange yielded at midspan at the relatively low load of 4000 lb per panel and the top flange did not yield at all at midspan (Fig. 10). On the other hand, the top flange over the center pier yielded at 4000 lb per panel (Fig. 11) while the bottom flange in the vicinity of this support did not yield at all. If corrected for the residual stress, the yield load would be 6940 lb for yielding at midspan and 7440 lb for yielding over the center pier.

In order to express the loads at first yielding of the I-beams in terms of live loads corresponding to a standard H-20 truck, a correction must be made for the difference in the dead loads of the model and of the prototype, and the remaining load divided by 1300 lb. If based on the loads corrected for residual stresses, the yield capacity of the beams thus corrected is 4.9 LL at midspan and 4.8 LL over the center pier. The corresponding value for the simple-span bridge N15 was 3.9 LL (Bulletin 363, Table 10). However, the beams of bridges N15 and N30 were not comparable because of differences in span lengths and size of the beams.

It can be seen from Table 11 that the prototype structure yielded first over the center pier whereas the model bridge yielded first as midspan. This apparent inconsistency in behavior between the prototype and model bridges results from the difference in the effects and magnitude of the dead load. The maximum positive moment due to dead load was only about a half of the maximum negative moment due to dead load. On the other hand, the maximum positive moment due to live load was slightly greater than the maximum negative moment due to the live load of equal magnitude per panel. Thus it could be expected that the critical section would be at midspan for a bridge with a small dead load, but over the center pier for a bridge with a large dead load. Since the dead load of the prototype bridge would be four times as large as the dead load of the model bridge, the shift of the critical section from the center pier for the prototype to the midspan for the model bridge could be expected.

Punching of Slab. Final failure of the slab by punching was produced by application of one pair of loads. The loads at which punching was produced at various locations on the bridge are given in Table 12. The positions of the loads and the order of their application are shown in Fig. 18. In tests 12 and 13, loads were located 6 in. away from the steel beams; in all other tests they were located at midpanel.

Attention is called to the fact that when loads were applied a second time at the same transverse section of the bridge, a smaller load was required for punching on the second loading. The only exception to this rule was test 1, for which the punching load was lower than in either test 2 or 3 at the same section. Furthermore, out of ten tests in which load was applied in the outside and adjacent inside panels, failure occurred

in the inside panel only twice. The load required to punch an inside panel was, as a rule, higher than that required to produce punching of an exterior panel. These results suggest that the degree of continuity of the punched panel affects the magnitude of the punching load.

The average punching loads were 9470 lb at midspan and 8330 lb over the center pier. Whether this difference was a result of the variations in stiffness of the beams or whether it was accidental cannot be said from these tests. Undoubtedly, the lower average punching capacity over the center pier was caused in part by the fact that all three punching tests over the support were made at the same section.

In both tests with loads 6 in. away from the beams punching occurred at loads lower than in any other test in the span.

The average punching loads are listed in Table 12 and also expressed in terms of live loads. It took 7.3 LL to punch the slab at midspan and 6.4 LL to punch it over the center pier. Punching of the slab of bridge N15 required 7.93 LL (Bulletin 363, Table 10). The difference between the average punching loads for bridges N15 and N30 may be explained in the same way as the difference between the loads at first yielding of the slab reinforcement of these two bridges: that is, in terms of the ratio of longitudinal to tranverse reinforcement.

Bridge Capacity. In this test four symetrically located loads were applied at Section W5 at the middle of each of the four panels. At 8000 lb per panel interior beams B, C and D had yielded extensively both in the bottom and top flanges, exterior beam A had yielded in the bottom flange only, and beam E had not yielded at all. The transverse reinforcement had yielded in all spans but not over the beams. As the load was

was increased to approximately 8490 lb per panel, the three interior beams began to buckle or twist and no more load could be applied.

The theoretical flexural capacity of the bridge assuming full yield capacity of all beams at both positive and negative moment sections was 12,300 lb per panel. This load could not be reached, however, because of the occurrence of a secondary failure by buckling of the beams. Even if buckling had not occurred, failure by punching of the slab would have undoubtedly occurred at a load lower than that indicated by this calculation.

V. TESTS OF COMPOSITE BRIDGES C30 AND X30

18. Description of Tests

The tests of composite bridges C30 and X30 were, in all important respects, similar to the tests of bridge N30 described in Section 12. However, sections E2-E6 and W2-W6 on bridges C30 and X30 were located 3 in. farther away from the center pier than the corresponding sections of bridge N30, and there were also small differences in the arrangement of gage lines. The locations of the sections and strain gage lines for these composite bridges are shown in Fig. 19.

The testing of bridge C30 was begun when the slab was 118 days old and was completed when the slab was 242 days old. At the beginning of the tests of bridge X30 the slab was 62 days old and at the conclusion 128 days old.

Tests were made in the following order: cracking tests, slab strain tests, influence line tests for beams, maximum beam strain tests, influence line tests for slab (X30 only), and tests to failure.

Cracking Tests. The location of loads and the order of loading in the cracking of bridges C30 and X30 are shown in Fig. 20. Loads were applied in 250 lb increments to a maximum of 2500-4250 lb over the center pier and 4000-4750 lb in the spans. In the tests of bridge C30 strains were measured when loads were applied at positions 1, 2, 3, 10, 11, 28, 29 and 30. In the tests of bridge X30 strains were measured when loads were applied at positions 1, 2, 3, 12, 13, 14, 27 and 28. In all other respects these tests were identical with those of bridge N30.

Influence Line Tests. These tests were identical to those of bridge N30 except that loads were also applied at Sections W6 and E6.

Slab Strain Tests. In the tests for determining the magnitude of strain in the slab reinforcement, load was applied in eight 500-lb increments. Otherwise these tests for bridges C30 and X30 were identical to those for the non-composite bridge.

An additional series of tests was made on bridge X30 to determine the position of a pair of loads which would cause maximum strains in the transverse reinforcement over the beams. In these tests, a pair of loads spaced at 18 in. was applied successively at eight different transverse positions at Sections W5 and O. The loads were first applied at the middle of panels AB and BC, and were then shifted together to other positions 3, 6 and 9 in. closer to the center of the bridge; in the last position the loads were applied over beams B and C. Strains were measured over beam B. Next, the loads were applied at the middle of panels BC and CD and then shifted 3, 6 and 9 in. toward beam E; in the last position the loads were thus over beams C and D. Strains were measured over beam C.

Maximum Beam Strain Tests. For maximum strains in the span, two pairs of loads were applied at Section W5 and B, C, CD and DE; they were then applied at AB, BC, C and D, and both tests were repeated with loads at Section E5. Beam strains were measured on all beam gages at Sections E1, O, W1 and W5 in the first two tests, and at W1, O, E1 and E5 in the last two tests. In the second test at W5, strains were read also on the transverse slab reinforcement under the loads at AB and BC, over beam B between the loads, and on the longitudinal reinforcement under the loads at AB and BC. Loads were applied in eight 500-lb increments.

Maximum beam strains over the center pier were determined in two tests with two pairs of loads at Section E3 and two pairs at W3. First, loads were applied at AB, BC, C and D and strains were measured on all beam gages at Sections W3, W1, 0, E1 and E3. Strains in the top longitudinal reinforcement were read over the center pier, and strains in the bottom longitudinal reinforcement were read at Section E3 in the loaded panels. In the second test, loads were applied at B, C, CD and DE and strains were measured at the same locations as in the first test. The maximum load applied was 3000 lb per panel, and increments of 500 lb were used.

Tests to Failure. (1) Yield tests were made with two pairs of loads at Section W5 and with two pairs of loads at Section E5 and with four pairs of loads at Sections E3 and W3, as for N30. For yielding in the spans, loads were located at AB, BC, C and D, and for yielding over the pier at B, C, CD and DE. Strains were measured at locations corresponding to those described for bridge N30. Loads were applied in increments of 500 and 1000 lb. The maximum loads for the test at midspan were 7000 and 6500 lb; for the test over the center pier 8000 and 9000 lb, for bridges C30 and X30, respectively.

(2) Twelve punching tests were made on bridge C30 and 13 were made on bridge X30. One test on each bridge was made with two pairs of loads, the others with one pair of loads. The locations of the loads are described in Section 23. Strains were measured in tests 1, 11 and 12 on bridge C30 and in tests 1, 2, 6 and 7 on bridge X30. Loads were applied in 500-lb and 1000-lb increments until failure by punching occurred.

(3) The punching tests with two pairs of loads were planned as tests for maximum flexural capacity of the bridge. However, a flexural failure was prevented by early punching of the slab.

As was done for bridge N30, only representative data for bridges C30 and X30 are presented in this bulletin since the test results were usually quite consistent. The agreement between the results for symmetrically placed gages and loads was excellent for deformation of beams; some scatter was present in the measurements made on the slab reinforcement.

19. Cracking Tests

The pattern of cracks on the bottom face of the slab of bridge C30 is shown in Fig. 21 for the east span after the cracking tests. The crack pattern on the west half of the bridge was similar. The crack pattern for bridge X30 was similar except that a somewhat larger number of diagonal cracks was observed at locations close to the center pier. The pattern of cracks for the composite bridges was decidedly different from that observed on the non-composite bridge N30. Cracks in the composite bridges were predominantly longitudinal (Fig. 21), whereas cracks in the non-composite bridge radiated in all directions from the point of load application (Fig. 6). The slabs on all bridges had the same amount of longitudinal reinforcement and the strength of mortar was not appreciably different. On the other hand the amount of transverse reinforcement in the composite bridges was about 82 percent of that used in the non-composite bridges, and the slab of the composite bridges was tied down to the beams by the shear connectors. It is believed, however, that the differences in the crack patterns resulted primarily from the fact that the slab was tied down to the beams.

Load-strain curves for the transverse reinforcement and the surface of the slabs are shown in Fig. 22. The open symbols represent strains at Section W5 and the solid symbols represent strains over the center pier. All of the stress-strain curves bent over at strains equal to 10-20 x 10^{-5}, indicating that first cracking occurred at this strain. The magnitude of the strains at first cracking is in good agreement with that observed in the tests of bridge N30.

As in bridge N30, the strains at midspan were much larger in the panels than over the beams, and strains over the center pier were somewhat larger over the beams than in the panels. However, a comparison of Fig. 22 with Fig. 7 shows that strains in the panels at midspan were larger for the composite bridges than for the non-composite one.

During the testing period, shrinkage cracks appeared in the slabs of bridges C30 and X30. The cracks were perpendicular to the direction of the bridge axis, and most of them extended from one edge of the slab to the other and penetrated the full depth of the slab. The density of the shrinkage cracks in the slab of bridge C30 reached a maximum 167 days after casting. At this time, the cracks were distributed fairly evenly throughout the middle two-thirds of the bridge. The density was somewhat greater over the center pier than at midspan. The average spacing of cracks on C30 was 9 in. The maximum density of cracks on the slab of bridge X30 was reached at 120 days after casting, that is no additional cracking occurred after that time. The distribution of cracks was similar to that on bridge C30, but cracks occurred over about three-fourths of the bridge length and the average crack spacing was about 12 in. The chose spacing of the shrinkage cracks in the composite bridges

was undoubtedly caused by the shear connectors restraining the slab from free shrinkage.

20. Influence Line Tests

In Fig. 23 maximum measured strains are shown for various locations along beam C in the span. The open circles represent strains measured on the beams of bridge C30 and the solid circles represent those for bridge X30. There is very little difference between the results for the two bridges. The test results showed that Section 5 was the critical section. Section 5 was 8.25 ft away from the center pier. Theoretical calculations taking into account the differences in the stiffness in the positive and negative moment regions gave the distance of the critical section from the center pier as 8.33 ft.

Influence lines for the maximum negative moment section are drawn in Fig. 24. The test data in this figure indicate that the position of loads required for obtaining the maximum strains over the center pier was somewhere between Section 2 and 3. The theoretical location of loads for maximum moments over the center support was found to be 5.90 ft from the center pier. The distances between the center pier and the Sections 2 and 3 were 5.25 ft and 6.25 ft, respectively.

In the following sections of this bulletin, Section W5 is called the maximum positive moment section or midspan. Accordingly, maximum beam strains in the span are those measured at Section W5 for loads applied at Section W5. Maximum strains over the center pier are those corresponding to loads placed at Sections E3 and W3.

21. Beam Strain Tests

Load-strain curves for the beams at the maximum positive moment section are plotted in Fig. 25. Strains for bridge C30 are plotted as full lines, strains for bridge X30 as dashed lines and theoretical strains are plotted as broken thin lines. As the differences between the theoretical values for the two bridges were very small, only one set of theoretical strains is included. In Fig. 25, load-strain curves for the bottom and top flanges are given for each beam for two types of loading. The experimental data for one pair of loads are those measured in the influence line tests, and for two pairs of loads are those measured in the tests to failure by yielding of the beams.

The load-strain curves for bridges C30 and X30 are in good agreement. Thus the test results show conclusively that the presence or absence of shear connectors over the center pier had no significant effect on the strains in the beams at midspan.

Strains measured on the bottom flanges were in good agreement with the theoretical strains, but those measured on the top flanges were always larger than would be expected from the theory. At low loads the slope of the measured load-strain curves is greater than that of the theoretical curves, but at higher loads the experimental and theoretical curves are approximately parallel. These differences between the test results and the theory can be explained by the presence of shrinkage cracks. At low loads the shrinkage cracks were open, and the slab at the cracks offered no resistance to compressive stresses; the beams thus acted as if little or no composite action existed. As the load increased, the cracks closed and composite action was resoted in the beams; therefore

the measured load-strain curves became parallel to the theoretical ones.* The presence of cracks had a slight influence also on the bottom flange strains, but this effect was small and is barely noticeable on the curves in Fig. 25.

Maximum beam strains over the center pier are shown in Fig. 26. Only strains on the top flanges were measured. The two theoretical lines represent strains for complete interaction between the beams and the longitudinal slab reinforcement over the pier, and strains for the beams only as the load-carrying elements. In this figure, the measured strains for bridge X30 are about 25 percent larger than those for bridge C30. With the exception of the edge beams A and E, there is a fairly good agreement between strains measured on bridge C30 and the theoretical strains for complete interaction between the beams and the slab reinforcement. Strains for X30 lie about midway between the two theoretical values. Thus the test results in Fig. 26 indicate the presence of some degree of composite action over the center piers of both bridges.

The presence of composite action is indicated even better in Fig. 27 in which the distribution of strains through the depth of beam C is shown for a location 6 in. from the center pier. Both the full line connecting the open circles (bridge C30) and the dotted line connecting the solid circles (bridge X30) intersect the zero strain line above the neutral axis of the beam. If there were no interaction between the beams

* A similar effect caused by a shrinkage crack was observed on a composite T-beam and was described in Section 28 of Bulletin 396 of the Univ. of Ill. Eng. Exp. Sta: "Studies of Slab and Beam Highway Bridges, Part III: Small-Scale Tests of Shear Connectors and Composite T-beams," by C. P. Siess, I. M. Viest and N. M. Newmark, 1952.

and the slab reinforcement, zero strains would have occurred at the neutral axis of the beam. The data presented in Fig. 27 demonstrate also that for bridges C30 and X30, respectively, the bottom flange strains were about 42 and 27 percent greater than the top flange strains. The governing bottom flange strains for bridge X30 were only about 7 percent greater than the strains for bridge C30.

On bridge C30 the slab was connected to the beams by means of shear connectors throughout the entire length of the bridge. As long as bond existed between the slab and the reinforcement, composite action must have been present between the slab reinforcement and the beams, and the stress in the reinforcement undoubtedly increased from zero at the point of contraflexure to a maximum over the center pier. On bridge X30, shear connectors were omitted between the points of contraflexure; in the remaining portions of the bridge the slab was anchored to the beams. Thus when the upper flanges of the beam elongated between the points of contraflexure, the slab had to undergo an approximately equal total elongation between these points. Because of its resistance to this elongation, the slab reinforcement offered some restraint to the steel beams; in other words, some degree of interaction was present between the beams and the slab reinforcement. Theoretically, the stress in the longitudinal reinforcement should have been an approximately uniform tension throughout the region of negative moment. Thus the stress in the bars and the degree of interaction over the center pier had to be smaller in bridge X30 than the corresponding values in bridge C30.

A comparison of the theoretical and test data in Figs. 25 and 26 indicates that the distribution of strains across the maximum positive

and negative moment sections were about the same. A better comparison of the strain distributions is given in Table 13. Strain distribution at midspan for four types of loading, and strain distribution over the center pier for one type of loading, are included in this table. Strains for individual beams are presented in percent of the total strain. The agreement between the theory and the test data is good for both bridges and for all types of loading, but is significantly better for four loads, representing both lanes loaded.

Load-deflection curves for beam C at midspan are shown in Fig. 28. Deflections for both bridges are those measured in the tests to failure. A theoretical load-deflection curve is also included in this figure.

22. Slab Strain Tests

Strains in Transverse Reinforcement. In all tests of bridges C30 and X30, strains measured on gages C located on the reinforcing bar passing directly under the load were larger than strains measured on the adjacent gages 1E and 1W. Typical longitudinal distributions of transverse strains are shown in Fig. 29. No irregularities similar to those observed on bridge N30 and described in Section 16 were recorded in the tests of the two composite bridges.

Load-strain curves for the transverse reinforcement of bridges C30 and X30 are plotted in Fig. 30. This figure includes only data from tests with a pair of loads applied in the outside and adjacent inside panel, and strains measured under the loads and over the beam between the loads. One set of data is given for each of the following sections

of the bridge: W5, E3 and O. It can be seen from Fig. 30 that in the span the load-strain curves for bridges C30 and X30 differed very little and that these differences were not consistent. Over the center pier the strains in the panels of bridge X30 were somewhat smaller, and over the beam were somewhat larger, than the corresponding strains in C30. As for bridge N30, the measured strains were larger than the theoretical values computed for the uncracked section and smaller than the theoretical values computed for the cracked section.

A comparison between the non-composite and composite bridges may be made by comparing Figs. 14 and 30. A better quantitative comparison is presented in Table 14 in which measured strains for the three bridges are compared at a load of 3000 lb per panel. Two sets of strains are included for bridge N30. The slab of this bridge had 25 percent more transverse reinforcement than the slabs of bridges C30 and X30. In order to put the strains for N30 on a basis comparable to those for the other two bridges, strains for N30 were multiplied by 1.25. Although this correction does not account for various secondary effects of the increased percentage of reinforcement, such as the degree of cracking and the longitudinal distribution of load, it is believed that the factor 1.25 accounts for the major effect. Furthermore, it is probable that the value of strain listed for bridge C30 over the beam at midspan is too high. The strain of 50×10^{-5} was obtained by averaging the strains shown in Fig. 30. A comparison with corresponding strains at Section E3 indicates that a value of 34×10^{-5} would probably be more representative.

At midspan, strains in the bottom transverse reinforcement in the panels were 35-80 percent greater in the non-composite bridge. Strains

in the top transverse reinforcement over the beam in the non-composite bridge were less than half of those in the composite bridges. These differences can be explained as the result of the greater stiffness of the composite bridges, the torsional restraint caused by shear connectors, and the greater width of flanges of the beams in the non-composite bridge. It is shown in Section 16 that the transverse slab strains in the panel decreased with increasing bridge stiffness in the longitudinal direction, and the transverse slab strains over the beams increased with increasing stiffness. An increase in the width of the beam flanges decreases the effective span of the slab and thus causes a decrease of strains, especially those over the supports. The presence of shear connectors produced some torsional restraint at the edges of the slab and thus decreased strains in the panels. Furthermore, it is possible that the presence of shear connectors contributed to the formation of transverse cracks over the beams which in turn led to a substantial increase of strains at such locations.

Over the center pier, strains in the panels were nearly equal for bridges N30 and X30, and about 15 percent larger for bridge C30. Although this difference is relatively small, it is difficult to explain. Seemingly, the only significant difference was the presence of shear connectors in bridge C30. It would be expected that in such a case strains in the panels of bridge C30 should be smaller than those in the other two bridges. However, just the opposite was observed. It is possible that the close spacing of shrinkage cracks in bridge C30 caused these unexpected results. Strains over the beams were about the same in N30 and C30 and about 36 percent larger in X30. The effect of the greater

width of the supporting flanges in N30 was probably the cause of the difference between N30 and X30. In beam C30, this effect was probably counteracted by the torsional restraint exerted by shear connectors on the edge of the slab.

These explanations of the differences in the transverse slab strains are only qualitative. The preceeding discussion has shown that both the absolute and relative magnitudes of the transverse strains in the panel and over the beams might be affected by the following factors: percentage of the transverse reinforcement, stiffness of the bridge in the longitudinal direction, torsional restraint over the beams offered by shear connectors, width of the flanges of I-beams, and possibly also the spacing of the transverse shrinkage cracks. However, the test data available are insufficient for a quantitative determination of the influences of the individual factors.

All comparisons of transverse slab strains described so far were based on tests with one pair of loads. In Table 15, maximum strains are compared for four different types of loading. In all three bridges, the critical loading was that with two pairs of loads located at B, C, CD and DE, and the largest strains were found in the loaded outer panel. However, the effect of the pair of loads at B and C was fairly small - 3 percent in bridge N30 and 7 percent in bridge X30. The data for bridge C30 for one pair of loads at CD and DE are unreliable because the slab was accidentally damaged in panel DE in the vicinity of midspan, but it is believed that an effect similar to that observed for X30 might be expected.

One series of tests was carried out on bridge X30 for the purpose of determining the position of a pair of loads which caused the largest strains over a beam. The results are shown in Fig. 31. A pair of loads was applied successively at positions 1, 2, 3 and 4. The influence lines in Fig. 31 show that the most unfavorable loading is with loads at midpanels.

Strains in Longitudinal Reinforcement. Load-strain curves for the longitudinal bars in the bottom of the slab at midspan are given in Fig. 32 for two pairs of loads, each load located at midpanel; and strain distribution curves in the panels are given in Fig. 33 for two pairs of loads with two loads at midpanels and two over the beams. Data for the non-composite bridge are included in Fig. 33. In both figures, positive strains represent tension, negative strains represent compression.

Nearly all strains in bridges C30 and X30 shown in Figs. 32 and 33 are compressive. The compressive strains increased rapidly in magnitude until a load of about 2000 lb per panel was reached. At higher loads a decrease in the compressive strains was observed, and in some cases tensile strains were recorded.

Obviously, the presence of compressive stresses was caused by composite action between the slab and the beams. Stresses in the unloaded panels were distributed approximately uniformly throughout the full width of the panel (Fig. 33, panels CD and DE). In the loaded panels nonuniformly distributed tensile stresses, resulting from the dishlike deformations of the slab under the load, were present in addition to the compressive stresses due to the composite action. These additional tensile stresses were comparable to those observed on bridge N30.

The presence of compressive stresses in the longitudinal reinforcement of a composite bridge is to be expected and was observed also in the tests of simple-span bridges. However, the magnitude of the compressive stresses in the simple-span bridges (Figs. 12 and 45 in Bulletin 363 and Figs. 12 and 21 in Bulletin 375) was much smaller than in the continuous bridges. Furthermore, the load-strain curves for the continuous bridges were curved (Fig. 32) while those for the simple-span right bridges were straight. An explanation of these differences lies in the presence of the transverse shrinkage cracks. At low loads the shrinkage cracks in bridges C30 and X30 were open and all compressive stresses in the slab had to be carried by the reinforcement alone. As the load increased, the cracks closed and the mortar took a greater part of the additional compressive stresses. The slab of bridge C30 had more shrinkage cracks than the slab of X30; accordingly, longitudinal compressive stresses in the slab of C30 were somewhat larger than the corresponding stresses in X30.

The distribution of strains in the top longitudinal reinforcement over the center pier is shown in Fig. 34 for all three bridges for the loading producing maximum negative moments over the pier. All strains were tensile. The smallest strains were those in the non-composite bridge N30; the largest were those in the composite bridge C30, with shear connectors distributed over the full length of the bridge. Strains in bridge C30 were about twice as large as those measured in N30. Strains in bridge X30, in which the shear connectors were omitted over the center pier, were somewhat smaller than those for C30 but appreciably larger than those for N30. The differences between these longitudinal strains in the three

bridges were caused by the presence or absence of shear connectors. In the non-composite bridge the bending of the slab was independent of that of the beams; the bottom of the slab was in compression, the top in tension; the slab carried only a very small portion of the total load (estimated in Section 16 as one percent). Thus the strains in the longitudinal reinforcement had to be comparatively small. In the composite bridges C30 and X30 the full cross section of the slab was in tension and strains in the longitudinal reinforcement had to be compatible with those in the beams. Thus strains in these bridges had to be relatively large. The differences between C30 and X30 were caused by the differences in the compatibility conditions, as discussed in Section 21. The magnitude of the longitudinal slab strains over the support of the composite bridges was comparable to that of the strains in the transverse reinforcement at midspan (Fig. 30).

Owing the composite action, the contribution of the slab to the load-carrying capacity of the bridge was large. At midspan, where the slab was in compression, the section modulus of the composite section was 56 percent greater than the section modulus of the non-composite section. Over the center pier, where only the slab reinforcement interacted with the beam, the section modulus of the fully composite bridge C30 was 11 percent greater than that for the non-composite bridge N30.

23. Tests to Failure

Yielding of Slab Reinforcement. Load-strain curves for the transverse slab reinforcement in the tests to failure are shown in Fig. 35. Although a definite break can be observed only in the two curves for

strains over the beam at Section 0, the strains at the break points in these cases practically coincide with the yield point strain of the tensile coupons. It was decided, therefore, to consider the load corresponding to this yield point strain as the load producing first yielding.

Load-strain curves for the top longitudinal reinforcement over the center pier are shown in Fig. 36. The shapes of these curves show numerous irregularities which may be explained by the presence of transverse cracks at both ends of the gages and by bond failures along the bars. At a strain approaching the yield point strain, some measurements indicated an increase of load without an increase of strain. It is believed that in such cases yielding took place at observed cracks located at both ends of the particular gage prior to the occurrence of yielding at the gage. As yielding progressed, strain in the gage which was located between these two yielded regions could not increase as long as the bar was bonded to the adjacent concrete. However, at some higher load the bond was broken and the gage registered a rapid increase of strain.

Yielding occurred first in the transverse reinforcement. First yielding at midspan took place in both bridges at the same load of about 5000 lb per panel. First yielding over the center pier also occurred in both bridges at the same load of 3000 lb per panel. The loads at which first yielding was observed in the slab reinforcement are given in Table 16. They are listed also in terms of live loads corresponding to a standard H-20 truck.

In all three bridges tested, the transverse reinforcement yielded first in the panels at midspan and over the beams at the center pier. The results for all bridges may be compared if a correction is made for the differences in the yield point stresses and the amounts of reinforcement.

Correction to a common yield point of 44,000 psi and to an amount of reinforcement equal to that used in the composite bridges requires that the loads for N30 be multiplied by 0.80, for C30 by 1.05, and for X30 by 1.02. The corrected yield point loads at midspan are 3.1, 4.0 and 3.9 LL, and over the center pier 3.4, 2.4, and 2.3 LL for bridges N30, C30 and X30, respectively.

A comparison of the loads at first yielding of reinforcement with the corresponding strains listed in Table 14 shows that yielding in the span of the three bridges occurred in the sequence which would be expected on the basis of the elastic strains. On the other hand, yielding over the center pier occurred in a sequence different from that indicated by the elastic strains. All strains included in Table 14 were taken from the slab strain tests made early in the testing period. First yielding of the reinforcement was observed during the punching tests made toward the end of the testing period, except for yielding over the center pier of bridge X30 where the transverse reinforcement had yielded during the slab strain tests. The strains measured during the two tests did not differ significantly on bridge N30 (compare Figs. 14 and 17) nor at midspan of bridges C30 and X30 (compare data for midspan in Figs. 30 and 35). On the contrary, strains measured over the center piers of bridges C30 and X30 were larger than the corresponding strains measured in the slab strain tests (compare data for C30 over the pier, Figs. 30 and 35). An explanation of these phenomena seems to be in the transverse cracking of the slab due to shrinkage. No extensive cracking due to shrinkage was observed in bridge N30, whereas in the composite bridges this cracking was extensive and the density of the cracks increased with time. At

midspan, the cracks closed long before the loads causing first yielding of reinforcement was reached. Over the center pier, however, the shrinkage cracks were open at high loads so that the slab was composed of essentially separate strips interconnected only by the longitudinal reinforcement. The width of these strips decreased with time owing to the occurrence of new shrinkage cracks, and the stress in the transverse reinforcement increased accordingly.

Yielding of I-beams. The load-strain curves for the I-beams of bridges C30 and X30, obtained from the tests to failure, are shown in Figs. 25 and 26 for midspan and over the center pier, respectively. In both bridges, first yielding was observed at midspan on the bottom flange of beam C. The loads were 4000 lb for C30 and 3600 lb for X30. The corresponding stresses in the top flanges were small. They remained far below the yield point value up to the maximum load applied, indicating that composite action between the slab and the beams was maintained throughout these tests. Over the center pier, first yielding of the beams occurred in bridge C30 in the top flange of beam C at a load of 7500 lb per panel and in bridge X30 in the top flange of beam D at a load of 6500 lb.

Before comparisons of the two composite bridges can be made, the loads at first yielding must be corrected to a comparable basis. It can be seen from Table 2 that the yield point stress of coupons differed for the two bridges. Furthermore, it is shown in Section 9 that the residual stresses due to rolling and due to welding shear connectors were different for the beams of bridges C30 and X30. It can be seen from Table 5 that the apparent yield point stresses, which account for the residuals, were also different for bridges C30 and X30 and in each bridge

were different for midspan and center pier sections.

Correction of the loads at first yielding was made as follows: First, the loads were multiplied by the ratio of a chosen yield point strain (138×10^{-5}) to the actual yield point strain. Next, the loads were multiplied by the ratio of the expected to the measured strain at first yielding. The expected strain at first yielding was computed as the difference between the yield point strain of test coupons and the dead load strain. The first correction was for differences in the yield point stress of the material and the second for the residual stresses.

The corrected measured loads at first yielding are compared with the corresponding calculated loads in Table 17. The calculated values were obtained as outlined in Section 6. The following relative stiffnesses H were used for determining the transverse distribution of strains: 3.76, 5.68 and 4.10 for bridges N30, C30 and X30, respectively; $b/a = 0.12$ was used for all three bridges. To account for the incomplete interaction between the slab reinforcement and the beams over the pier of bridge X30, strains at this location were computed for both full and no interaction and an average value was taken for further calculations. The measured and calculated values in Table 17 are in good agreement. In the light of the results reported in Sections 15 and 21 this agreement was to be expected.

Corrected loads at first yielding of bridges C30 and X30 are listed in Table 16. If corrected for the additional dead load for a full size structure, and expressed in terms of 1.0 DL + n LL, where LL is the live load corresponding to that for standard H-20 truck loading, loads at first yielding of the beams are 3.2 LL and 3.9 LL for midspan

and center pier of bridge C30, and 3.0 LL and 2.9 LL for the corresponding sections of bridge X30. As would be expected, the loads for the maximum positive moment section are approximately equal for both bridges, and the loads for the maximum negative moment section are higher for C30 than for X30. However, the difference between the loads for Section 0 is larger than would be expected from the differences in the two bridges. At this section in the test of bridge C30 beam C yielded first, while in the test of bridge X30 beam D was the first to yield. Yielding of beam D progressed rather slowly and the strains in beam C became larger than those in beam D soon after beam C began to yield. This behavior seems to indicate that the yielding of beam D might have been the result of some local condition. If this were true, the first yielding of beam C should have been taken as the critical load. The load at first yielding of bridge X30 over the center pier would then be equal to 1 DL + 3.4 LL, which would compare with that for bridge C30 as expected.

The measured loads at first yielding of the beams were smaller for the composite structures than for the non-composite bridge N30. If corrected for the residual stresses, dead load, and to a coupon yield strain of 138 x 10^{-5}, the loads at first yielding of the prototype of bridge N30 would be 1 DL + 4.2 LL and 1.0 DL + 3.9 LL for the maximum positive and negative moment sections respectively. Thus the first yielding at midspan of the beams of the prototype bridges N30, C30 and X30 would have occurred on the application of 4.2, 3.2 and 3.0 LL, respectively; and the first yielding over the center pier would have occurred on the application of 3.9, 3.9 and 3.4 LL. It can be seen that the critical section of the non-composite bridge was over the center pier, whereas the

critical section of the composite bridges was that at midspan. These test results are in agreement with the findings of the design calculations. Only prototype bridges N30 and C30 were designed. The design of the non-composite bridge was governed by the compressive stress of 16,870 psi in the unsupported bottom flange of the I-beam over the pier (a reduced allowable stress of 16,775 psi). The design of the composite bridge was governed by the tension of 18,720 psi at midspan (an allowable stress of 18,000 psi). On account of the danger of buckling, the governing design stress for N30 was lower than the governing design stress for C30. As would be expected, yielding of the beams began before any buckling could occur. Thus the number of live loads required to produce first yielding was larger for bridge N30 than for bridge C30.

Punching of Slab. Final failure of the slab occurred by punching. Loads at which punching took place are given in Table 18 for bridge C30 and in Table 19 for bridge X30. The locations of the loads during the punching tests are shown in Figs. 37 and 38. Punching occurred in a manner similar to that described in Bulletin 363 for the simple-span bridges.

It can be seen from Fig. 37 that the location of the punched holes on the continuous bridge C30 was divided about equally between the outer and inner panels. This indicates that, as a result of the presence of shear connectors, the outer panels had edge restraints similar to those for the inner panels. That the shear connectors help to restrain the edges of the individual slab panels can be seen also when punching loads are compared for tests made at the same transverse section of the bridge. It was observed in the tests of bridge N30 that after a section of the slab had been punched the successive punching tests at that section required

a smaller load. A similar phenomenon was observed also in a few tests on C30, but in the majority of the tests on this bridge the second punching load was either equal to or somewhat higher than the first one. In bridge X30 failures occurred predominatly in the outer panels (Fig. 38) and the differences between the first and second punching loads at the same section were inconsistent.

A few tests on bridges C30 and X30 were made with loads located 6 in. away from the beams rather than at midpanels. The punching loads did not differ significantly from those observed for loads at midpanels.

In the tests of bridge N30, the average punching load over the center pier was smaller than the average punching load in the span. A similar phenomenon was observed in the tests of composite bridges. A summary of the average punching loads for all three bridges is given in Table 20. The data in this table demonstrate clearly that the loads required to punch the slab over the support or in its immediate vicinity are smaller than those required for punching in the span. Furthermore, the punching loads in the span are lower for the non-composite bridge than for the two composite bridges. The situation over the pier is just reversed: the punching loads decrease with increasing degree of composite action. At midspan, slabs of the composite bridges were subject to some longitudinal compression, thus it could be expected that the shearing resistance of the slab was higher in the composite than in the non-composite bridges. Accordingly, composite action increased the punching-load capacity. A similar phenomenon was observed in the tests of simple-span bridges (Bulletin 363, Table 10). It is believed that the difference between C30 and X30 resulted from the higher strength of the

mortar in bridge X30 (Table 4). Over the center pier, the slabs of the composite bridges were in tension, and it would be expected that the tension would decrease the shearing resistance of the slabs. The punching loads over the pier are in line with this assumption: the highest punching load was observed in the non-composite bridge N30, the lowest in the fully composite bridge C30.

Bridge Capacity. As in bridge N30, four loads were applied at Section W5 for the purpose of determining the capacity of bridges C30 and X30. In the test of bridge C30, all five beams yielded extensively in the bottom flange, but the stresses in the top flanges remained well below yielding. At the last increment of load before failure occurred (10,000 lb per panel), the top flanges of the three inside beams were in tension whereas the top flanges of the outside beams were still in compression. Final failure occurred by punching of the slab at 10,400 lb per panel. No strain measurements were taken in the test of bridge X30 which failed also by punching at a load of 10,400 lb per panel.

The capacities and modes of failure for all three bridges are listed in Table 21. Ultimate flexural capacities computed from the principles of limit design are included for comparison. It can be seen from this table that the ultimate capacities of the composite bridges were 23 percent higher than the capacity of the non-composite bridge, in spite of the smaller size of the beams. Bridge N30 failed by buckling of the beams, whereas the composite bridges failed by punching of the slab at a considerably higher load. Presumably the connection between the slab and beams prevented buckling of the beams.

VI. DISCUSSION OF TEST RESULTS

24. Preliminary Remarks

Three 1/4-scale models of two-span continuous bridges were tested for the purpose of obtaining experimental evidence concerning the distribution of moments and strains and the effects of composite action on the behavior of such bridges. Each bridge consisted of five steel I-beams and a mortar slab resting on the tops of the beams. In two bridges, the slab was tied to the beams with channel shear connectors; in the third bridge no connection was provided between the beams and the slab. The specimens, methods of testing, and test results have been described in detail, and the experimental data compared with the results of the tests of simple-span bridges (Bulletin 363) in the preceding chapters. The important test results are discussed and summarized in the following sections.

25. Behavior of Steel I-Beams

General. As in the tests of simple-span I-beam bridges, elastic strains measured on the I-beams of the continuous bridges were in excellent agreement with the computed values. First yielding of the beams was characterized by an abrupt change in the slope of the load-strain curves. Yielding occurred first in the center beam and was followed shortly thereafter by large deflections. With further increase of the load, yielding spread to the other beams and penetrated deeper into the sections, but yielding through the entire cross-section of all beams was never reached. Final failure of the non-composite bridges occurred by buckling of the interior beams, and of the composite bridges by punching of the slab.

Beam Strains and Moments. In the non-composite bridge, the top and bottom flange strains were of equal magnitude. At midspan of the composite bridges, the top flange strains were much smaller than the bottom flange strains. Over the center pier of the composite bridges, the top flange strains were somewhat smaller than the bottom flange strains. Thus bridge N30 behaved as a truly non-composite structure, and bridges C30 and X30 as composite structures. In the composite bridges tested, the full area of the slab cooperated with the beams at midspan, but only the longitudinal reinforcement cooperated with the beams over the center pier.

The bottom flange strains measured at midspan and the top flange strains measured over the center pier were equal to the corresponding computed values. This agreement indicates two things: First, the total strains, and therefore approximately also the total moments on the critical sections of continuous I-beam bridges, were equal to those computed for a continuous beam having the same span and stiffness as the bridge. Second, the strains, and therefore also the moments, were distributed to the individual beams in the same manner as they would be distributed at the maximum positive moment section of a simple-span bridge of identical cross section and with a span length equal to the distance between the point of contraflexure and the end support of the continuous bridge. The distribution of strains across the maximum positive and maximum negative moment sections were approximately the same.

Moments in the center beam over the center pier were critical in the non-composite bridge, whereas in the composite bridges critical moments were those occurring in the center beam at midspan. This shift of the critical section was the result of the decreased stiffness of the section over the center pier of the composite bridges which caused a significant shift of moments from the pier to midspan.

Beam Deflections. Measured deflections were in satisfactory agreement with the computed ones. The average deflection was computed for a continuous beam of identical span and stiffness, and distributed according to the deflections of the equivalent simple-span bridge at midspan. It was observed also that for the particular bridges tested the distribution of deflections across the maximum positive moment section was more uniform than the distribution of strains.

Yielding of Beams. The load at first yielding of the I-beams was influenced significantly by residual stresses existing in the beams at the time of the test. Three types of residual stresses were found to be present in the beams - residual stresses due to rolling, due to welding of shear-connectors, and due to shrinkage of the slab. The two types mentioned last were present only in the composite bridges. In these tests it was possible to determine the residual stresses by means of various auxiliary tests, and thus the loads at first yielding could be computed with satisfactory accuracy. However, in practice, these stresses are uncertain and prediction of the load at first yielding would be virtually impossible.*

Yielding of the I-beams was indicated clearly by an abrupt change in the slope of the load-strain curves. In bridges N30 and C30, first yielding occurred at the location of maximum strains, whereas in bridge X30 first yielding took place over the pier in beam D instead of in beam C although maximum strains were measured in beam C. It is believed

* A similar conclusion was reached from the results of tests of full-size composite T-beams described in the Eng. Exp. Sta. Bul. "Studies of Slab and Beam Highway Bridges, Part IV: Full-Scale Tests of Channel Shear Connectors and Composite T-beams," by I. M. Viest, C. P. Siess, J. H. Appleton and N. M. Newmark. See Section 39, p. .

that some local variation in the material or in the residual stresses might have caused this discrepancy.

A further discrepancy was observed in the magnitude of strain at first yielding of bridges C30 and X30 over the center pier. Strains at which yielding began were substantially larger than the yield strains determined from the tests of coupons and corrected for residual stresses.

Buckling of Beams. In the final test of bridge N30, yielding penetrated the full depth of the three interior beams at midspan and was soon followed by buckling. The beams of the composite bridges, however, never yielded throughout the full depth, and large permanent deformations constituted the only damage done to the beams during the tests to failure.

26. Behavior of Mortar Slabs

General. The behavior of the slabs of the continuous I-beam bridges was similar to the behavior of the slabs of the corresponding simple-span I-beam bridges. First cracking of the slab occurred at a steel strain of 10-20 x 10^{-5}. Upon the release of load after first cracking some residual stresses were observed, probably caused by the release of residual shrinkage strains. The cracked slab exhibited a fairly straight load-strain relationship. As in the simple-span bridges, the measured strains were appreciably smaller than the computed strains, the difference varying with the location on the bridge.

First yielding of the slab reinforcement was a localized phenonenon. It took place in the transverse reinforcement, in panels under the loads at midspan, and over the beam between two loads over the center pier. As the loading continued, yielding spread to the adjacent bars and

the degree of cracking increased. However, no appreciable warning in the form of a visible increase of deflections was observed before the final failure occurred. The slab failed by punching in the manner described in Bulletin 363.

Strains in Transverse Reinforcement. At midspan, the strains in the bottom transverse reinforcement in the panels were larger than those in the top transverse reinforcement over the beams. This difference was especially noticeable in the non-composite bridge in which strains over the beams were so small that these sections did not crack before first yielding took place in the panels. Strains in the outside panels were critical.

Strains over the center pier were larger in the top transverse reinforcement over the beams than in the bottom reinforcement at midpanels. In the composite bridges the magnitude of these strains was greatly affected by the transverse shrinkage cracks. Strains increased with the increasing density of these cracks.

The maximum slab strains occurred at midspan in the non-composite bridge and over the center pier in the composite bridges. It is believed that this difference was caused primarily by the presence of shrinkage cracks.

The magnitude of strains in the transverse reinforcement depended primarily on loads located over the gage and in the adjacent panels. Loads located further away from the gage location affected the strain but little. The difference between the strains for one and two pairs of loads did not exceed 3 percent in the non-composite bridge and 7 percent in the composite bridges.

Strains in Longitudinal Reinforcement. Strains in the longitudinal reinforcement were always smaller than the maximum strains in the transverse reinforcement. Thus the longitudinal reinforcement was of secondary importance. However, the test results indicated that even though the stresses in the longitudinal steel are not critical, the relative percentage of this steel might have a considerable effect on the magnitude of the transverse strains. The smaller the ratio of the longitudinal to transverse reinforcement, the larger is the portion of the load that will have to be carried by the transverse bars located directly under the load. This results from the decreasing effectiveness of the longitudinal steel in transferring the load to the more distant transverse bars.

There is a basic difference between the behavior of the slabs of a non-composite and a composite bridge. In a non-composite bridge, the slab bends independently of the beams; as a result, the slab is subject to both tension and compression at each cross section. On the other hand, in a composite bridge, the slab and the beams act as a solid cross section and the slab is thus predominantly in compression in the regions of positive moment and in tension in the regions of negative moment. Consequently, the bottom longitudinal reinforcement at midspan is in tension in the non-composite bridge and in slight compression or tension in a composite bridge. Over the center pier, the top longitudinal reinforcement of both types of bridges is in tension.

Contribution of Slab as Load-Carrying Element. The stiffness of the slab was small as compared to the stiffness of the I-beams. Since the ratio of the load carried by the slab and the beams of a non-composite bridge is approximately the same as the ratio of their stiffnesses, the

slab carried only a small portion of the total load. It was estimated that the contribution of the slab to the load-carrying capacity of bridge N30 was about one percent.

This situation was radically different in the composite bridges. At midspan, the slab was very effective as a load-carrying element because it was fully in compression. The section modulus for the composite structure was 56 percent greater than that for the I-beams alone. Over the center pier, only the longitudinal reinforcement in the slab contributed to the longitudinal load-carrying capacity, since the slab was fully in tension. The increase of the section modulus at this location was 11 percent.

Yielding of Reinforcement. First yielding of the slab reinforcement was indicated by more or less sharp changes of the slope of the load-strain curves at strains which were in good agreement with the yield strains found in the tensile tests of coupons.

The reinforcement of the non-composite bridges yielded first at midspan in the outside panels. Yielding over the pier occurred at a higher load and took place over the beams. In the composite bridges, first yielding of the reinforcement occurred in the top transverse reinforcement over the beams at the center pier. First yielding in the span occurred in the transverse reinforcement in the panels. First yielding of the longitudinal reinforcement in all bridges occurred at higher loads. The location and sequence of first yielding were in agreement with those expected from the elastic strain measurements.

Punching of Slabs. The maximum capacity of the slab at midpanels was reached when the load punched a hole through the slab. The magnitudes of the punching loads were smaller over the center pier than

in the span. In the span, the punching loads were larger for the composite than for the non-composite bridges whereas over the center pier the opposite was true. When the slab is in direct compression, as it was at midspan of composite bridges, the neutral axis for local bending under the load is at a lower level than normal and there is a larger area available to resist shear; consequently the punching load is high. Just the opposite situation exists when the slab is subject to a direct tension as was the case over the center pier of composite bridges.

In addition, the tests indicated that the resistance to punching increased with restraint to rotation at the edges of the punched panel.

27. Ultimate Failure of Bridges

Each bridge was loaded at midspan with four loads, one in each panel, until failure occurred. These tests demonstrated a profound difference in behavior between the non-composite and composite bridges. The non-composite bridge failed by buckling of three interior beams at a load of 8490 lb per panel. Both composite bridges failed by punching of the slab at a load of 10,400 lb per panel.

28. Effects of Shear Connectors

At Midspan. The shear connectors welded to the top flanges of the I-beams restrained the mortar slab against free shrinkage. This resulted in transverse cracking throughout the major portion of the lengths of bridges C30 and X30. The average spacing of the shrinkage cracks in C30 was 9 in. and in X30 was 12 in. Upon loading, the shrinkage cracks at midspan closed and the slab was fully effective in carrying the longitudinal compressive stresses. The effect of the presence of shrinkage

cracks on the magnitude of the governing bottom flange stresses in the beams was barely noticeable, whereas the top flange stress increased rapidly until the cracks closed. Consequently, these stresses were more than three times as large as would be expected in the absence of shrinkage cracks. Nevertheless, the top flange stresses were only a fraction of the bottom flange stresses and the slopes of the load-strain curves for the top flanges indicated that practically full interaction existed between the beams and the slab once the cracks had closed.

The omission of shear connectors in the negative moment region of bridge X30 did not seem to affect the stresses at midspan. Strain measurements at midspan of bridges C30 and X30 showed practically no difference between the behavior of these two bridges at midspan.

The presence of shear connectors affected the behavior of the slab as follows: The transverse strains were decreased at midpanels and increased over the beams. The loads at first yielding of reinforcement and at punching were about 25 percent higher in the composite bridges.

Over Center Pier. Because the slab was in longitudinal tension at this location, the maximum beam strains were not affected by the presence of shrinkage cracks. In both composite bridges, interaction was observed between the longitudinal slab reinforcement and the beams. In bridge C30 with shear connectors in the negative moment region, this interaction over the center pier was practically complete whereas in the bridge X30, built without any shear connectors in the negative moment region, the strain measurements over the center pier indicated that the degree of interaction was about half-way between complete and no interaction. Consequently, the governing bottom flange strains were about 7 percent

larger in bridge X30 than in bridge C30.

The principal effect of shear connectors on the transverse slab strains resulted from the additional number of transverse cracks in the regions where shear connectors were provided. The strains in the transverse reinforcement were increased in regions at extensive cracking owing to the loss in longitudinal distribution of the load or moments. Otherwise the transverse strains were not affected greatly by the presence of shear connectors, and the distribution of strains between the sections at midpanel and over the beams was about the same in the composite and non-composite bridges. The measured strains in the top longitudinal reinforcement were over twice as large in the composite bridges as in the non-composite bridges. Loads at first yielding and at punching of the slab were on the average about 30 percent lower in the composite than in the non-composite bridges.

29. Relation of Test Results to Design

Tests of three bridges with the extent of composite action as the only major variable are not sufficient in themselves to provide a basis for a specific design recommendation. However, these tests of continuous bridges form a link in the chain of theoretical studies (Bulletin 336) and tests (Bulletins 363 and 375) of slab-and-girder bridges. The results of the tests of continuous bridges were in good qualitative and quantitative agreement with the results of the tests of corresponding simple-span bridges and with the results of analyses. Thus it seems reasonable to assume that conclusions drawn from these tests would be more widely applicable than would perhaps be justified by the rather limited scope of the tests.

Moments in Beams. The tests indicated that the total moments at the critical sections were practically equal to the total moment computed for an equivalent continuous beam. The distribution of moment to the various beams was the same in the span and over the center pier and was essentially the same as that for an equivalent simple-span bridge. Therefore, it seems reasonable to compute the equivalent wheel load acting on one beam as that for an equivalent simple-span bridge* and then to compute the maximum positive and negative moments by the usual methods for continuous beams.

The cross section to be considered in the computation of moments for a non-composite bridge should be that of the steel I-beam alone. For a composite bridge, the cross-section at midspan should be assumed to consist of one I-beam acting compositely with the slab.[x] Over the center pier, one should consider either I-beam alone or the I-beam plus the longitudinal slab reinforcement. Full interaction may be assumed between the components of the cross-section.

Slab Reinforcement. Strains in the transverse and longitudinal reinforcement at midspan of the continuous bridges were comparable to the corresponding strains in simple-span bridges. Thus the design procedure proposed by N. M. Newmark** on the basis of the results

* N. M. Newmark, "Design of I-beam Bridges," Transactions of the American Society of Civil Engineers, 1949, Vol. 114, pp. 1020-1021.

[x] For computing the strains and deflections of the model bridges, the effective width of the slab was assumed to be equal to the beam spacing. A good agreement was found between the computed and measured values.

** N. M. Newmark, "Design of I-beam Bridges," Transactions of the American Society of Civil Engineers, 1949, Vol. 114, pp. 1018-1019.

of the tests reported in Bulletin 363 should be applicable also the the positive moment sections of continuous bridges.

Strains in the transverse reinforcement in the region over the center pier were distributed more like the theoretical strains for a continuous slab resting on non-deflecting supports than like the strains at midspan where the supporting beams were flexible. It seems that if the percentage of reinforcement in the panels and over the beams were equal, the strains also would have been about equal at this location. The maximum transverse strains in the region over the center pier were somewhat smaller than those at midspan in the non-composite bridge and somewhat larger in the composite bridges; consequently, a design procedure using the same maximum moments as in the panels at midspan might be acceptable for the slab over the center pier. However, the tests of the continuous bridges did not furnish sufficient evidence regarding the strains in the reinforcement over the pier, and this question requires additional experimental study.

The longitudinal reinforcement over the center pier of composite bridges is subject to relatively high participation stresses depending on the deformation of the I-beams. The required area of this reinforcement may be estimated from the magnitude of the maximum negative moment obtained by assuming complete interaction between the reinforcement and the beam. In such a case the strain distribution and therefore also the stress distribution depends only on the relative areas and positions of the reinforcement and the beam. For a known cross-section of the beam and a known relative position of the reinforcement and the beam, the stress distribution depends only on the area of the reinforcement. If this area

is very small, the neutral axis of the composite section will practically coincide with the centroidal axis of the beam and the corresponding stress in the reinforcement will be the maximum attainable. If the area of the reinforcement is increased, the neutral axis of the composite section rises and the stress in the reinforcement decreases. Thus the required area of the longitudinal reinforcement over the center pier may be determined as follows: First, the stress distribution in the composite section should be determined for the minimum required area of the reinforcement. If the resulting stress in the reinforcement is lower than the allowable stress, the minimum required area should be used. If, however, the resulting stress is greater than the allowable, the area of the reinforcement should be increased and the stress distribution recomputed. This procedure should be repeated until an area is found which gives a stress in the reinforcement equal to the allowable value.

Composite Action. At midspan the effects of the presence of shear connectros on the behavior of the structures tested were the same as in the simple-span bridges. Thus, at midspan, composite action has a definite strengthening effect on the bridge, and it may be taken into account in the same manner as in simple-span bridges.

Over the center pier, the question arises as to whether the presence of shear connectors in the region of negative moment has detrimental or beneficial effects on the behavior of continuous I-beam bridges. The tests indicated that the presence of shear connectors will result in a slight decrease of the governing stresses in the I-beams and a slight increase in the stresses in the longitudinal reinforcement over the pier. It also seems to cause a larger number of transverse shrinkage cracks

which may be followed by some increase of the strains in the transverse reinforcement. Thus the tests seem to indicate that no particular advantage or disadvantage can be gained by providing the shear connectors in the region of negative moment.

APPENDIX: THEORETICAL ANALYSIS OF TWO 2-SPAN CONTINUOUS I-BEAM BRIDGES

30. Introduction

Theoretical moments and deflections for a two-span, continuous, right I-beam bridge may be computed by the method of analysis described in Bulletin 304.* Two bridges, each with two equal spans, were analyzed by this method. The relative proportions of both bridges were $b/a = 0.2$ (Fig. 39) and the relative stiffnesses were $H = 2$ for one bridge and $H = 4$ for the other. The relative proportions b/a and the relative stiffnesses H were chosenso as to permit the use of the moment and deflection coefficients tabulated in Bulletin 336.x

The results of these analyses were used in planning the tests reported in the preceding sections. However, since the dimensions of the test models were such that they did not permit the use of the moment and deflection coefficients tabulated in Bulletin 336, an exact analyses applicable to the test structures could not be made conveniently, and an approximate method of computing the moments and deflections, described in Section 6 of this Bulletin, was used instead. To investigated the accuracy of this approximate method, the results of the analyses presented in this appendix are compared with the results obtained from the approximate method.

The relative dimensions of the bridges and the notations used

* N. M. Newmark, "A Distribution Procedure for the Analysis of Slabs Continuous Over Flexible Beams," Univ. of Ill. Eng. Exp. Sta. Bul. 304, 1938.

x N. M. Newmark and C. P. Siess, "Moments in I-beam Bridges," Univ. of Ill. Eng. Exp. Sta. Bul. 336, 1942.

in this appendix are shown in Fig. 39. For simplicity, in the following sections the method based on Bulletin 304 is called "the exact method of analysis" and the approximate method outlined in Section 6 is called "the simplified method of analysis."

31. Exact Method of Analysis

The method of analysis described in Bulletin 304 is a numerical procedure for computing moments and deflections of a slab, simply supported in one direction and continuous over a number of beams in the other direction. Since it is an elastic analysis, it may be used for computing the deformations of a continuous bridge by application of the principle of superposition in the following manner: The bridge is considered to be simply supported at its end supports and the load to consist of the applied loads and of the reactions of the interior supports. The moments at the points in question are computed separately for each load and reaction, and the sum of these moments is the moment for the continuous bridge.

The detailed procedure for the two-span continuous bridges was as follows: The bridge was considered as a simple-span bridge with span length 2a. A unit concentrated load was applied successively at sections 4/12, 6/12 and 8/12 at locations A, AB, B, BC and C (Fig. 39), a total of 15 positions. For each load position, deflections of all five I-beams (A, B, C, D and E) were computed for the section designated in Fig. 39 as the center pier. Next, forces were applied to all five beams at the center-pier section to eliminate the deflections at this location. This procedure required the solution of a system of simultaneous equations which resulted in forces equal to the reactions of the continuous bridge.

The next step was the computation of the transverse slab moments at midspan for loads at midspan. For this purpose simple-span moments were computed for a unit load applied at midspan on lines A, AB, B, BC, C, CD, D, DE and E, and for the corresponding five reactive forces at the location of the center pier. The sum of the moments due to the unit load and due to the five corresponding center pier reactions gave the moments for the continuous bridge.

The moments in beams A, B and C at midspan and over the center pier were computed next. The simple-span moments were computed for the unit load applied successively at sections 4/12, 6/12 and 8/12 at locations A, AB, B, BC, C, CD, D, DE and E, and for the corresponding five reactive forces at the location of the center pier. The sum of the moments due to the unit load and to the five corresponding center pier reactions gave the moment for the continuous bridge.

32. Results of Exact Analysis

The results of the exact analysis are given in Tables 22-24.

The influence coefficients for the transverse moment in the slab at midspan were computed only for loads at midspan and are given in Table 22. The moments per unit width of a section of the slab may be obtained by multiplying the influence coefficients by the magnitude of the load.

Transverse moments over the center pier were not computed because the moments in a slab supported by non-defleoting beams are practically independent of the ratio b/a and can be obtained directly from the tables of Bulletin 336 for $H=\infty$ for any value of b/a. The longitudinal moments were not computed because of their relative unimportance as compared to the transverse moments.

The influence coefficients for moments in the beams at midspan are listed in Table 23. The coefficients are given for three longitudinal locations of the load; namely at 4/12, 6/12 and 8/12 of the span length a from the left support. The moments may be obtained by multiplying the influence coefficient by the magnitude of the load and by the span length a. It should be noted that the maximum coefficients listed in this table, those for the loads at $\frac{6}{12}$ a (midspan), are not the maximum positive moments due to a moving load but only a close approximation. The maximum positive moments would be located closer to the end support of the bridge.

The influence coefficients for moments in the beams over the center pier are listed in Table 24. The coefficients are given for the same positions of the load as the coefficients for moments at midspan, and the moments may be computed in the same manner as those at midspan. The moment coefficients over the center pier for load at $\frac{8}{12}$ a are approximately equal to the maximum negative moment coefficients due to a concentrated load moving along the bridge.

33. Total Beam Moments

In Table 25, the sums of the influence coefficients for moments in the beams at midspan for loads at midspan (Columns 3 and 5) are compared with the corresponding moment coefficients computed for a continuous beam of constant cross-section (Column 2). Since the slab carries a part of the total moment, the ratios of the sum of the bridge beam moments to the continuous beam moment should be smaller than 1.0. This ratio should be larger for the bridge with stiffer beams, that is larger for $H = 4$ than for $H = 2$. The average ratio for the bridge with $H = 4$ is 0.933 and for bridge with $H = 2$ is 0.890.

The total moment may be computed from the sum of the beam moments on the assumption that the longitudinal moment is distributed between the beams and the slab in proportion of their stiffnesses. If the stiffness of the slab is assumed to be 4bEI and the stiffness of the beams 5 $E_b I_b$, then the total moment may be computed by multiplying the sum of the beam moments by the factor

$$1 + 0.8 \frac{b}{aH}$$

If this is done, the average ratios of the total bridge moments to the continuous beam moments are 0.971 and 0.962.

A comparison between the sums of the bridge beam moments and the continuous beam moments over the center pier is presented also in Table 25. The average ratios of the sum of the bridge beam moments to the continuous beam moments are 0.902 and 0.952 for bridges with H = 2 and 4, respectively. If correction is made for the longitudinal moments carried by the slab, the average ratios of the total bridge moments to the continuous beam moments are 0.975 and 0.991.

Even better agreement between the continuous beam moments and the total bridge moments may be obtained if the correction factor is taken as

$$1 + \frac{b}{aH}$$

If this factor is used, the ratios at midspan are 0.980 and 0.981 for bridges with H = 2 and 4, respectively, and the ratios over the center pier are 0.994 and 1.000.

It can be seen from the comparisons made above that the total moment carried by the continuous bridge at either midspan or over the center pier may be computed as the moment for a continuous beam of equal span length. This total moment consists of the moments carried by the slab and the beams. The stiffness of the slab is usually small when compared with the stiffness of the beams and the cracking reduces the stiffness of the slab even further. Thus for the purposes of design it may ordinarily be assumed that the total moment is carried by the beams. However, if the slab is comparatively stiff, this procedure would be very conservative; in such case the sum of the beam moments may be computed by correcting the total moments carried by the slab.

34. Distribution of Moments to Beams

In Tables 26 and 27 the distribution of moments to the five beams of the bridge at midspan for load at midspan is compared with the distribution over the center pier for loads at $\frac{8}{12}\,\underline{a}$ and for bridges with H = 2 and 4, respectively. The moments carried by the individual beams are expressed in percent of the sum of the beam moments at the section considered. It can be seen from these tables that the distribution is more non-uniform over the center pier than at midspan. For a single concentrated load on the bridge with H = 2, the moment in the beam carrying the largest portion of load is 19.2 percent larger over the support than at midspan. The corresponding figure for the bridge with H = 4 is 16.6 percent. However, if more than one concentrated load is applied at the same cross-section of the bridge, which is the case for usual truck loadings, the differences between the distribution of moments over the pier and at midspan would be smaller than indicated in Tables 26 and 27

for single loads. For instance, for four concentrated loads applied at AB, BC, C and D the difference is only 4.8 percent for the bridge with H = 2 and 4.9 percent for the bridge with H = 4 (Tables 26 and 27).

35. Comparison of Exact and Simplified Analysis

It is shown in Section 34 that the sum of the beam moments at any cross-section of the I-beam bridge may be computed as the moment of a continuous beam of equal span, corrected if desired for the longitudinal moment carried by the slab. The question remains as to how this total moment should be distributed to the individual beams.

Tables 26 and 27 include also the distribution of beam moments at midspan of the equivalent simple-span bridge. It can be seen that the distribution of moments at midspan of the equivalent simple-span bridge is practically identical with the distribution of moments at midspan of the continuous bridge. Thus the moments at midspan of a continuous bridge computed by the simplified method of analysis (Section 6) will differ very little from those computed by the exact method of analysis. However, the governing moments over the center pier of a continuous bridge computed by the simplified method of analysis will be slightly smaller than those computed by the exact method of analysis.

The transverse slab moments at midspan for load at midspan computed by the exact and simplified methods of analysis are compared in Table 28. There is practically no difference between the corresponding moment coefficients computed by the two methods.

Table 1

Design Details for Model Bridges

Bridge			N30	C30	X30
Span, ft			2 x 15	2 x 15	2 x 15
Spacing of Beams, ft			1.5	1.5	1.5
Size of Beams			9-in. 7.5-lb Junior Beams	7-in. 5.5-lb Junior Beams	7-in. 5.5-lb Junior Beams
Shear Connectors:		Type	None	Channel[x]	Channel[x]
		Width, in.	. . .	1.5	1.5
		Spacing, in.	. . .	6 1/4	6 1/4**
Nominal Depth of Slab, in.			1.75	1.75	1.75
Slab Reinforcement:			All bars 1/8-in. square		
Transverse	Bottom	Spacing, in.	1	1 1/4	1 1/4
		p*, percent	1.09	0.87	0.87
	Top	Spacing, in.	1 1/2	1 7/8	1 7/8
		p*, percent	0.72	0.58	0.58
Longitudinal	Bottom	Spacing, in.	2	2	2
		p*, percent	0.59	0.59	0.59
	Top Midspan	Spacing, in.	6	6	6
		p*, percent	0.20	0.20	0.20
	Top Over Pier	Spacing, in.	3	3	3
		p*, percent	0.40	0.40	0.40

* Ratio of the area of reinforcement to the product of the width of slab by the effective depth of the particular bars considered.

x 1 x 3/8 x 1/8-in. bar channels.

** Shear connectors omitted for a distance of 28 1/8-in. on each side of the center pier.

Table 2

Physical Properties of Steel in Beams

From tests of coupons cut from flanges. Cross-section of coupons was approximately 1/2 x 3/16 in.

Bridge	Size of Beam	Number of Tests	Yield Point, psi	Ultimate Strength, psi	Elongation in 2 in., percent
N30	9-in. 7.5-lb JB	10	45 200	69 300	33
C30	7-in. 5.5-lb JB	17	40 000	61 100	29
X30	7-in. 5.5-lb JB	10	42 900	65 000	32

Table 3

Physical Properties of 1/8-Inch Square Reinforcing Bars

Bridge	Number of Tests	Yield Point, psi	Ultimate Strength, psi	Elongation in 2 in., percent
N30	10	44 000	57 800	21
C30	12	41 800	57 600	28
X30	6	43 200	58 700	29

Table 4

Physical Properties of Mortar

Obtained from tests of 2 x 4-in. cylinders and 2 x 1 3/4-in. beams. All specimens were moist-cured under wet burlap for 28 days, painted with white enamel afterwards and stored in the laboratory until the time of test.

Bridge	Tests of Cylinders						Tests of Beams*		
	Age at Test, days	Compressive Strength No. of Tests	f'_c, psi	Initial Modulus of Elasticity No. of Tests	E_c, psi	n	Age at Test, days	Modulus of Rupture No. of Tests	Mc/I, psi
N30	29	10	1850	..	.....	....	92	1	603
	114	21	3330	12	3 310 000	9.1	96	1	793
	118	8	3400	..	.....	....	112	14	635
	160	11	3260	10	3 160 000	9.5	...	..	...
	188	16	3220	11	2 990 000	10.0	...	..	...
C30	29	8	2910	..	.....	....	147	13	693
	145	18	3420	11	2 750 000	10.9	...	..	...
	236	40	3050	23	2 560 000	11.7	...	..	...
X30	28	9	2640	..	.....	....	90	10	904
	79	21	4110	8	4 020 000	7.5	...	..	...
	127	20	4340	9	3 770 000	8.1	...	..	...

* Beams loaded at third points on 15-in. span.

Table 5

Residual Stresses in Flanges of I-Beams

All values listed are tensile stresses in psi.

Bridge	Yield Point from Coupon Tests*	Residual Stresses					Apparent Yield Point	
		Due to Rolling[x]	Due to Welding Shear Connectors** In Span		Over Pier		Bottom Flange at Midspan	Top Flange over Pier
			Bottom Flange	Top Flange	Bottom Flange	Top Flange		
N30	45 200	19 000	0	0	0	0	26 200	26 200
C30	40 000	2 500	1500	3400	1500	3400	36 000	34 100
X30	42 900	2 500	4100	9500	0	0	36 300	40 400

* From Table 2.

x Obtained from strain measurements on sections cut from flanges.

** Obtained by calculations from measured deflections corrected as described on p. .

Table 6

Strains at First Yielding of I-Beams

All strains are tensile strains multiplied by 10^5.

Section	Bridge	Yield Point Strain of Coupons			Strain at First Yielding of I-Beams**
		As Measured*	Corrected for Dead Load[x]	Corrected for Dead Load and Residual Strains*	
In Span	N30	156	152	86	90
	C30	138	131	117	106
	X30	148	141	116	102
Over Pier	N30	156	148	82	84
	C30	138	126	106	151
	X30	148	136	127	167

* Computed from stresses in Table 5.

[x] Computed.

** Measured in tests to failure of bridges.

Table 7

Transverse Distribution of Beam Strains, Bridge N30

Values based on measured strains were computed from slopes of the load-strain curves. Theoretical values were computed from moment coefficients at midspan of an equivalent simple-span bridge located at midspan; the moment coefficients were obtained from the Univ. of Ill. Eng. Exp. Sta. Bul. 336.

Position of Load	Basis for Computing Strain Percentage		Strain in Percent of Total				
			Beam A	B	C	D	E
AB - BC	Strains Measured	W5	30	35	25	10	0
Section W5	at Section	0	31	35	22	12	0
	Theory		31	36	23	9	1
BC - CD	Strains Measured	W5	10	24	32	24	10
Section W5	at section	0	11	23	31	24	11
	Theory		10	24	33	24	10
B - C - CD - DE	Strains Measured	W3	7	22	28	27	16
Sections W3 and E3	at Section	0	8	21	27	27	17
	Theory		9	21	28	25	17
AB - BC - CD - DE	Strains Measured	W5	17	21	25	20	17
Section W5	at Section	0	17	21	23	22	17
	Theory		16	22	24	22	16

Table 8

Transverse Distribution of Beam Deflections

Bridge N30

Values based on measured deflections were computed from slopes of load-deflection curves; deflections were measured at Section W5 for loads at Section W5. Theoretical values were computed from deflection coefficients for midspan of an equivalent simple-span bridge loaded at midspan; the deflection coefficients were taken from the Univ. of Ill. Eng. Exp. Sta. Bul. 336.

Position of Loads	Basis for Computing Deflection Percentage	Beam Deflection in Percent of Total				
		Beam A	B	C	D	E
AB - BC	Test Data	32.6	32.6	23.8	11.0	0
	Theory	32.6	32.2	22.8	10.9	1.5
BC - CD	Test Data	12.1	22.8	29.9	24.1	11.7
	Theory	12.5	23.2	28.6	23.2	12.5
B - C - CD - DE	Test Data	11.2	19.7	25.0	24.4	19.7
	Theory	11.2	19.7	25.2	24.4	19.5
AB - BC - CD - DE	Test Data	17.2	21.2	22.5	22.1	17.0
	Theory	17.1	21.5	22.8	21.5	17.1

Table 9

Comparison of Distribution of Beam Strains
and Deflections, Bridge N30

All values computed from coefficients (Univ. of Ill. Eng. Exp. Sta. Bul. 336) for midspan of an equivalent simple span bridge at midspan.

Position of Loads	Beam	Maximum Strain, Percent of Total	Maximum Deflection, Percent of Total	Difference Percent
AB - BC	B	36.0	32.6	-10.5
BC - CD	C	33.2	28.6	-13.8
B - C - CD - DE	C	27.5	25.2	-8.3
AB - BC - CD - DE	C	23.6	22.8	-3.4

Table 10

Comparison of Transverse Slab Strains
for Various Types of Loading, Bridge N30

Loads and strains were measured at Section W5. Measured values represent the slopes of load-strain curves for individual gages.

Load at	Strains in Percent of Strain in Panel DE			
	Computed		Measured	
	Inside Panel (CD)	Outside Panel (DE)	Inside Panel (CD)	Outside Panel (DE)
CD - DE	100	101	82	97
BC - CD	111	--	84	--
AB - BC - CD - DE	94	97	69	97
B - C - CD - DE	117	100	94	100

Table 11

Summary of Data for Tests to Failure

Bridge N30

Location on Bridge	Load per Panel in Pounds at				Number of Live Loads at		
	First Yielding of Reinf.	First Yielding of Beams*	Punching of Slab	Buckling of Beams	First Yielding of Reinf.	First Yielding of Beams	Punching of Slab
In Span	5000	6750	9470	8490	3.8	4.8	7.3
Over Center Pier	5500	7050	8330	....	4.2	4.5	6.4

* Loads corrected for residual stress.

Table 12

Punching Loads, Bridge N30

Bridge was subjected to a pair of equal loads applied at locations shown in Fig. 18. Loads were applied to bridge at various locations in the order given in the table.

Loads at	Punching Load, lb per panel	Loads at	Punching Load, lb per panel
1-1	7 500[x]	8-8	10 700*
2-2	9 000[x]	9-9	9 850*
3-3	8 500[x]	10-10	9 700*
4-4	10 000*	11-11	9 000*
5-5	8 500*	12-12	8 000
6-6	9 500*	13-13	7 400
7-7	8 500*		

* Average punching load in span: 9470 lb.

x Average punching load over center pier: 8330 lb.

Table 13

Transverse Distribution of Beam Strains,
Bridges C30 and X30

Values based on measured strains were computed from slopes of load-strain curves. Theoretical values were computed from moment coefficients at midspan of an equivalent simple-span bridge loaded at midspan; the moment coefficients were obtained from the Univ. of Ill. Exp. Sta. Bul. 336.

Position of Load	Basis for Computing Strain Percentage		Strain in Percent of Total Beam A	B	C	D	E
AB - BC Section W5	Strains Measured at Section W5	C30	31	36	24	9	0
		X30	27	37	26	10	0
	Theory		31	37	24	8	0
BC - CD Section W5	Strains Measured at Section W5	C30	9	24	30	30	7
		X30	9	26	34	22	9*
	Theory		9	24	34	24	9
AB - BC - C - D Section E5	Strains Measured at Section E5	C30	16	26	27	22	9
		X30	18	25	26	22	9
	Theory		17	26	28	21	8
AB - BC - CD - DE Section W5	Strains Measured at Section W5	X30	14	23	23	24	16
	Theory		15	23	24	23	15
B - C - CD - DE Sections W3 and E3	Strains Measured at Section 0	C30	11	19	25	24	21
		X30	9	20	25	25	20
	Theory		8	21	28	26	17

* Strains measurements on beam E were defective; strains measured on beam A were substituted.

Table 14

Comparison of Transverse Slab Strains
For Bridges N30, C30 and X30

All three bridges were loaded with one pair of loads, each load equal to 3000 lb, one located in the outside, the other in the adjacent inside panel. Strain gages in panels were located directly under the loads; strain gages over the beams were located between the two loads. All values are averages for symmetrical loading conditions.

Longitudinal Location of Loads and Strains	Transverse Location of Strains	Strains in $\epsilon \times 10^6$ for Bridge N30		C30	X30
		Measured	Corrected*	Measured	Measured
Section W5	Outside Panel	92	115	74	85
	Inside Panel	90	112	69	62
	Over Beam	12	15	50[x]	36
Section 0	Outside Panel	56	70	81	73
	Inside Panel	40	50	59	50
	Over Beam	80	100	97	136

* Measured strains multiplied by the factor 1.25 to account for 25 percent more transverse reinforcement.

[x] Probably too high a value.

Table 15

Comparison of Transverse Slab Strains for Various Types of Loading, Bridges N30, C30 and X30

All bridges were loaded and strains measured at Section W5. Strains represent the slopes of load-strain curves for individual gages.

Load P at	Strains in Percent of Largest Strain for Bridge					
	N30		C30		X30	
	Inside Panel	Outside Panel	Inside Panel	Outside Panel	Inside Panel	Outside Panel
CD - DE	82	97	104*	80x	79	92
BC - CD	84	--	85	--	85	--
AB - BC - CD - DE	69	97	63	100	55	99
B - C - CD - DE	94	100	93	100	81	100

* Probably a high value.

x Probably a low value.

Table 16

Summary of Data for Tests to Failure

Bridges C30 and X30

Bridge	Location on Bridge	Load per Panel in Pounds at			Equivalent Live Load at		
		First Yielding of Reinf.	First Yielding of Beams*	Punching of Slab	First Yielding of Reinf.	First Yielding of Beams	Punching of Slab
C30	In Span	5000	4940	11 420	3.8	3.2	8.8
	Over Center Pier	3000	6250	5 250	2.3	3.9	4.0
X30	In Span	5000	4640	12 100	3.8	3.0	9.3
	Over Center Pier	3000	4940	6 550	2.3	2.9	5.0

* Loads corrected for residual stress and reduced to a coupon tensile yield strain of 138×10^{-5}.

Table 17

Comparison of Calculated and Measured
Applied Loads at First Yielding of I-Beams
in Model Bridges

All loads are in lb per panel

Bridge	Yielding at Midspan		Yielding over Center Pier	
	Calculated Load	Measured Load*	Calculated Load	Measured Load*
N30	6100	5980	6230	6230
C30	4990	4940	6500	6250
X30	4850	4640	5580	5610[x]

* Corrected for residual stresses and reduced to a coupon tensile yield strain of 138×10^{-5}.

[x] First yielding of beam C.

Table 18

Punching Loads, Bridge C30

Bridge subjected to a pair of equal loads applied at locations shown in Fig. 37. Loads were applied to bridge at various locations in the order given in the table.

Loads at	Punching Load, lb per panel	Loads at	Punching Load, lb per panel
1-1**	10 400	7-7	11 300*
2-2	10 950*	8-8	12 000
3-3	12 300*	9-9	11 200
4-4	11 500*	10-10	11 300
5-5	12 300*	11-11	6 000x
6-6	10 150*	12-12	4 500x

* Average punching loads in span: 11,420 lb.

x Average punching load over center pier: 5250 lb.

** Two pairs of loads, one load in each panel.

Table 19

Punching Loads, Bridge X30

Bridge subjected to a pair of equal loads applied at locations shown in Fig. 38. Loads were applied to bridge at various locations in the order given in the table.

Loads at	Punching Load, lb per panel	Loads at	Punching Load, lb per panel
1-1	12 000*	8-8	8 300**
2-2	12 700*	9-9	8 800**
3-3	11 600*	10-10	9 900xx
4-4	11 700	11-11	9 900xx
5-5	11 500	12-12	11 200xx
6-6	7 000x	13-13***	10 400
7-7	6 100x		

* Average punching load in span: 12,100 lb.

x Average punching load over center pier: 6550 lb.

** Average punching load 12 in. from center pier: 8550 lb.

xx Average punching load 18 in. from center pier: 10,330 lb.

*** Two pairs of loads, one load in each panel.

Table 20

Comparison of Average Punching Loads
For Bridges N30, C30 and X30

All values are averages of several tests with one pair of equal loads P applied at midpanels of two adjacent panels.

Bridge	In Span	Average Punching Load P in lb 18 in. from Pier	12 in. from Pier	Over Pier
N30	9 470	.....	....	8330
X30	12 100	10 330	8550	6550
C30	11 420	.....	....	5250

Table 21

Comparison of Maximum Capacities of
Bridges N30, C30 and X30

All bridges loaded with four loads P, one in each panel, at the maximum positive moment section (W5 or E5).

Bridge	Size of I-Beams	Maximum Load P in lb Computed*	Measured	Mode of Failure
N30	9-in. 7.5-lb JB	12 300	8 490	Buckling of beams
X30	7-in. 5.5-lb JB	11 160	10 400	Punching of slab
C30	7-in. 5.5-lb JB	10 500	10 400	Punching of slab

* Flexural capacity computed on principles of limit design.

Table 22

Influence Coefficients for Transverse Moment of Slab at Midspan of Bridge

Relative Proportions of Bridge b/a = 0.2

Numerical values of transverse moment per unit width in slab on various longitudinal lines, the moment being due to a unit concentrated load applied at midspan along various longitudinal lines A, AB, B, etc., as shown in Fig. 39. The quantity H is defined in Section 5, the quantities b and a are shown in Fig. 39. Poisson's ratio is zero. The values $\overline{M}_{ot}$ are given in Table 96, Univ. of Ill. Eng. Exp. Sta. Bulletin 336.

Moment on Line	Transverse Location of Load								
	A	AB	B	BC	C	CD	D	DE	E
				Relative Stiffness H = 2					
		M_{ot}							
AB	-0.029	-0.008	0.038	0.002	-0.007	-0.009	-0.008	-0.007	-0.004
B	-0.058	-0.059	0.111	-0.038	-0.017	-0.016	-0.020	-0.020	-0.008
				M_{ot}					
BC	-0.038	-0.018	0.030	+0.003	0.035	-0.007	-0.015	-0.026	-0.031
C	-0.028	-0.029	-0.023	-0.043	0.135	-0.043	-0.023	-0.029	-0.028
				Relative Stiffness H = 4					
		M_{ot}							
AB	-0.023	-0.009	0.033	-0.003	-0.008	-0.008	-0.005	-0.006	-0.001
B	-0.045	-0.069	0.086	-0.054	-0.020	-0.015	-0.013	-0.008	-0.002
				M_{ot}					
BC	-0.028	-0.017	0.023	-0.008	0.025	-0.013	-0.015	-0.013	-0.009
C	-0.016	-0.018	-0.024	-0.058	0.086	-0.058	-0.024	-0.018	-0.016

Table 23

Influence Coefficient for Moment in Beams at Midspan of Bridge

Relative Proportions of Bridge b/a = 0.2

Numerical values of moment in beams divided by span of bridge, the moment being due to a unit concentrated load applied along various longitudinal lines AB, B, BC, etc., as shown in Fig. 39. The longitudinal position of the load is indicated by the distance from the left end of the bridge, shown as a portion of the span a. The quantity H is defined in Section 5, the quantities b and a are shown in Fig. 39. Poisson's ratio is zero.

Moment in Beam	Longitudinal Position of Load	Transverse Location of Load								
		A	AB	B	BC	C	CD	D	DE	E
		Relative Stiffness H = 2								
A	4/12	0.085	0.058	0.036	0.018	0.008	0.001	-0.001	-0.003	-0.003
	6/12	0.150	0.082	0.041	0.019	0.004	0.001	-0.001	-0.003	-0.003
	8/12	0.080	0.056	0.032	0.017	0.006	0.002	0.000	-0.002	-0.003
B	4/12	0.036	0.043	0.044	0.041	0.032	0.020	0.010	0.004	0.000
	6/12	0.041	0.070	0.099	0.067	0.036	0.018	0.012	0.004	-0.001
	8/12	0.032	0.040	0.043	0.039	0.028	0.018	0.010	0.004	0.000
C	4/12	0.007	0.020	0.032	0.040	0.042	0.040	0.032	0.020	0.007
	6/12	0.008	0.020	0.036	0.067	0.097	0.067	0.036	0.020	0.008
	8/12	0.006	0.018	0.028	0.037	0.040	0.037	0.028	0.018	0.006
		Relative Stiffness H = 4								
A	4/12	0.098	0.062	0.032	0.012	0.002	-0.002	-0.003	-0.002	-0.001
	6/12	0.164	0.086	0.036	0.012	0.001	-0.004	-0.003	-0.003	-0.002
	8/12	0.091	0.057	0.028	0.010	0.002	-0.002	-0.003	-0.003	-0.001
B	4/12	0.031	0.049	0.056	0.049	0.032	0.018	0.005	0.000	-0.002
	6/12	0.036	0.079	0.118	0.078	0.038	0.018	0.006	0.001	-0.003
	8/12	0.028	0.046	0.052	0.047	0.031	0.015	0.006	-0.001	-0.003
C	4/12	0.002	0.017	0.032	0.050	0.056	0.050	0.032	0.017	0.002
	6/12	0.001	0.017	0.038	0.078	0.116	0.078	0.038	0.017	0.001
	8/12	0.002	0.015	0.030	0.046	0.053	0.046	0.030	0.015	0.002

Table 24

Influence Coefficients for Moment in Beams Over Center Pier of Bridge

Relative Proportions of Bridge b/a = 0.2
See Subheading of Table 23

Moment in Beam	Longitudinal Position of Load	Transverse Location of Load								
		A	AB	B	BC	C	CD	D	DE	E
		Relative Stiffness H = 2								
A	4/12	-0.053	-0.035	-0.017	-0.006	-0.001	0.002	0.001	0.001	0.000
	6/12	-0.071	-0.043	-0.020	-0.007	-0.001	0.003	0.002	0.001	0.001
	8/12	-0.075	-0.041	-0.015	-0.002	0.001	0.002	0.001	0.001	0.002
B	4/12	-0.017	-0.026	-0.030	-0.026	-0.020	-0.011	-0.003	-0.001	0.001
	6/12	-0.020	-0.035	-0.043	-0.035	-0.022	-0.010	-0.004	-0.001	0.001
	8/12	-0.015	-0.040	-0.051	-0.039	-0.018	-0.006	-0.002	0.000	0.001
C	4/12	-0.001	-0.009	-0.019	-0.026	-0.028	-0.026	-0.019	-0.009	-0.001
	6/12	-0.001	-0.010	-0.021	-0.035	-0.041	-0.035	-0.021	-0.010	-0.001
	8/12	0.001	-0.005	-0.018	-0.037	-0.047	-0.037	-0.018	-0.005	0.001
		Relative Stiffness H = 4								
A	4/12	-0.060	-0.036	-0.015	-0.004	0.002	0.004	0.000	0.000	0.000
	6/12	-0.078	-0.047	-0.017	-0.003	0.002	0.002	0.003	0.000	0.000
	8/12	-0.079	-0.042	-0.013	0.000	0.003	0.002	0.002	0.001	-0.001
B	4/12	-0.016	-0.029	-0.036	-0.032	-0.019	-0.009	-0.003	0.001	0.002
	6/12	-0.017	-0.042	-0.052	-0.043	-0.023	-0.008	0.000	0.002	0.002
	8/12	-0.013	-0.045	-0.060	-0.045	-0.018	-0.004	0.000	0.001	0.001
C	4/12	0.003	-0.008	-0.019	-0.030	-0.035	-0.030	-0.019	-0.008	0.003
	6/12	0.002	-0.008	-0.023	-0.040	-0.050	-0.040	-0.023	-0.008	0.002
	8/12	0.003	-0.004	-0.018	-0.043	-0.057	-0.043	-0.018	-0.004	0.003

Table 25

Sum of Influence Coefficients for Moments in Beams

Relative Proportions of Bridge $b/a = 0.2$

Transverse Location of Load	Continuous Beam Analysis	Bridge Analysis H = 2	Ratio (3)/(2)	Bridge Analysis H = 4	Ratio (5)/(2)
(1)	(2)	(3)	(4)	(5)	(6)
	Moments at Midspan for Load at Midspan				
A	0.203	0.195	0.960	0.196	0.965
AB	0.203	0.173	0.853	0.180	0.887
B	0.203	0.187	0.921	0.195	0.960
BC	0.203	0.172	0.847	0.182	0.897
C	0.203	0.177	0.871	0.194	0.956
			Av 0.890		Av 0.933
	Moments Over Center Pier for Load at $\frac{8}{12}a$				
A	-0.093	-0.086	0.926	-0.089	0.958
AB	-0.093	-0.085	0.915	-0.089	0.958
B	-0.093	-0.085	0.915	-0.089	0.958
BC	-0.093	-0.082	0.882	-0.090	0.969
C	-0.093	-0.081	0.871	-0.087	0.936
			Av 0.902		Av 0.956

Table 26

Distribution of Moments to Beams of Continuous Bridge

Relative Stiffness H = 2

Relative Proportion of Bridge b/a = 0.2

Transverse Location of Load	Method of Analysis	Location of Moment Section	Moment in Percent of Total in Beam				
			A	B	C	D	E
A	Exact	Midspan	76.9	21.0	4.1	-0.5	-1.5
	Exact	Pier	87.4	17.4	-1.2	-1.2	-2.4
	Simplified	Midspan	77.3	21.1	3.4	-0.9	-0.9
AB	Exact	Midspan	47.4	40.5	11.5	2.3	-1.7
	Exact	Pier	48.3	47.0	5.9	0	-1.2
	Simplified	Midspan	47.4	40.8	11.3	1.9	-1.4
B	Exact	Midspan	21.9	53.0	19.2	6.4	-0.5
	Exact	Pier	17.6	60.0	21.2	2.4	-1.2
	Simplified	Midspan	21.8	52.8	20.6	5.7	-0.9
BC	Exact	Midspan	11.0	39.0	39.0	10.4	0.6
	Exact	Pier	2.4	47.5	45.2	7.3	-2.4
	Simplified	Midspan	10.4	38.7	38.2	12.3	0.4
C	Exact	Midspan	2.3	20.3	54.8	20.3	2.3
	Exact	Pier	-1.2	22.2	58.0	22.2	-1.2
	Simplified	Midspan	3.5	20.6	51.8	20.6	3.5
AB-BC-C-D	Exact	Midspan	15.1	26.5	31.1	21.5	5.8
	Exact	Pier	12.0	29.8	32.6	22.4	3.2
	Simplified	Midspan	15.1	26.4	30.5	21.9	6.1

Table 27

Distribution of Moments to Beams of Continuous Bridge

Relative Stiffness H = 4

Relative Proportion of Bridge b/a = 0.2

Transverse Location of Load	Method of Analysis	Location of Moment Section	Moment in Percent of Total in Beam				
			A	B	C	D	E
A	Exact	Midspan	83.7	18.3	0.5	-1.5	-1.0
	Exact	Pier	88.8	14.6	-3.4	-1.1	1.1
	Simplified	Midspan	84.4	17.7	0.4	-1.7	-0.8
AB	Exact	Midspan	47.8	43.9	9.4	0.6	-1.7
	Exact	Pier	47.1	50.6	4.5	-1.1	-1.1
	Simplified	Midspan	47.6	44.8	9.0	0	-1.4
B	Exact	Midspan	18.4	60.5	19.5	3.1	-1.5
	Exact	Pier	14.6	67.4	20.2	0	-2.2
	Simplified	Midspan	18.5	59.7	20.2	3.3	-1.7
BC	Exact	Midspan	6.6	42.9	42.9	9.8	-2.2
	Exact	Pier	0	50.0	47.8	4.4	-2.2
	Simplified	Midspan	5.8	43.1	42.7	10.2	-1.8
C	Exact	Midspan	0.5	19.6	59.8	19.6	0.5
	Exact	Pier	-3.5	20.7	65.6	20.7	-3.5
	Simplified	Midspan	0	20.3	59.4	20.3	0
AB-BC-C-D	Exact	Midspan	13.4	27.4	32.9	22.6	3.7
	Exact	Pier	10.4	30.3	34.5	22.9	1.9
	Simplified	Midspan	12.9	27.9	32.8	22.6	3.8

Table 28

Comparison of Influence Coefficients for Transverse Moment in Slab at Midspan

Computed by Exact and Simplified Analysis

Relative Proportions of Bridge b/a = 0.2

Moment Line	Location of Load	Relative Stiffness H = 2		Relative Stiffness H = 4	
		Exact Method	Simplified Method	Exact Method	Simplified Method
AB	A	-0.029	-0.030	-0.023	-0.022
	AB	M_{ot}-0.008	M_{ot}-0.008	M_{ot}-0.009	M_{ot}-0.009
	B	0.038	0.039	0.033	0.033
B	AB	-0.059	-0.059	-0.069	-0.069
	B	0.111	0.114	0.086	0.090
	BC	-0.038	-0.036	-0.054	-0.052
BC	B	0.030	0.030	0.023	0.024
	BC	M_{ot}+0.003	M_{ot}+0.003	M_{ot}-0.008	M_{ot}-0.007
	C	0.035	0.036	0.025	0.027
C	BC	-0.043	-0.041	-0.058	-0.056
	C	0.135	0.117	0.086	0.090
	CD	-0.043	-0.041	-0.058	-0.056

Transverse Section

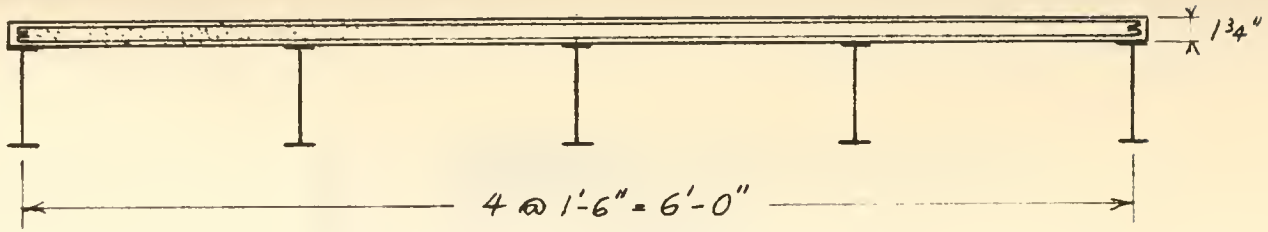

Longitudinal Sections

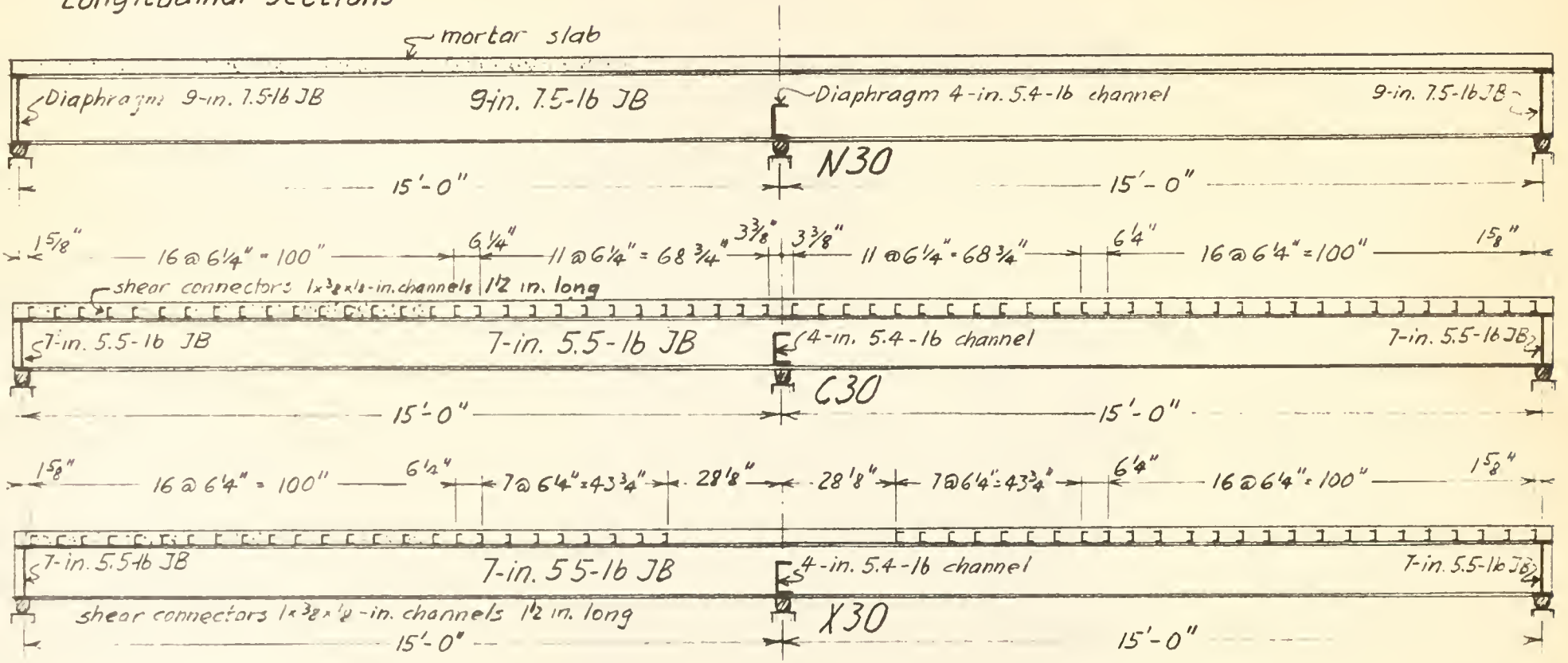

FIG.1 SECTIONS OF MODEL BRIDGES

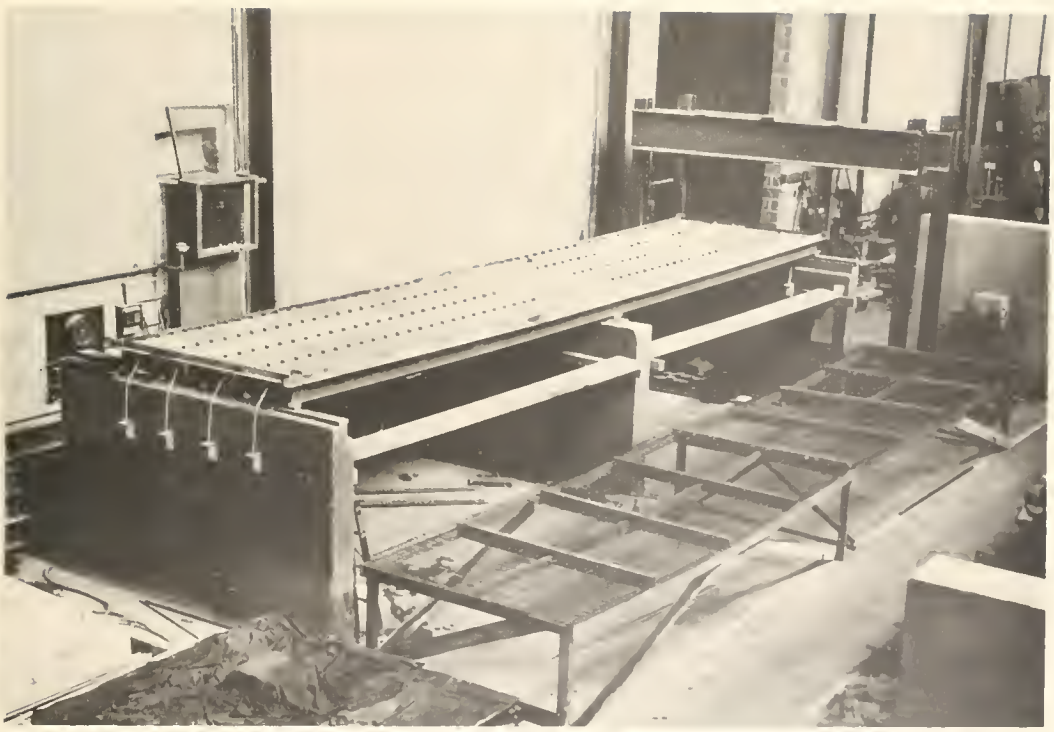

FIG.2 FORMS AND REINFORCEMENT FOR BRIDGE X30

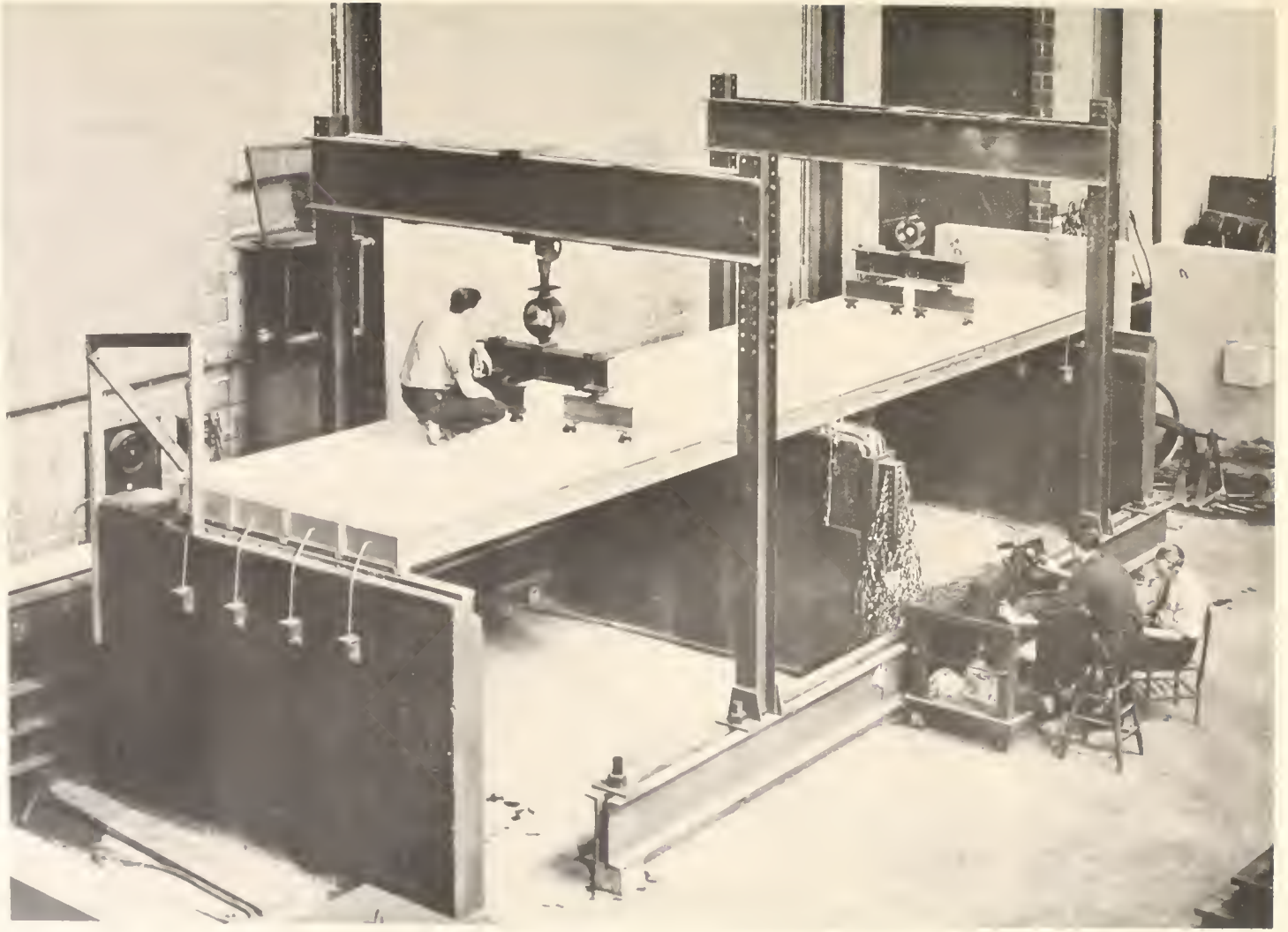

FIG.3 BRIDGE C30 DURING TESTING

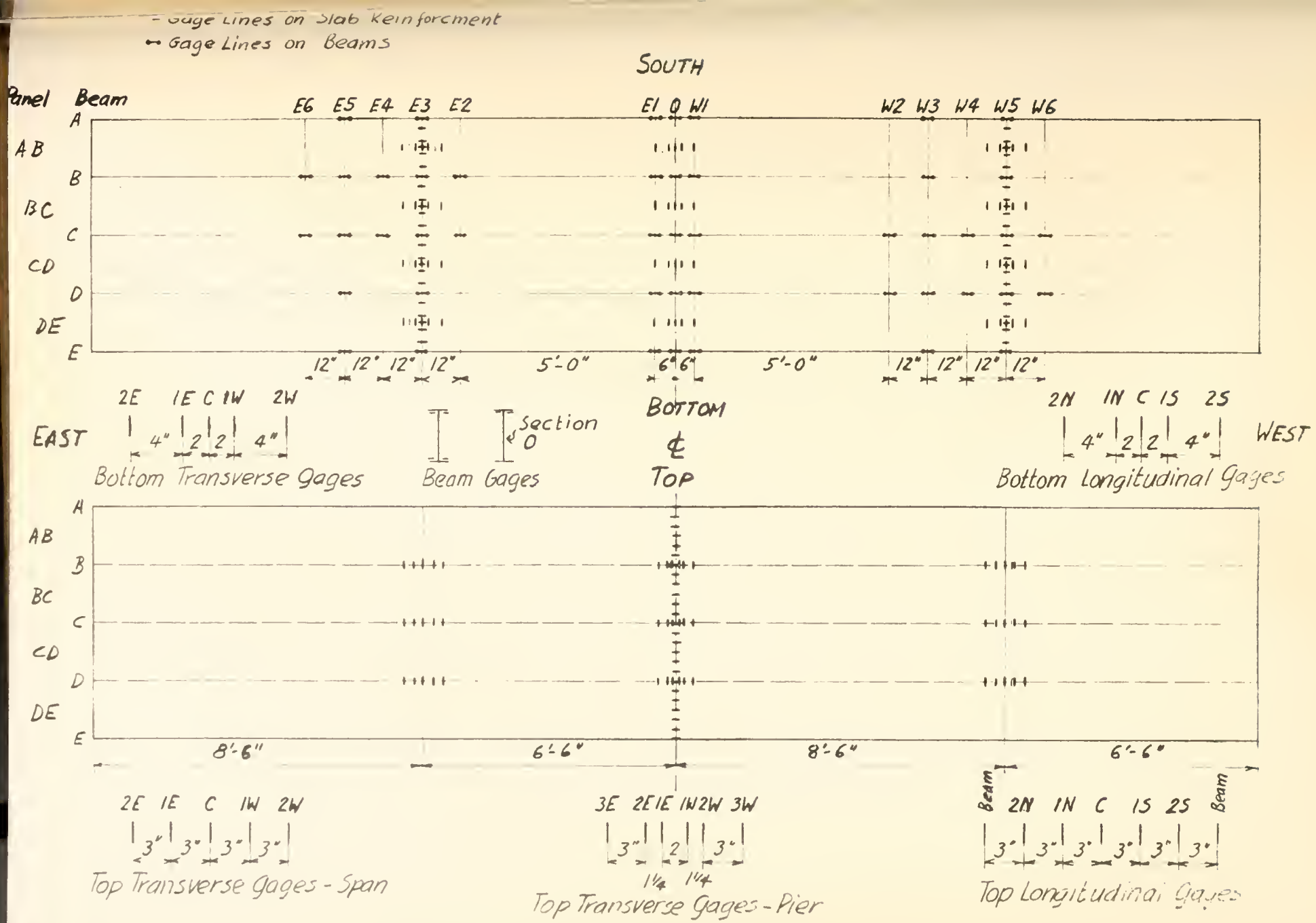

FIG. 4 LOCATION OF STRAIN GAGE LINES, BRIDGE N30

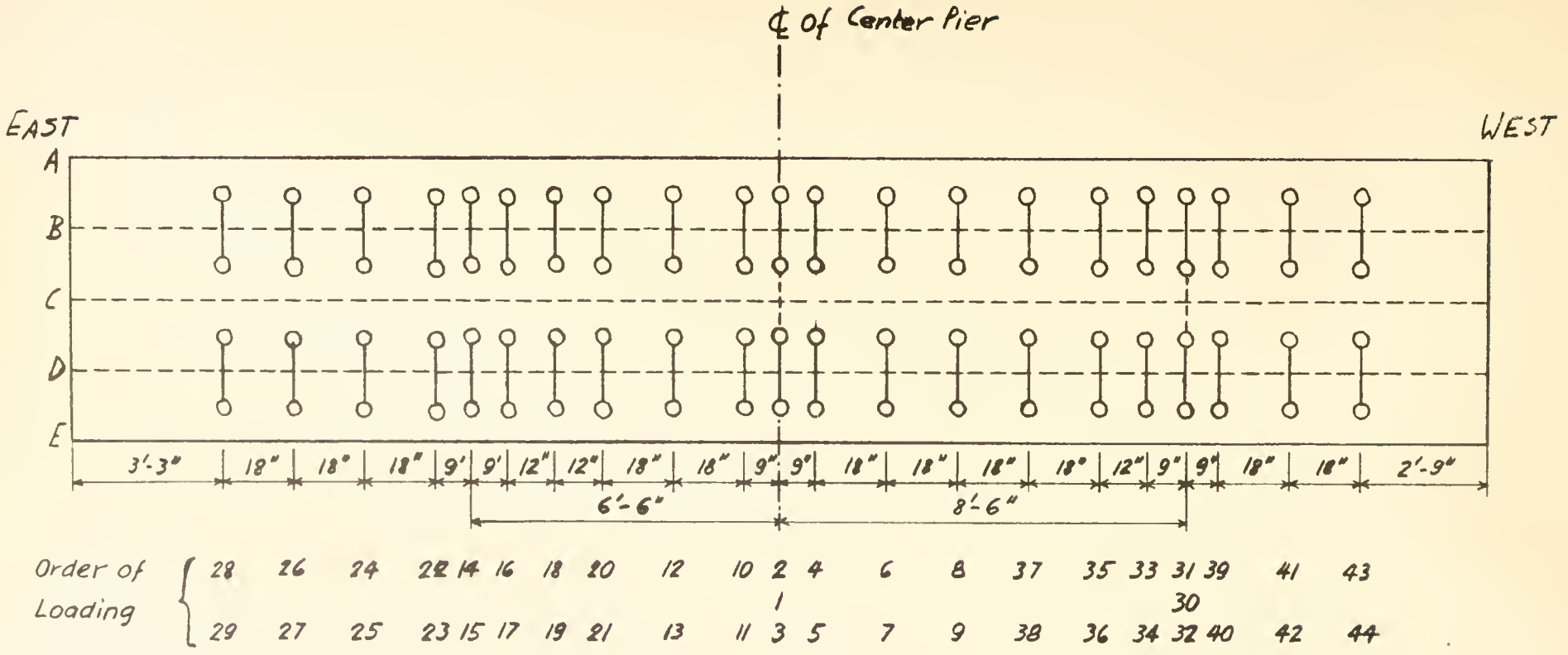

FIG.5 LOCATION OF LOADS AND ORDER OF LOADING IN CRACKING TEST, BRIDGE N30

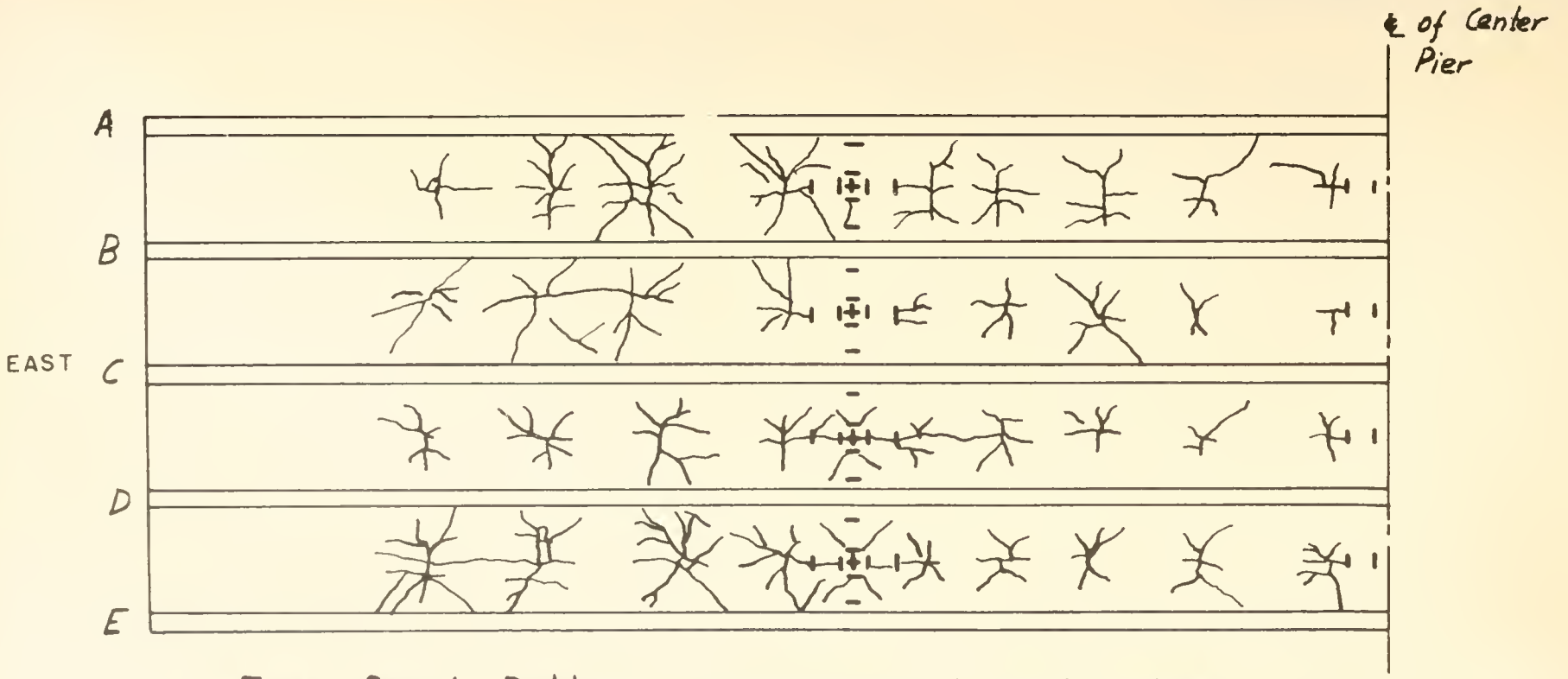

FIG.6 Crack Pattern on Bottom of Slab after Cracking Test, Bridge N30

Note: Symbols marked ✓ are described in text as solid circles

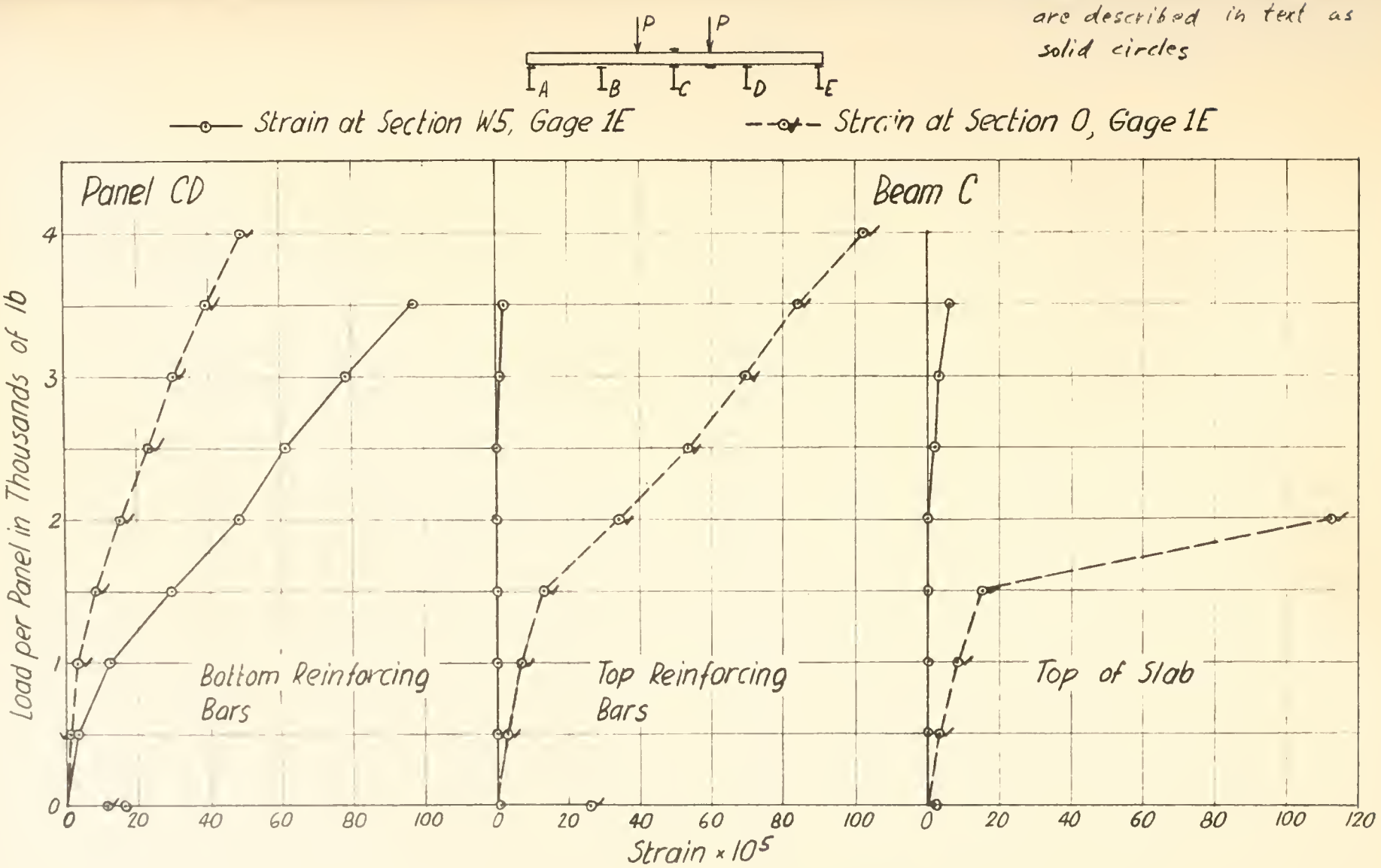

FIG. 7 TRANSVERSE STRAINS PRODUCING FIRST CRACKING OF SLAB, BRIDGE N 30

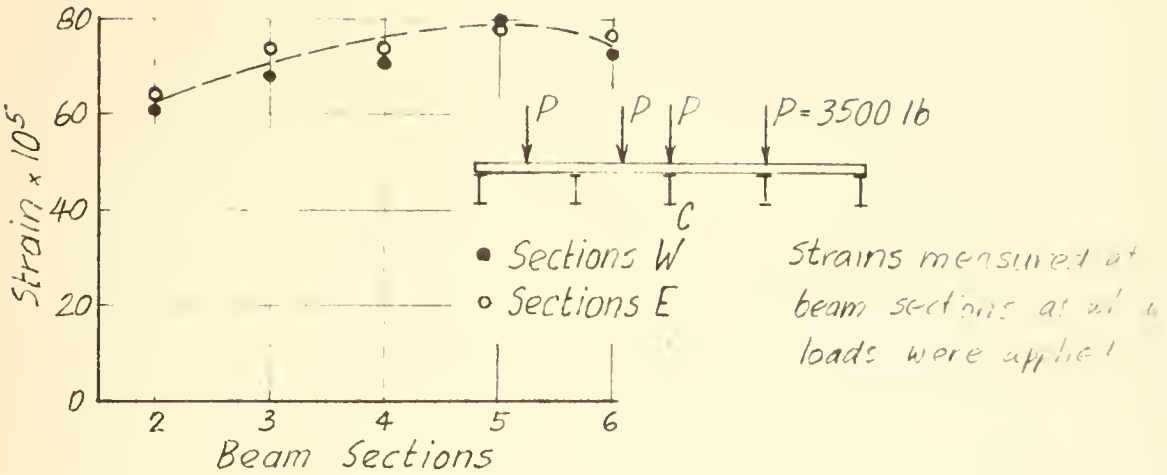

FIG. 8 CURVE OF MAXIMUM BOTTOM FLANGE STRAINS IN SPAN, BRIDGE N30, BEAM C

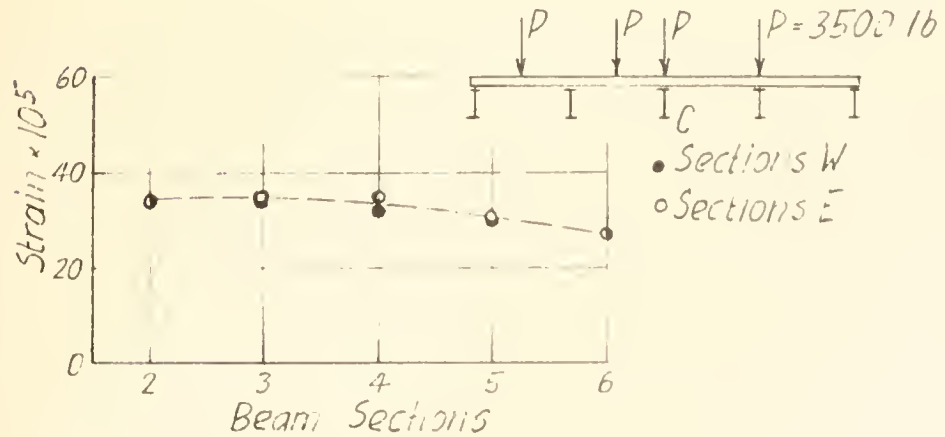

FIG. 9 INFLUENCE LINE FOR TOP FLANGE STRAINS OVER CENTER PIER, BRIDGE N30, BEAM C

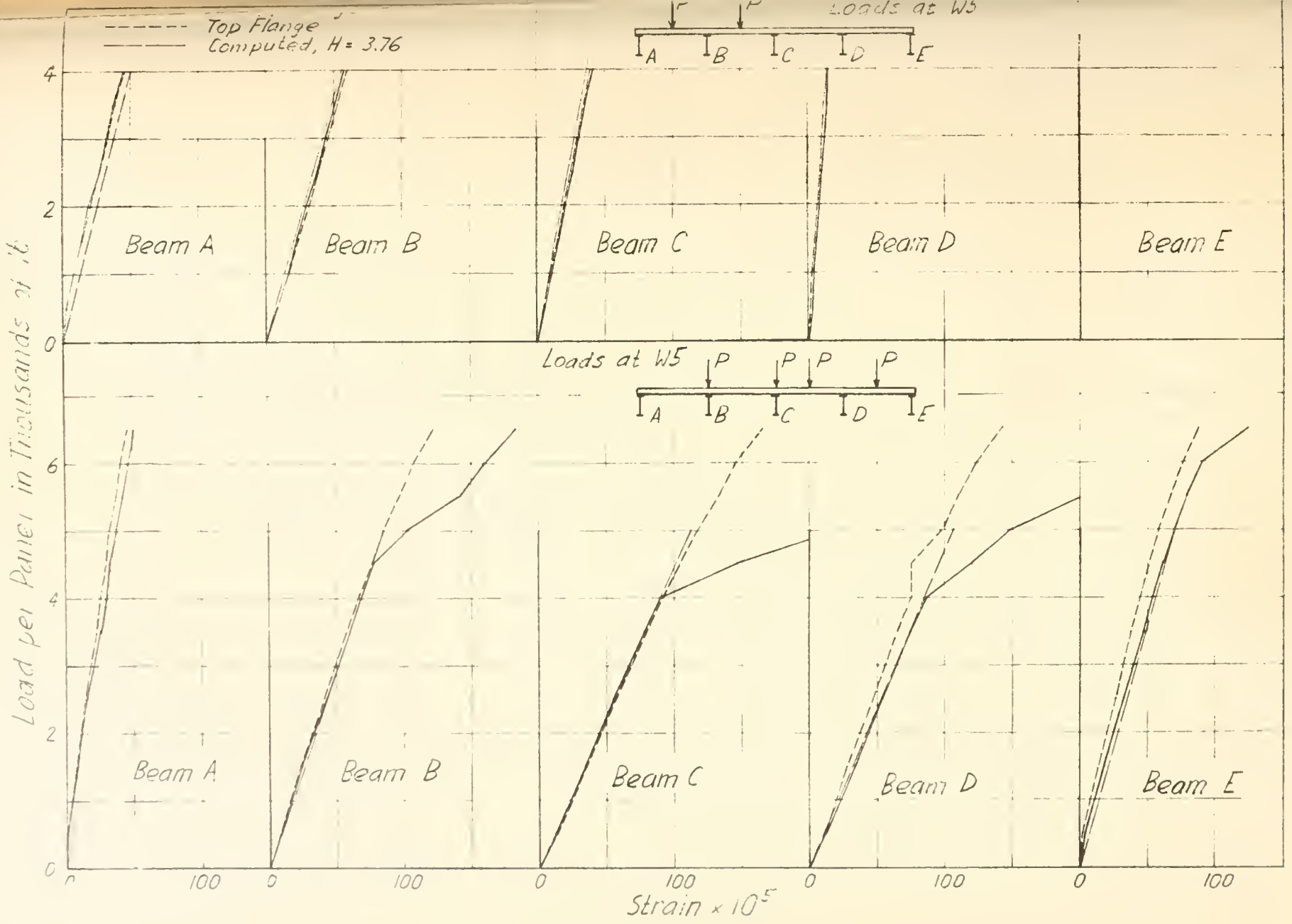

FIG. 10 BEAM STRAINS AT MAXIMUM POSITIVE MOMENT SECTION, BRIDGE N30

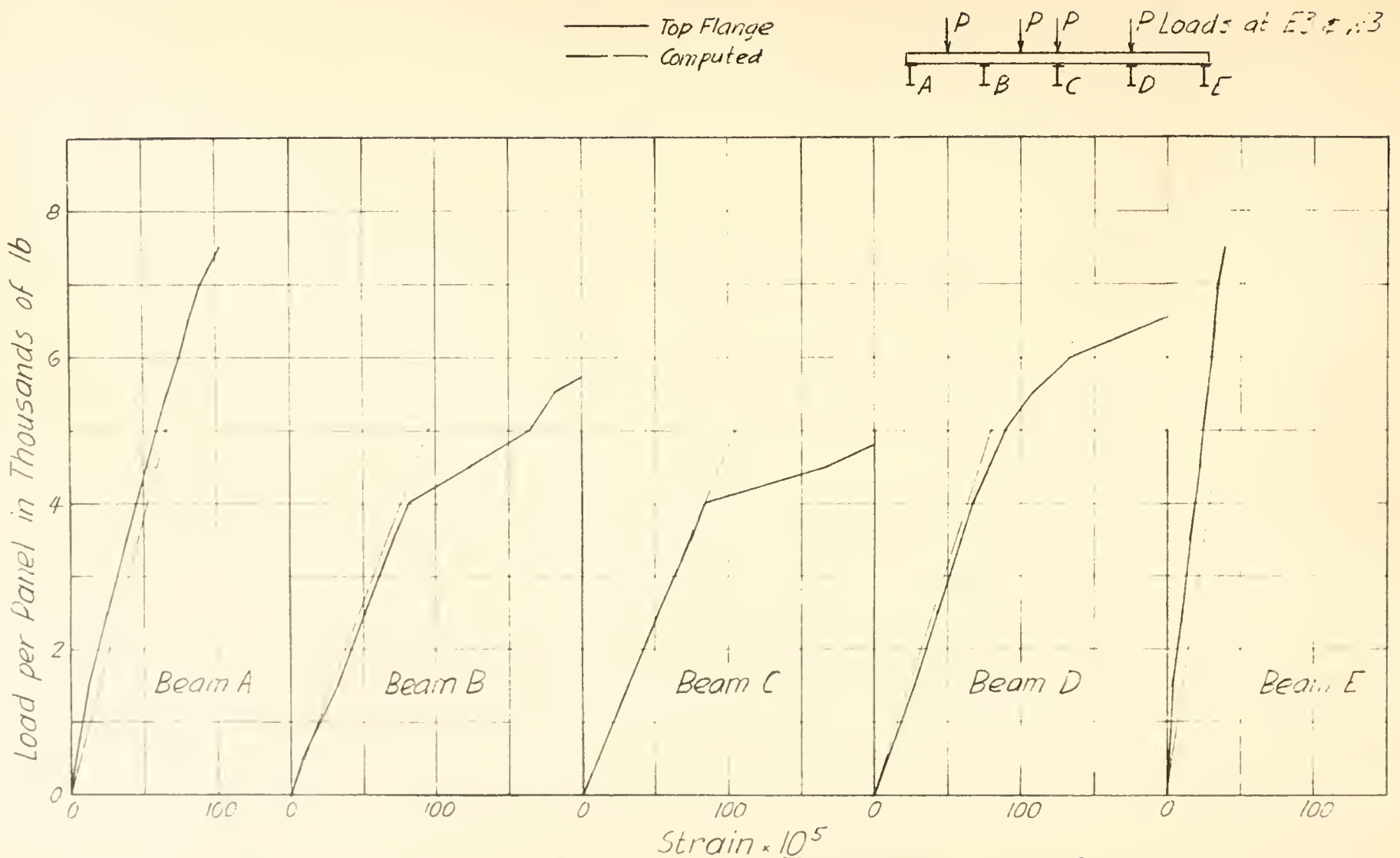

FIG. 11 BEAM STRAINS OVER CENTER PIER, BRIDGE N30

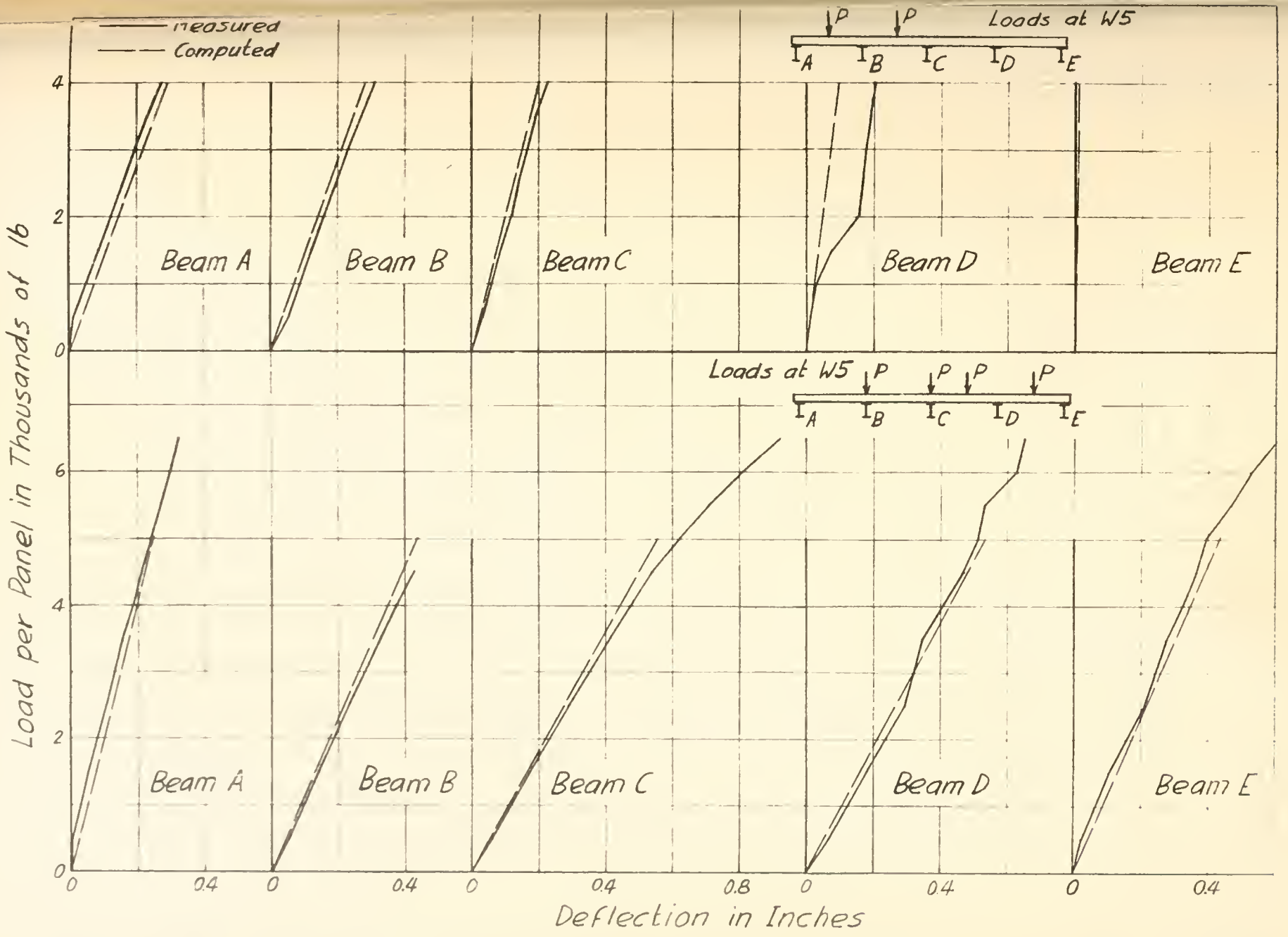

FIG.12 BEAM DEFLECTIONS AT MAXIMUM POSITIVE MOMENT SECTION, BRIDGE No. 5

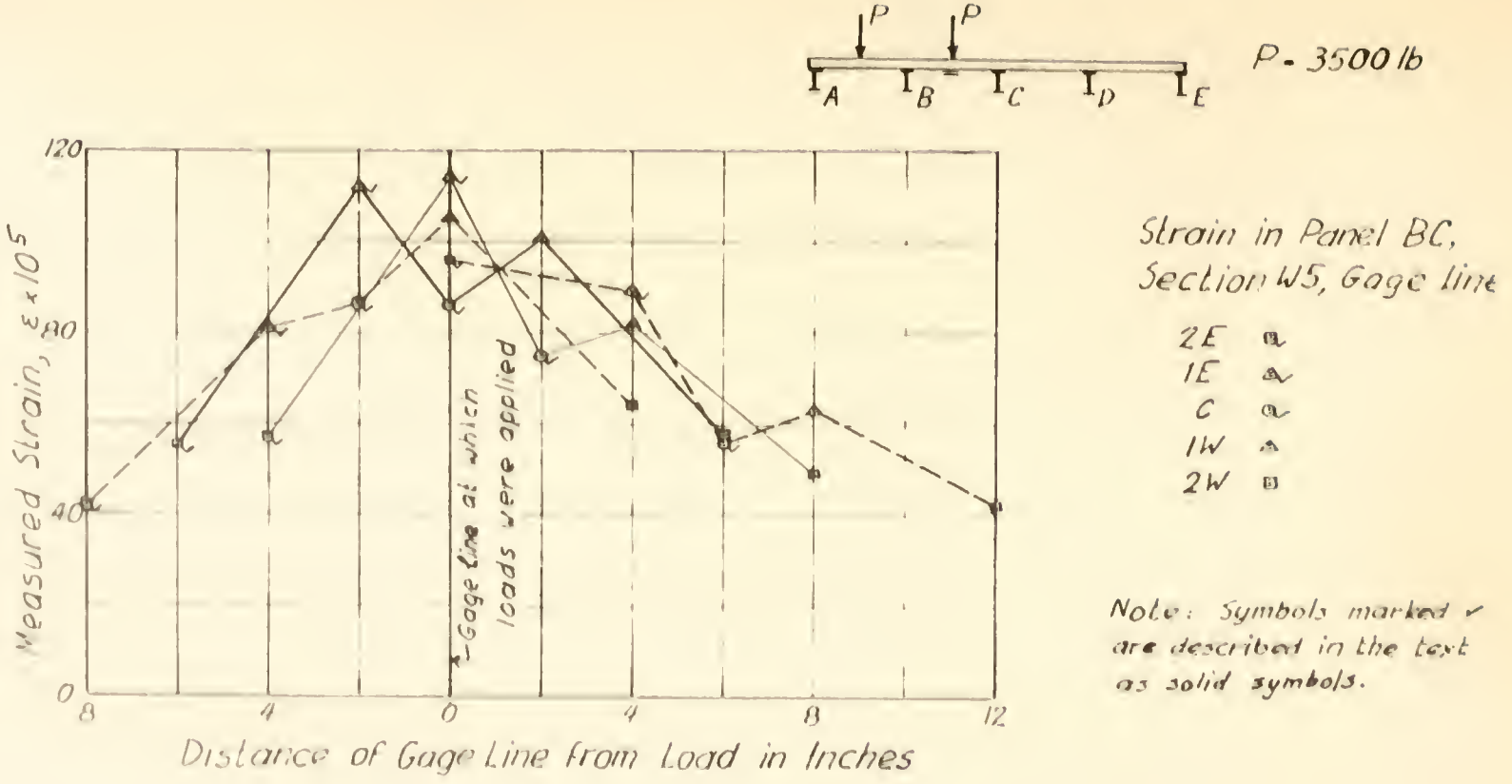

FIG. 13 LONGITUDINAL DISTRIBUTION OF STRAINS IN TRANSVERSE SLAB REINFORCEMENT IN SPAN, BRIDGE N30

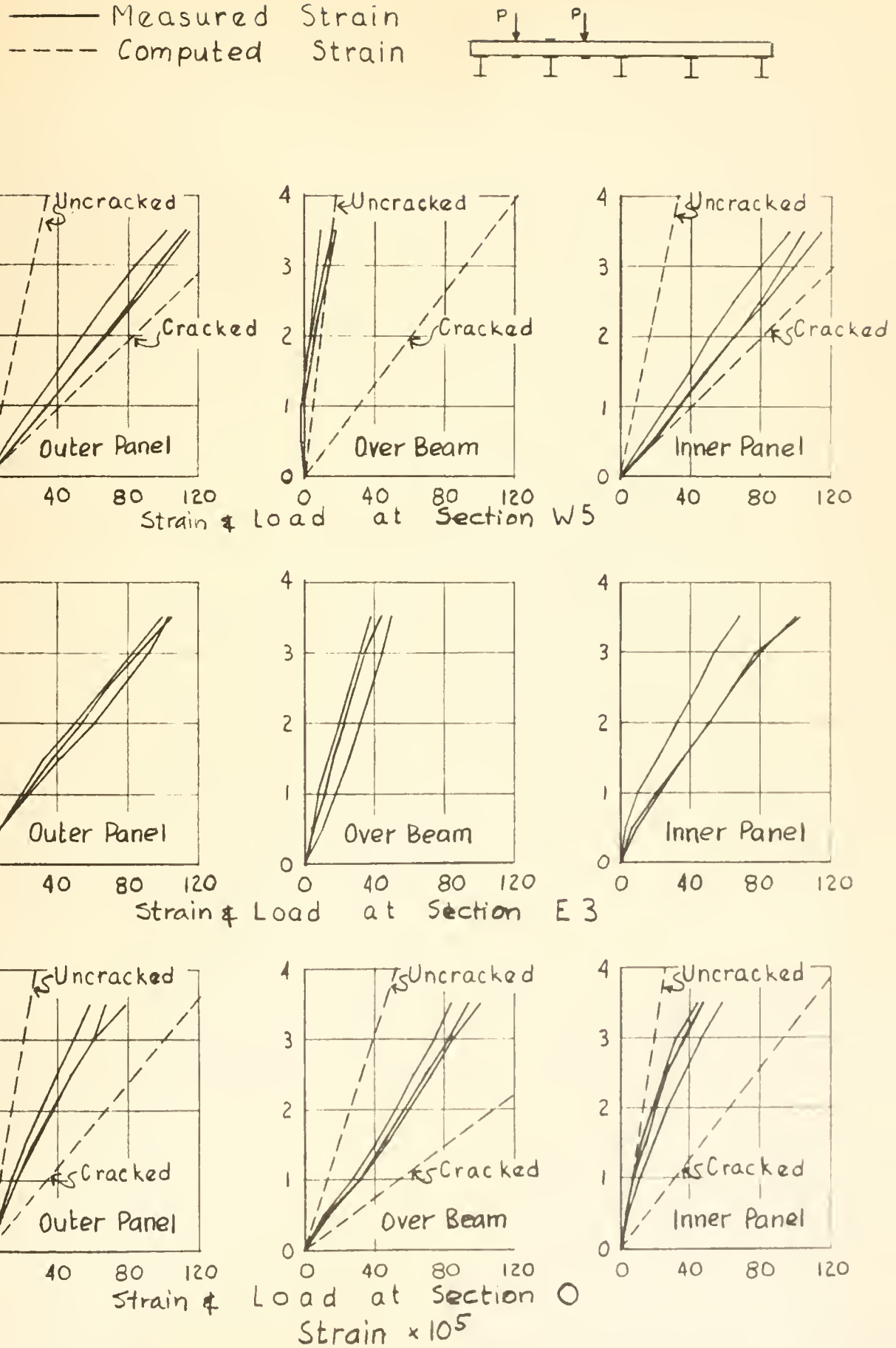

FIG.14 INDIVIDUAL LOAD-STRAIN CURVES FOR TRANSVERSE SLAB REINFORCEMENT, BRIDGE N30

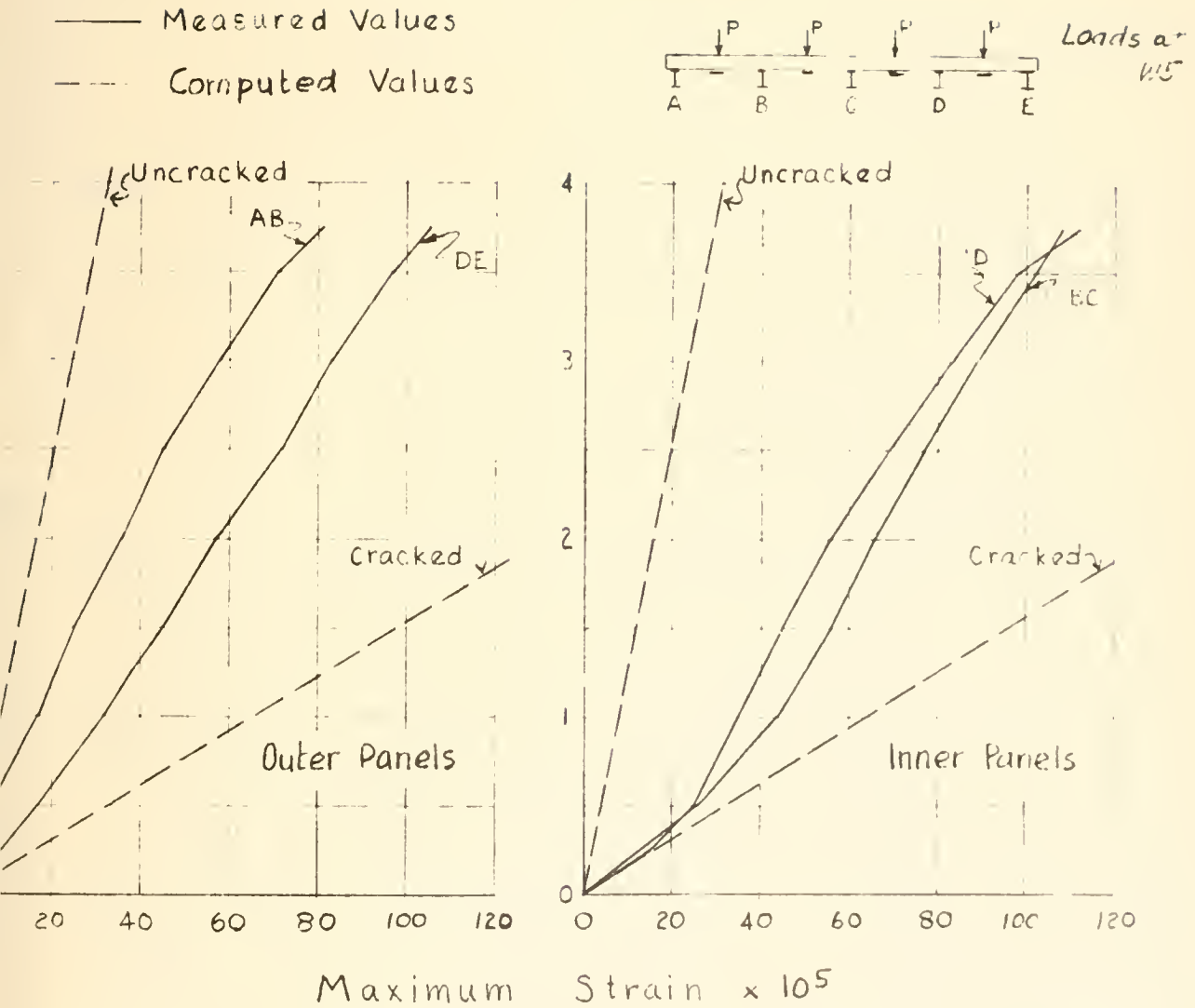

16.15 INDIVIDUAL LOAD-STRAIN CURVES FOR LONGI[illegible]
SLAB REINFORCEMENT AT MAXIMUM MOMENT [illegible]
BRIDGE N30

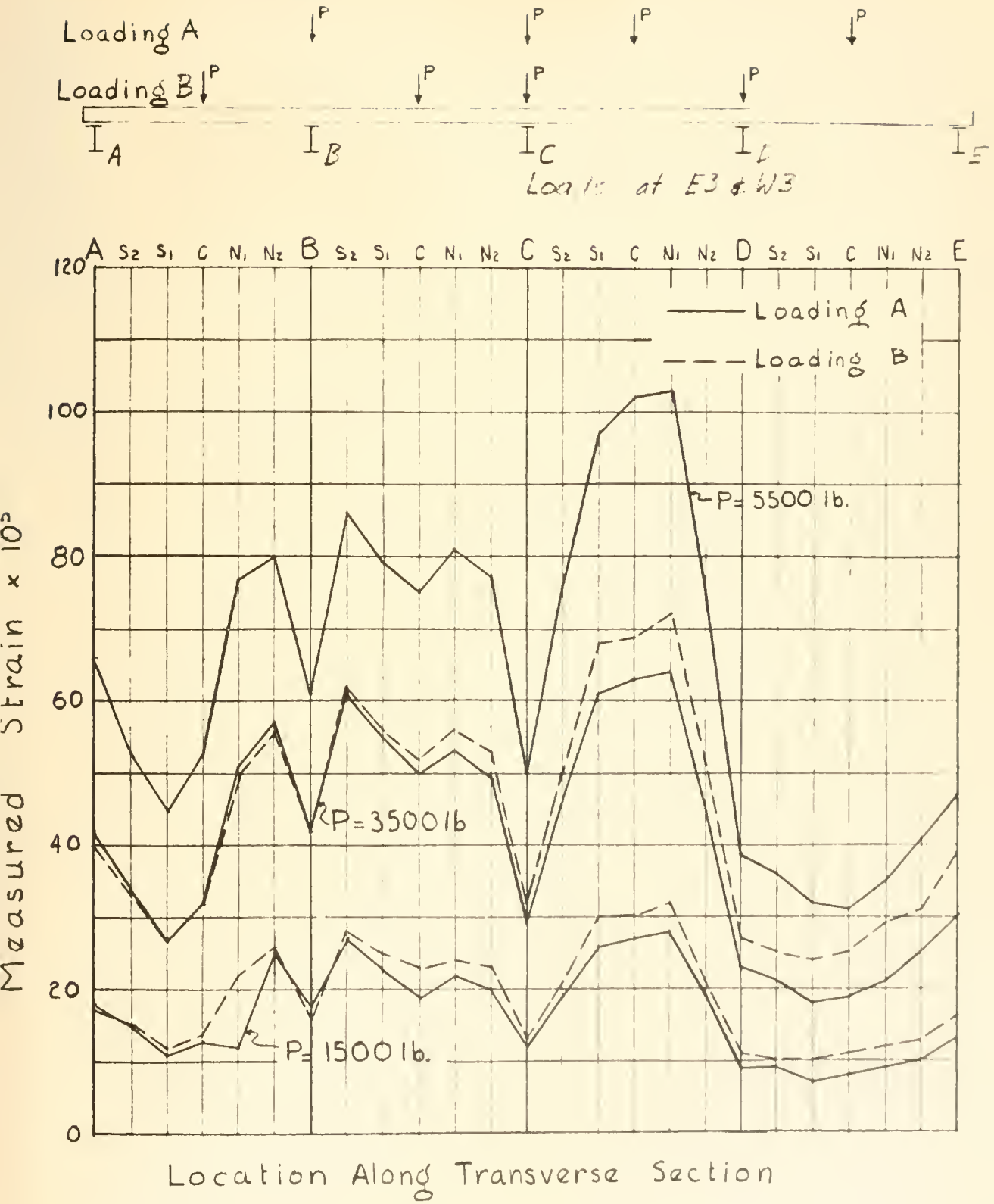

FIG. 16 TRANSVERSE DISTRIBUTION OF STRAIN IN LONGITUDINAL SLAB REINFORCEMENT OVER CENTER PIER, BRIDGE M30

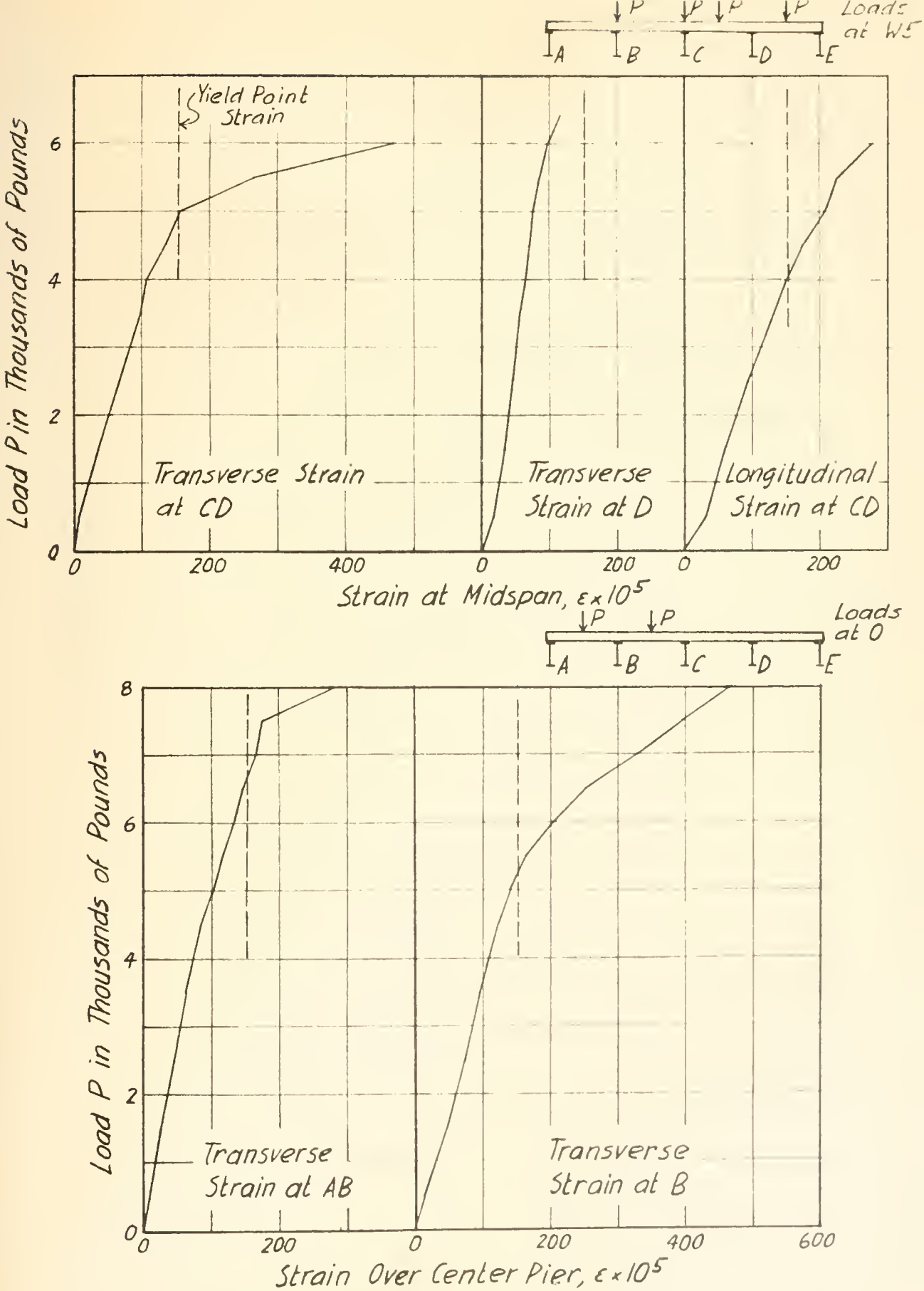

FIG.17 YIELDING OF SLAB REINFORCEMENT, BRIDGE N30

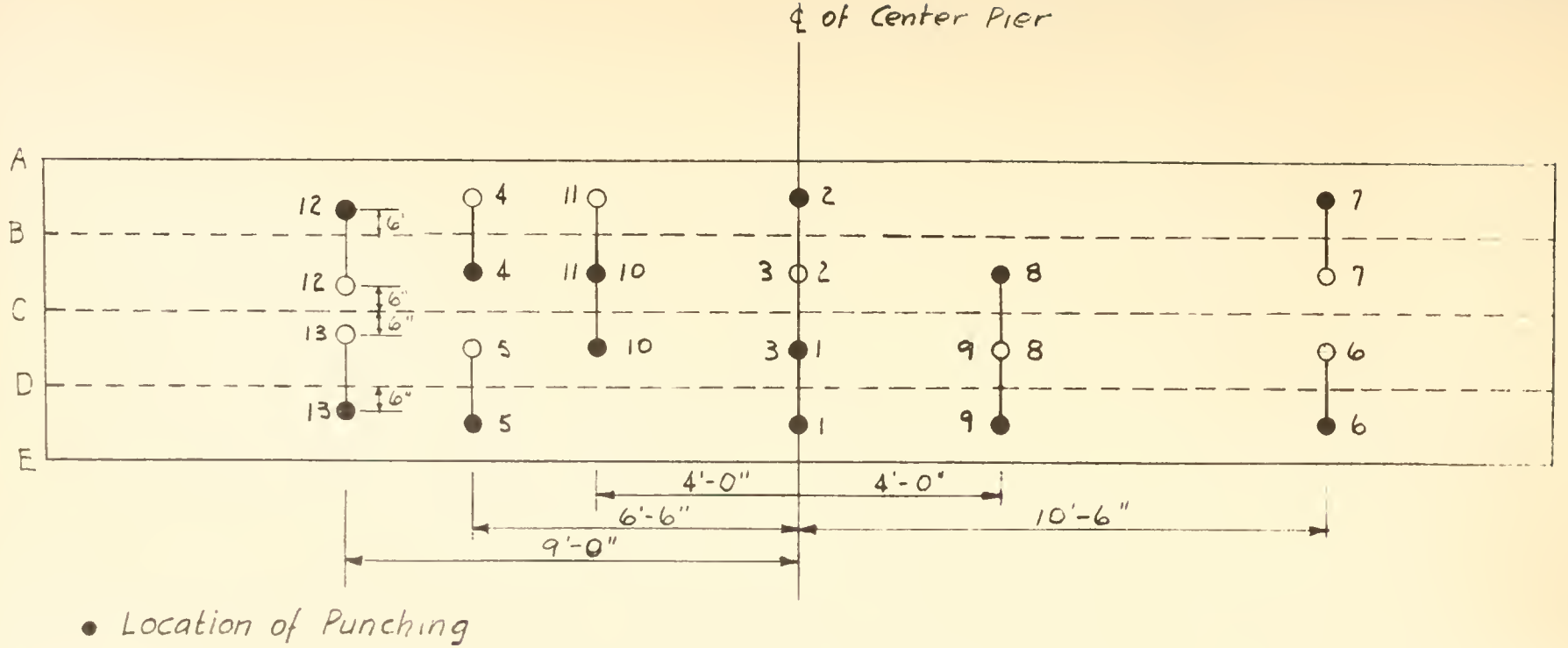

FIG. 18 LOCATION OF LOADS IN PUNCHING TESTS, BRIDGE N30

= Gage Lines on Beam

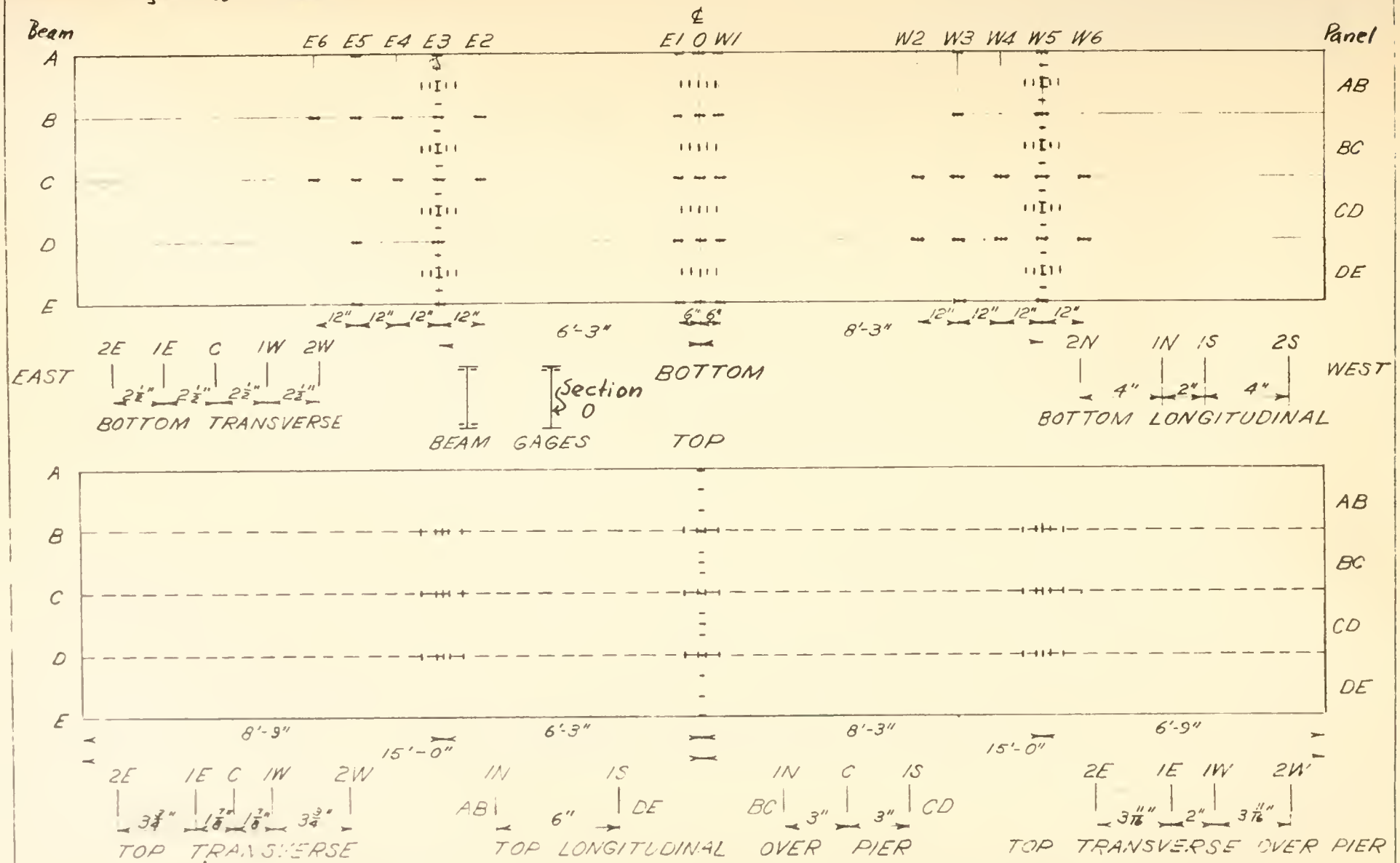

FIG. 19 LOCATION OF STRAIN GAGE LINES, BRIDGES C30 & X30

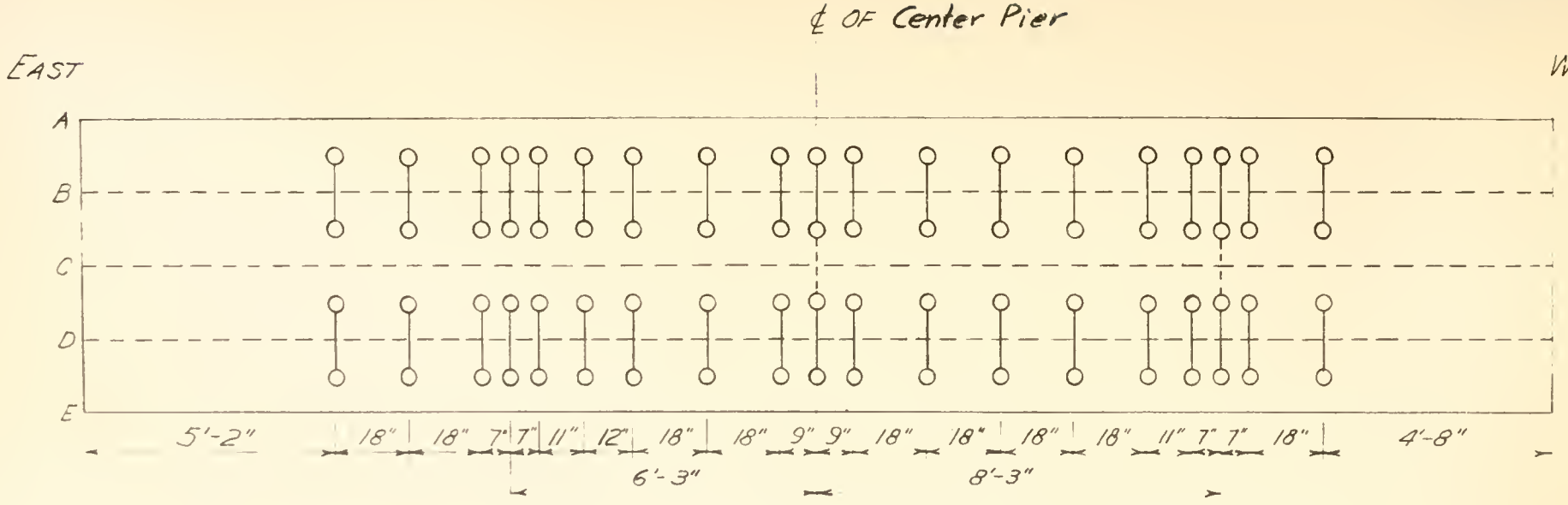

Order of Loading	C30	22	21	18	10	13	14	17	8	6	2	7	25	26	36	33	32	29	37	40
											1							28		
		23	20	19	11	12	15	16	9	5	3	4	24	27	35	34	31	30	38	39
	X30	34	31	30	27	35	38	39	25	5	2	4	9	10	24	21	20	13	16	17
											1							12		
		33	32	29	28	36	37	40	26	6	3	7	8	11	23	22	19	14	15	18

FIG.20 LOCATION OF LOADS AND ORDER OF LOADING IN CRACKING TEST, BRIDGES C30 & X30

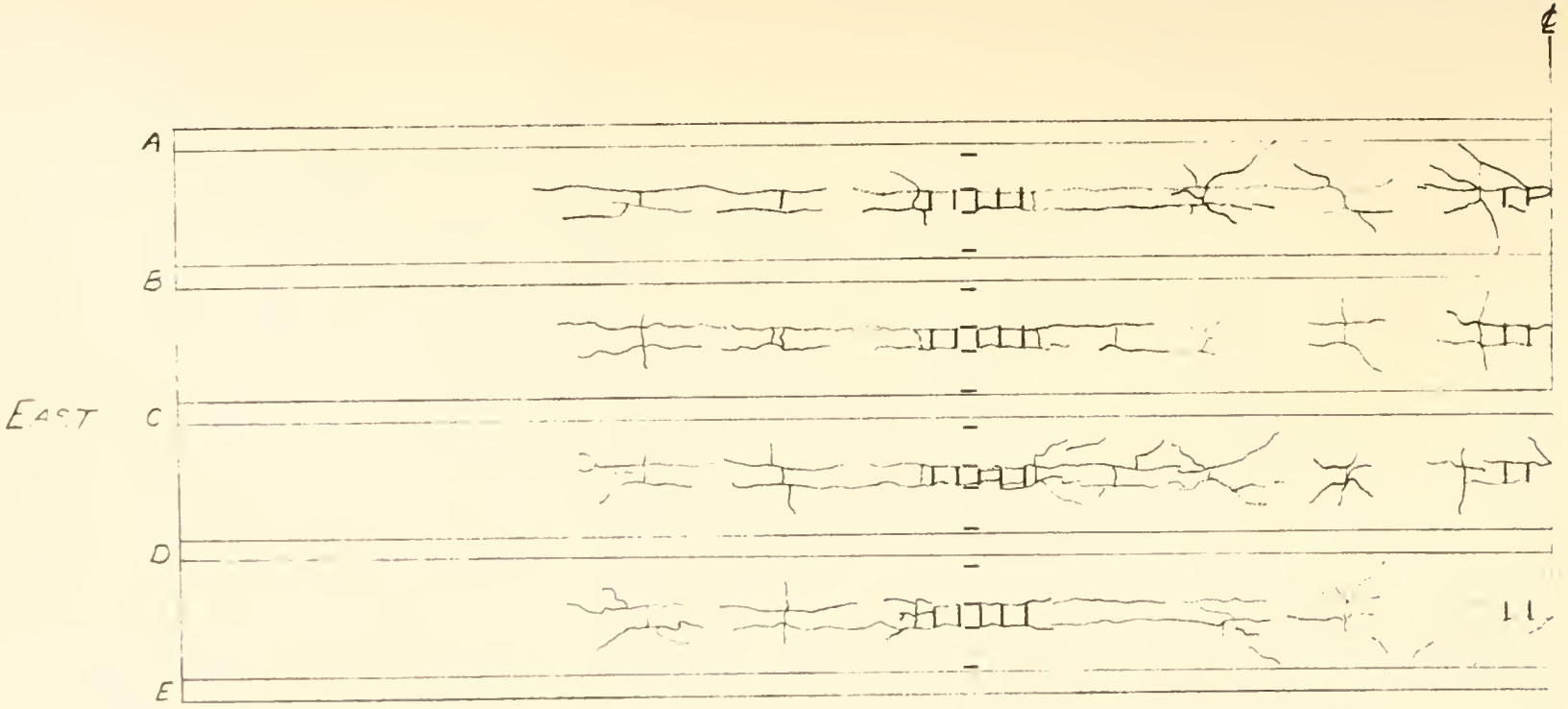

FIG. 21 CRACK PATTERN ON BOTTOM OF SLAB AFTER CRACKING TEST, BRIDGE C30

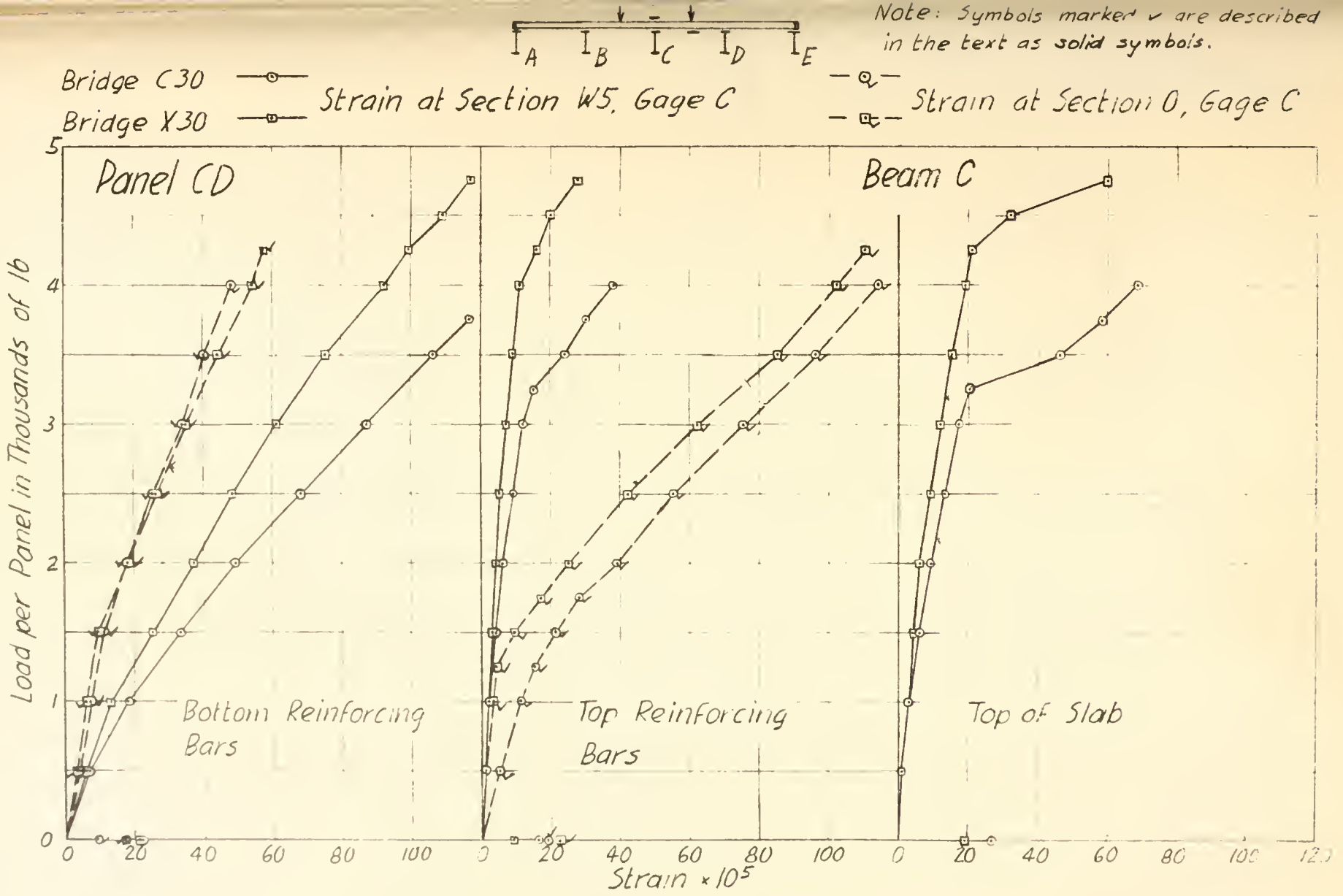

FIG. 22 TRANSVERSE STRAINS PRODUCING FIRST CRACKING OF SLAB, BRIDGES C30 & X30

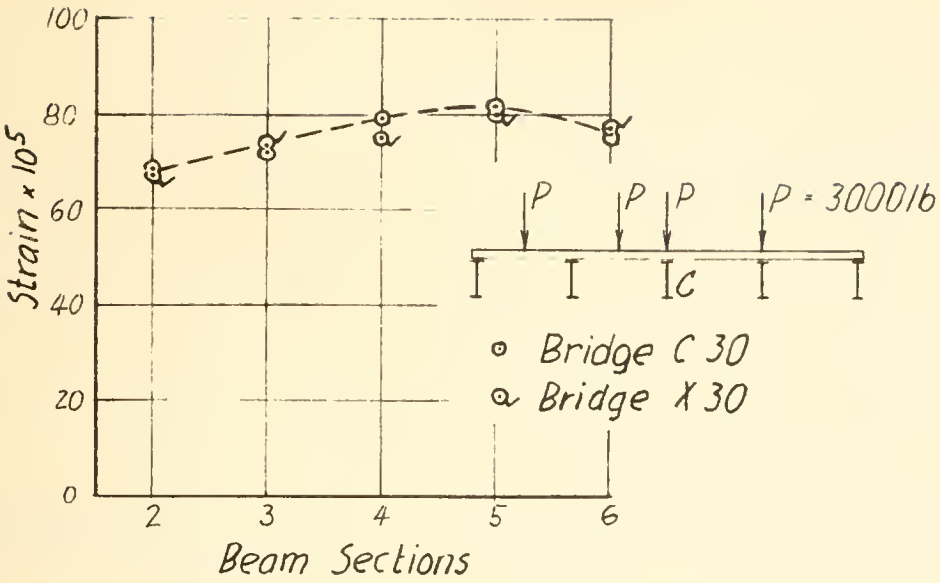

FIG. 23 CURVE OF MAXIMUM BOTTOM FLANGE STRAINS IN SPAN. BRIDGES C30 & X30, BEAM C

Note: Symbols marked ∨ are described in the text as solid symbols.

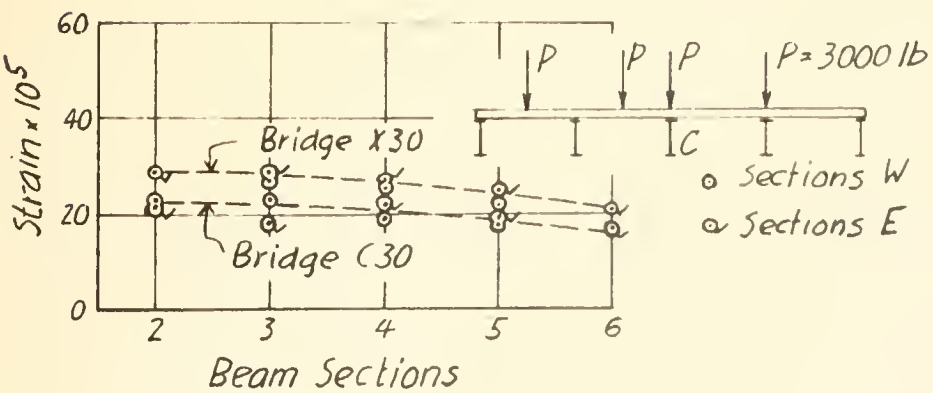

FIG. 24 INFLUENCE LINES FOR TOP FLANGE STRAINS OVER CENTER PIER, BRIDGES C30 & X30, BEAM C

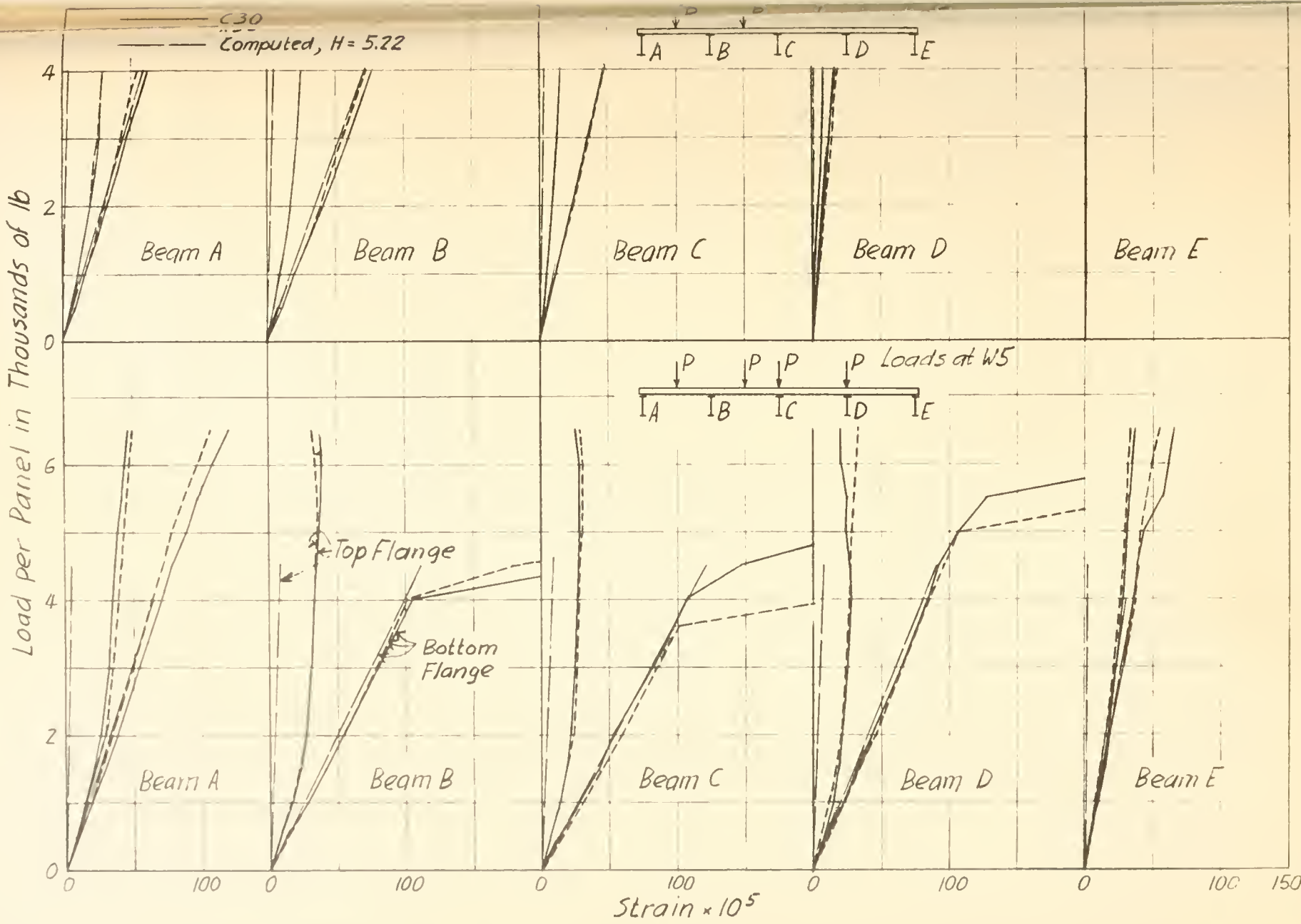

FIG. 25 BEAM STRAINS AT MAXIMUM POSITIVE MOMENT SECTION, BRIDGES C30 & C31

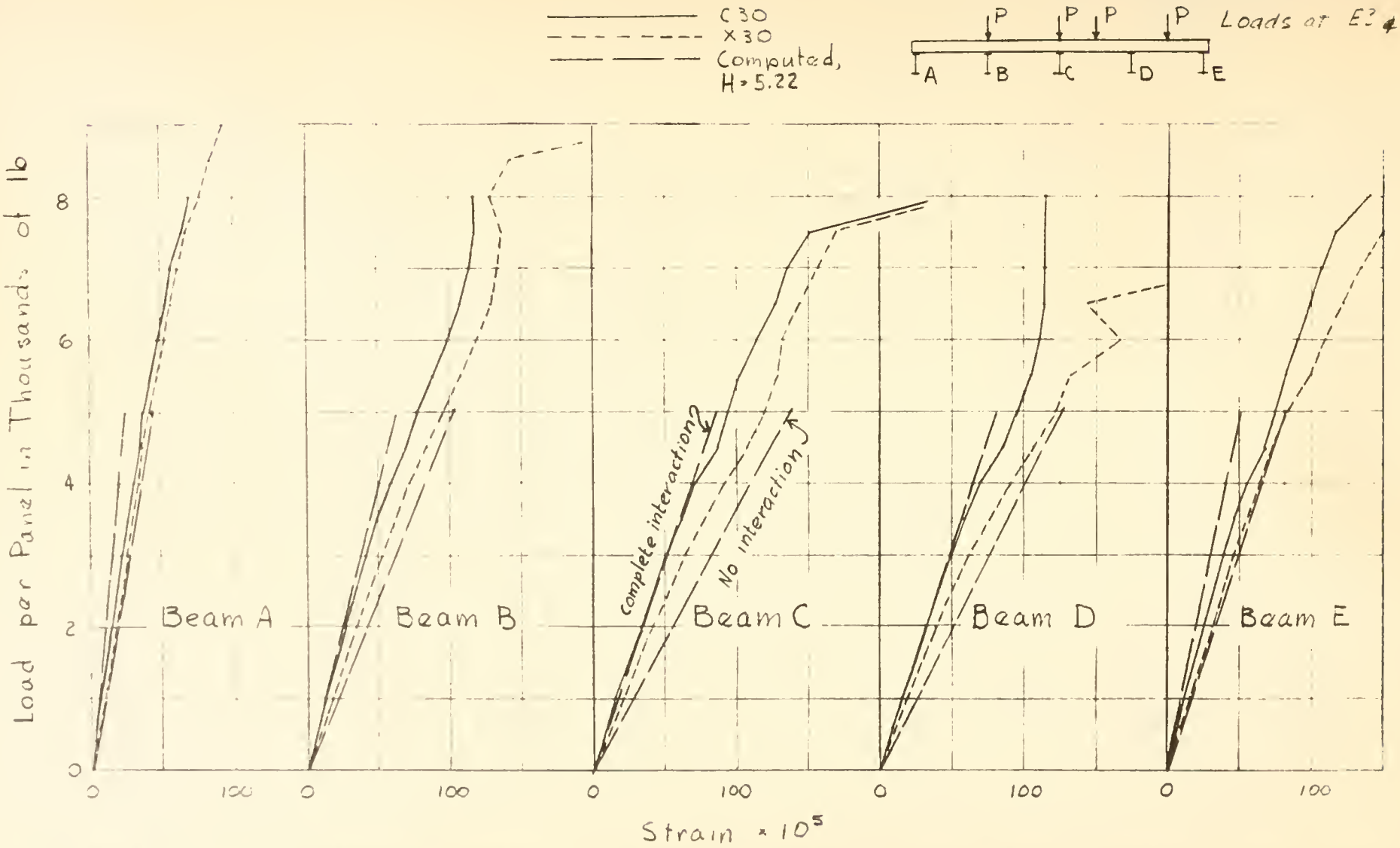

FIG 6 TO FLANGE STRAINS IN BEAMS ON CENTER PIER, BRIDGES C.P. 1.1.

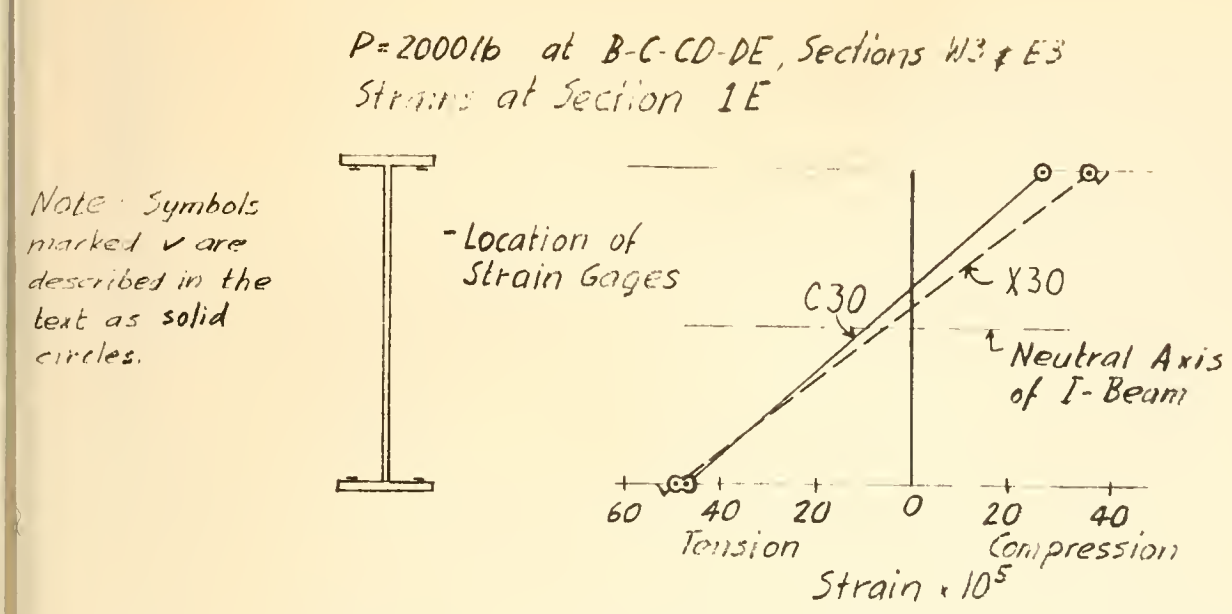

FIG. 27 DISTRIBUTION OF STRAIN IN BEAM C 6 INCHES FROM CENTER PIER, BRIDGES C30 & X30

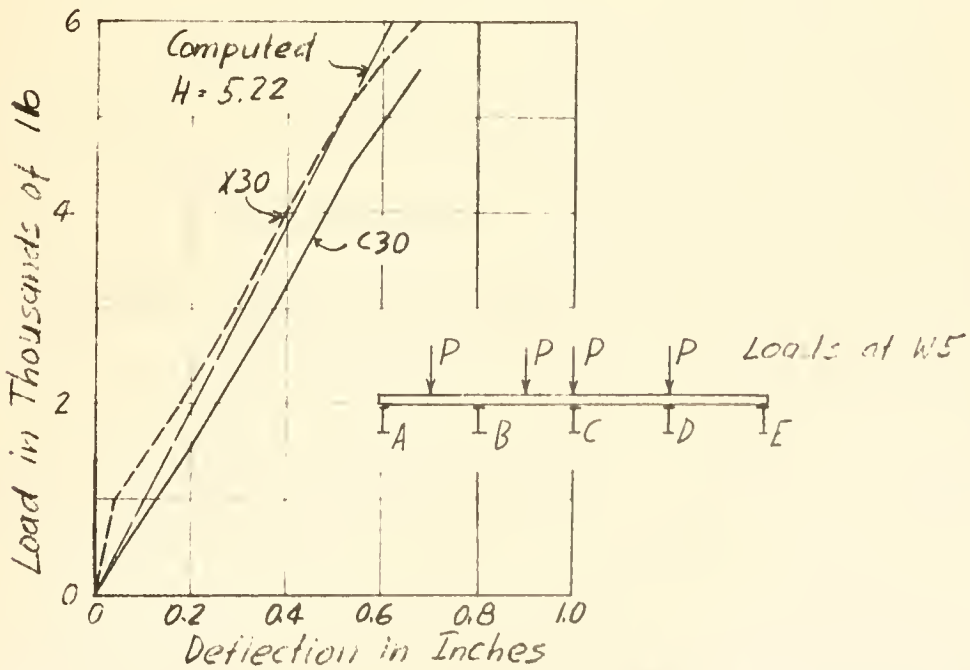

FIG. 28 LOAD-DEFLECTION CURVES FOR BEAM C AT SECTION W5, BRIDGES C30 & X30

Note: Symbols marked ✓ are described in the text as solid symbols.

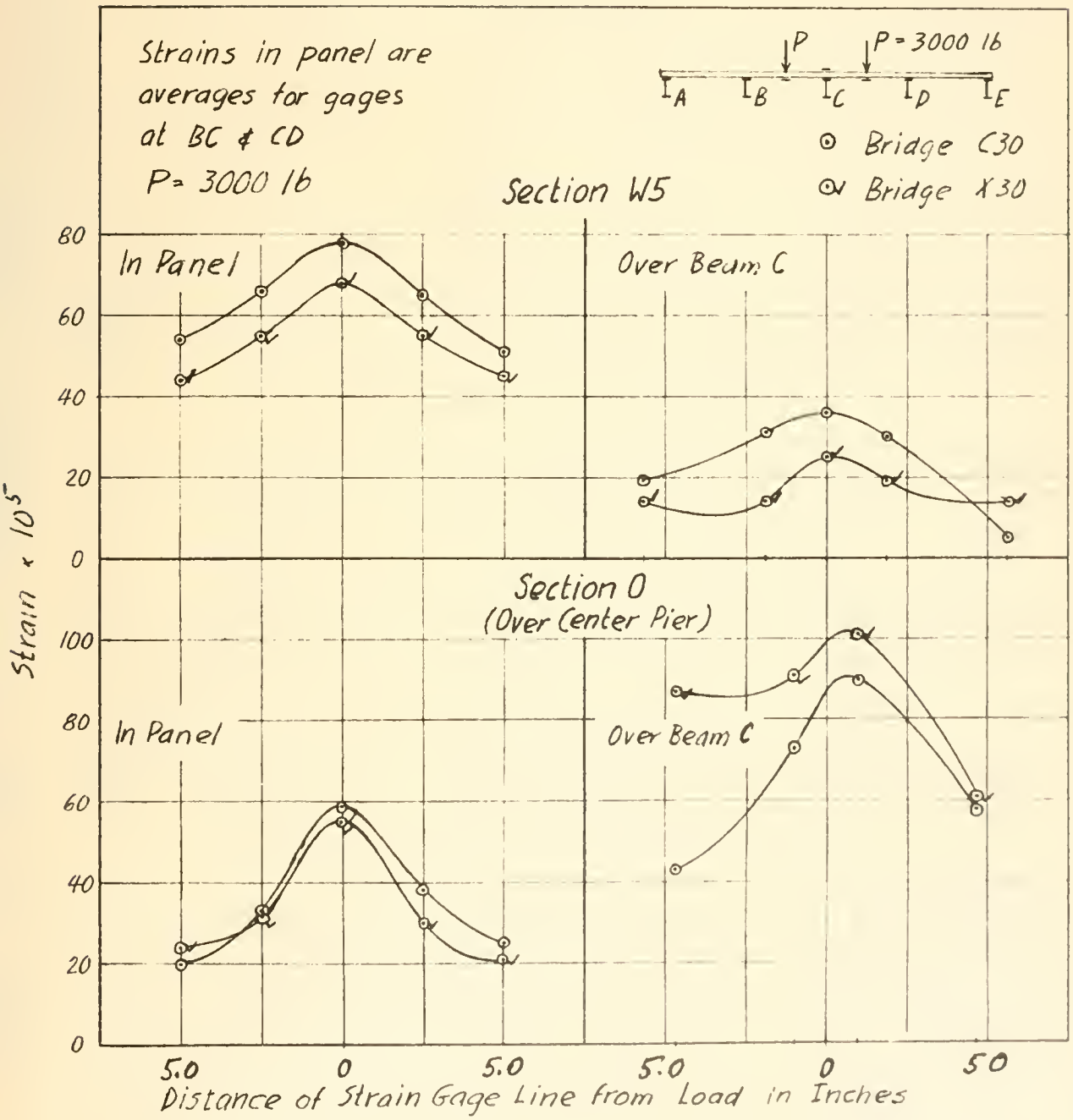

FIG. 29 LONGITUDINAL DISTRIBUTION OF STRAINS IN TRANSVERSE SLAB REINFORCEMENT, BRIDGES C30 & X30

——— Measured Strain Bridge C30
- - - - Measured Strain Bridge X30
—— —— Computed Strain

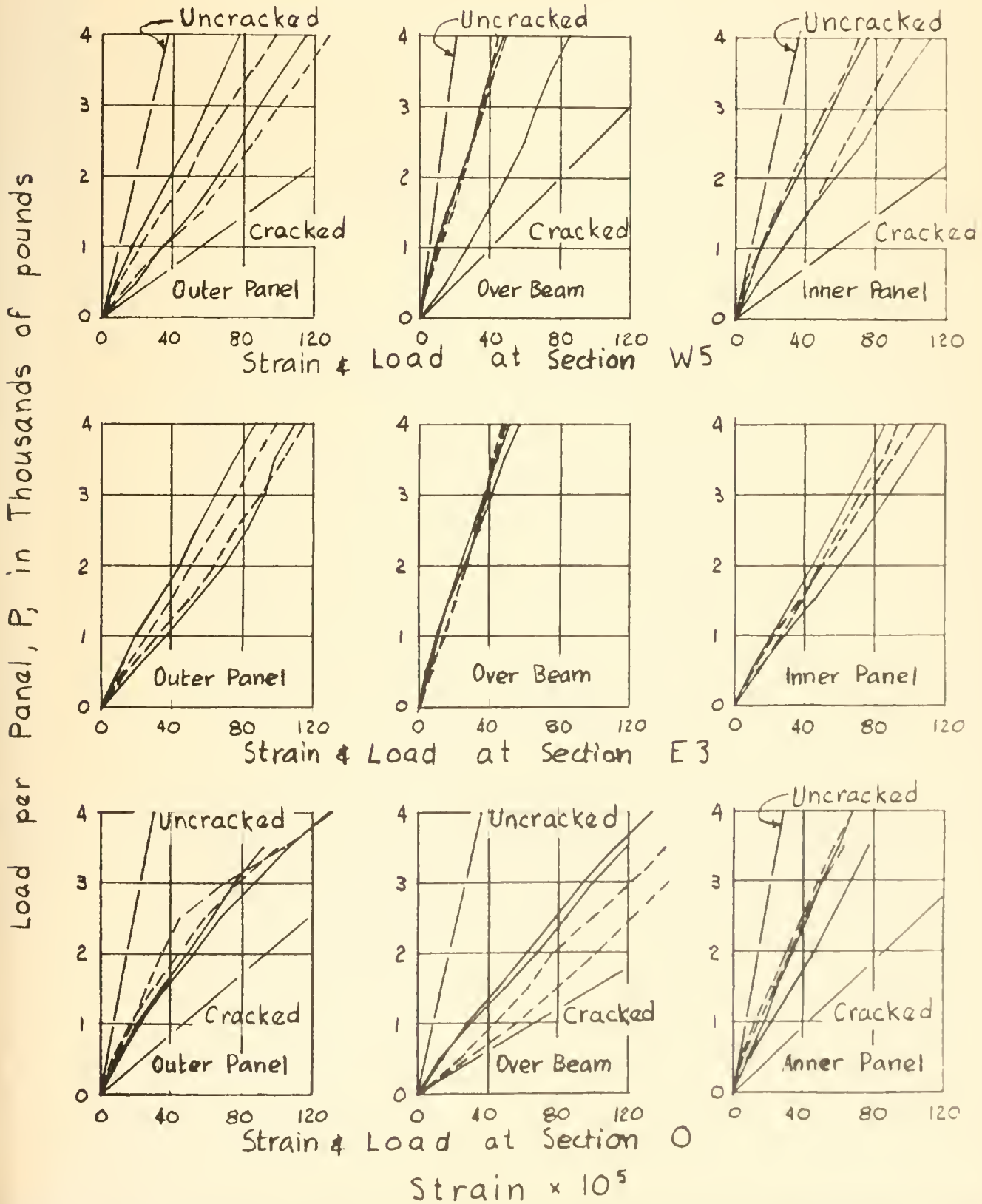

FIG.30 INDIVIDUAL LOAD-STRAIN CURVES FOR TRANSVERSE SLAB REINFORCEMENT, BRIDGES C30 & X30

Note: Symbols marked ✓ are described in the text as full symbols.

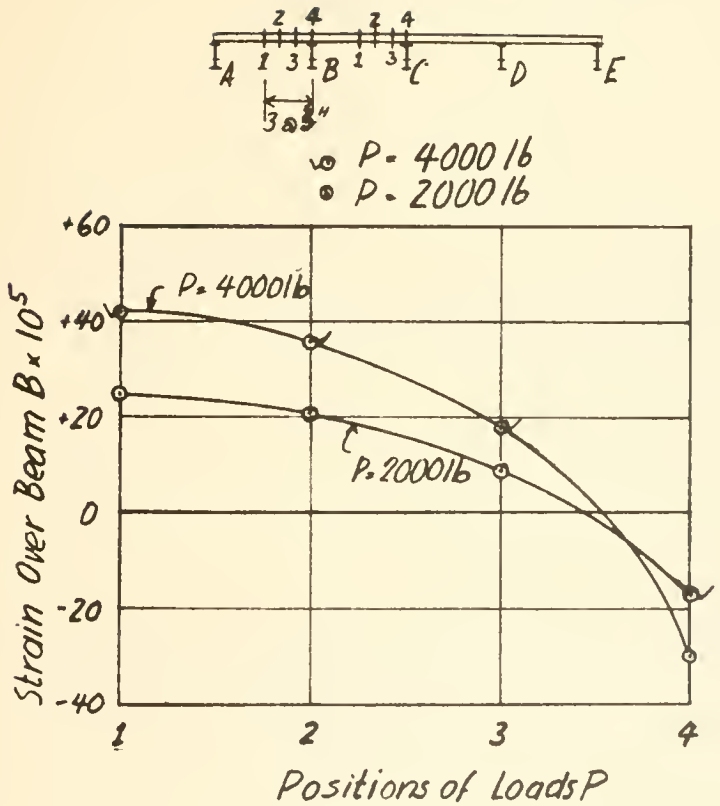

FIG. 31 INFLUENCE LINES FOR MAXIMUM STRAIN IN TRANSVERSE SLAB REINFORCEMENT OVER BEAM B, BRIDGES X30

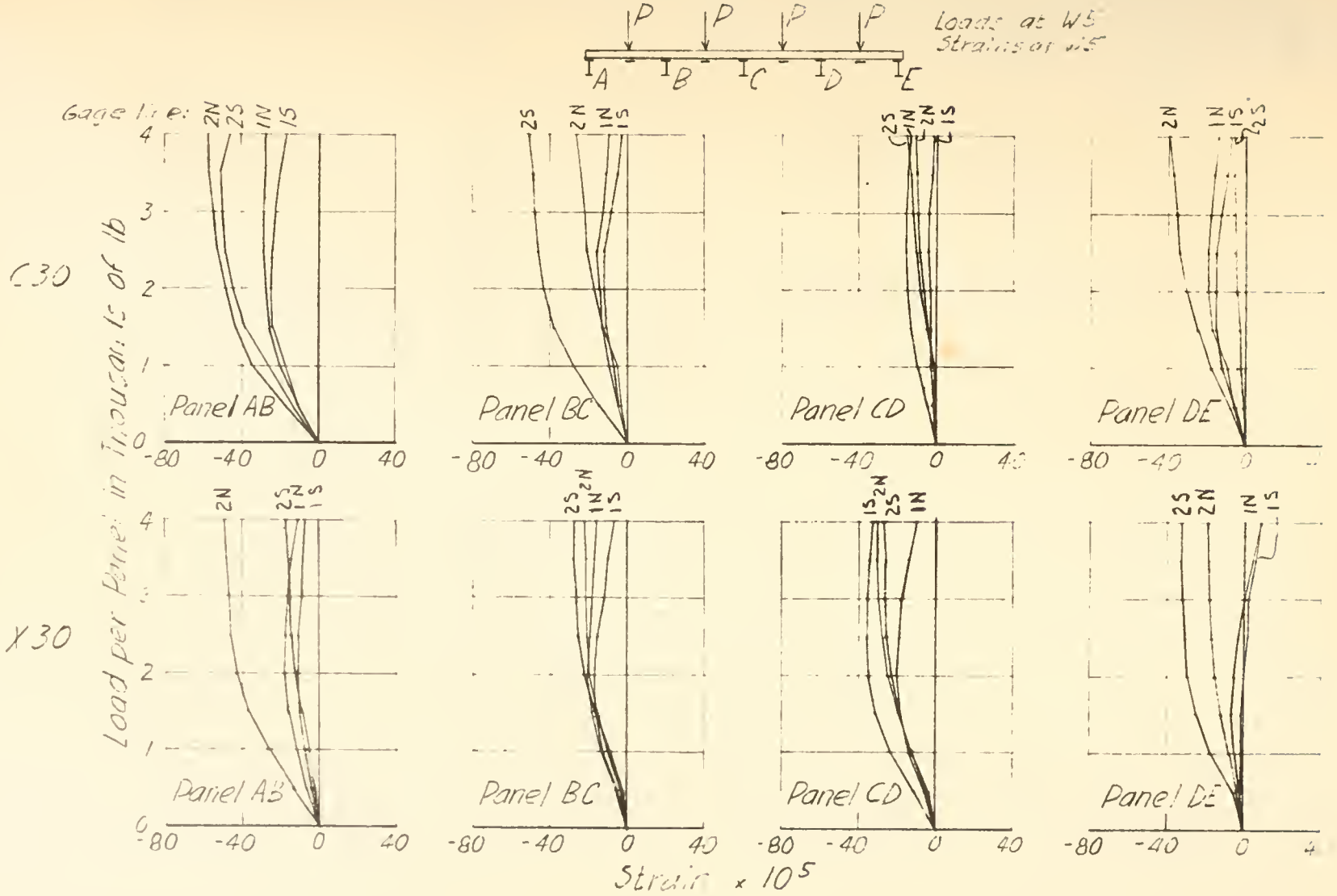

FIG.32 INDIVIDUAL LOAD-STRAIN CURVES FOR LONGITUDINAL SLAB REINFORCEMENT IN SPAIN, BRIDGES C30 + X30

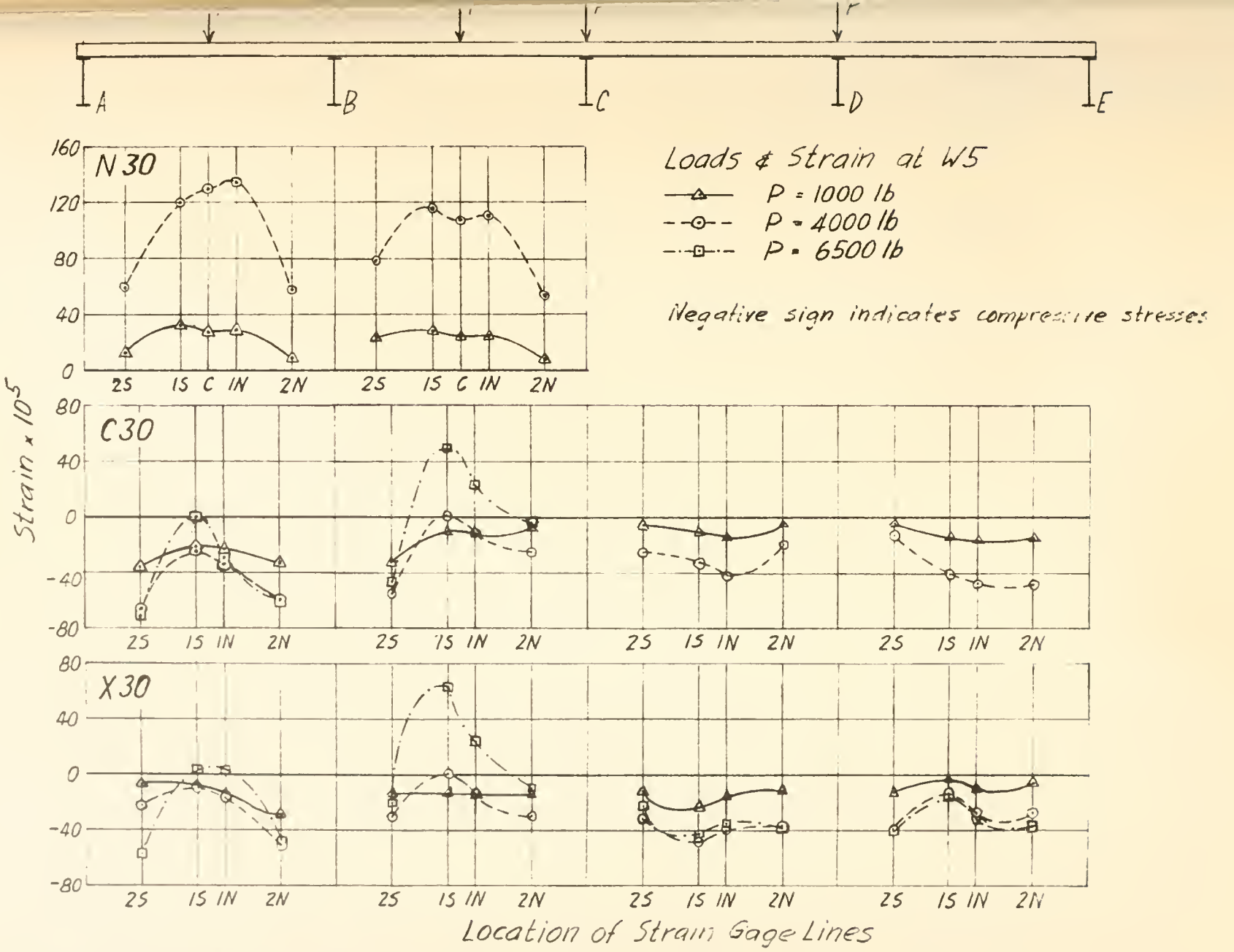

FIG. 33 DISTRIBUTION OF STRAINS IN LONGITUDINAL SLAB REINFORCEMENT IN SPAN, BRIDGES N30, C30 & X30

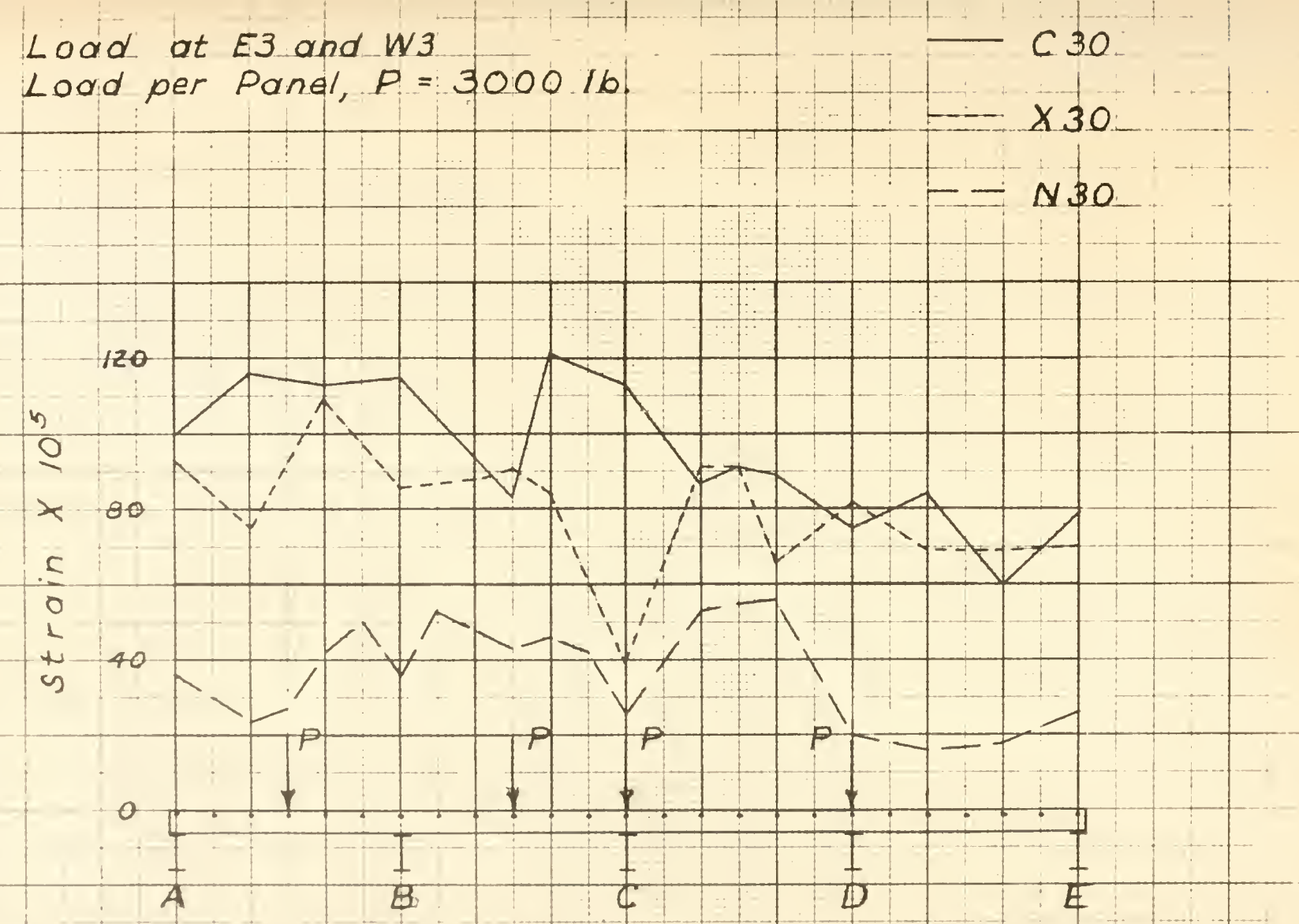

FIG.34 STRAIN DISTRIBUTION IN TOP LONGITUDINAL REINFORCEMENT OVER CENTER PIER, BRIDGES N30, C30 & X30

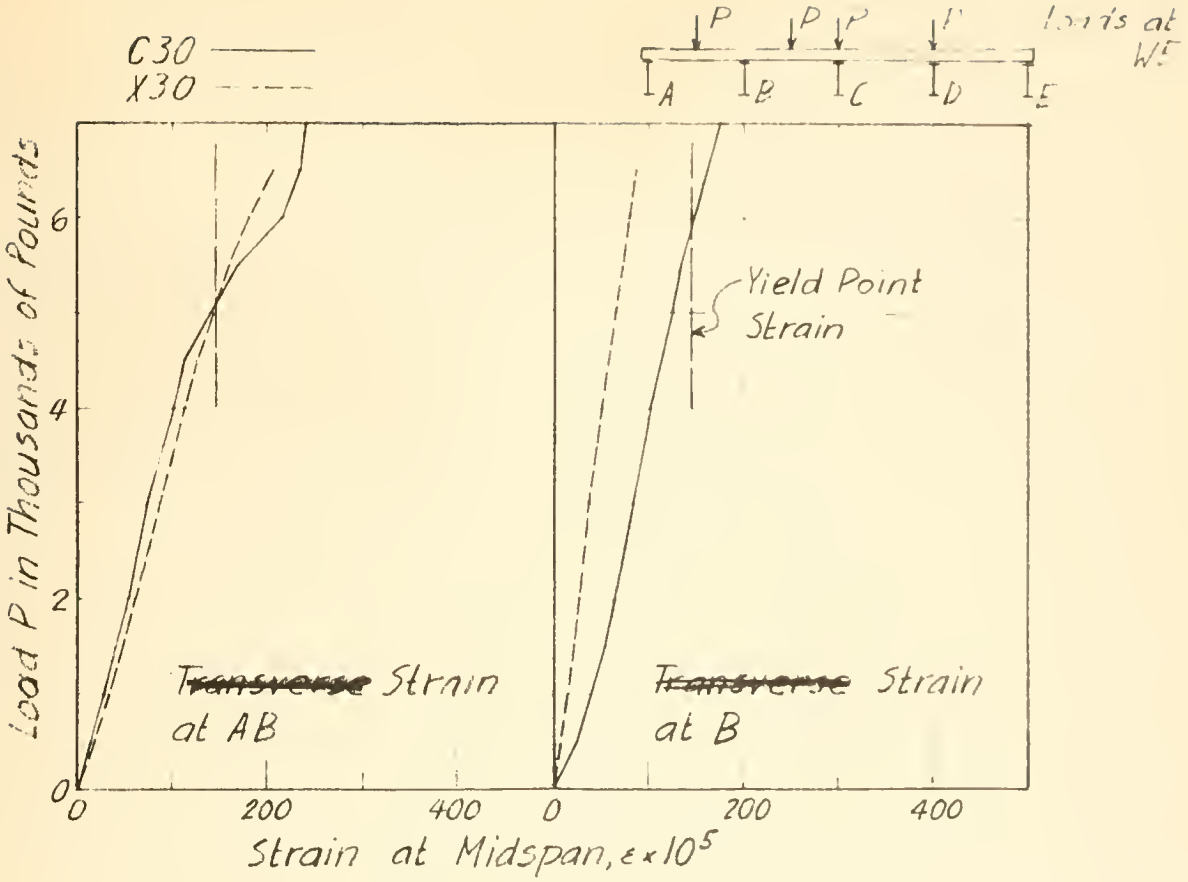

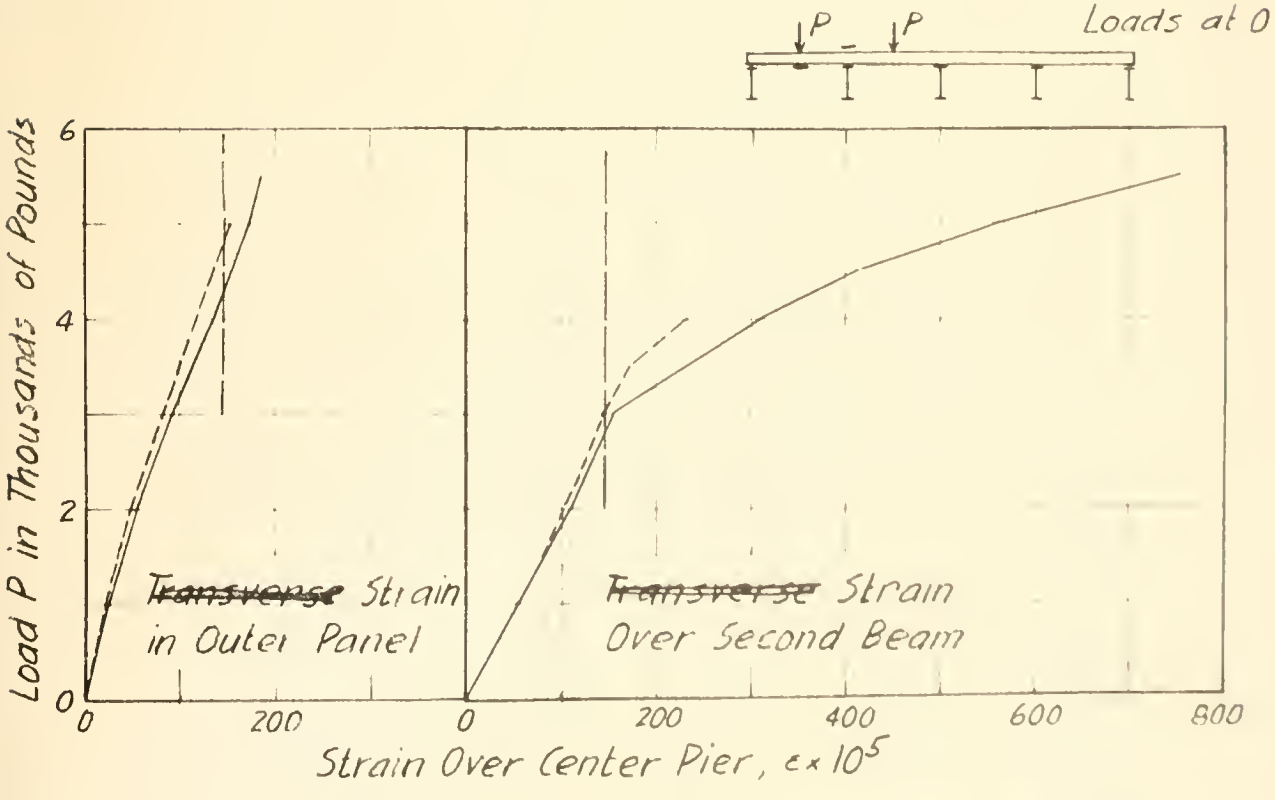

FIG. 35 YIELDING OF TRANSVERSE SLAB REINFORCEMENT, BRIDGES C30 & X30

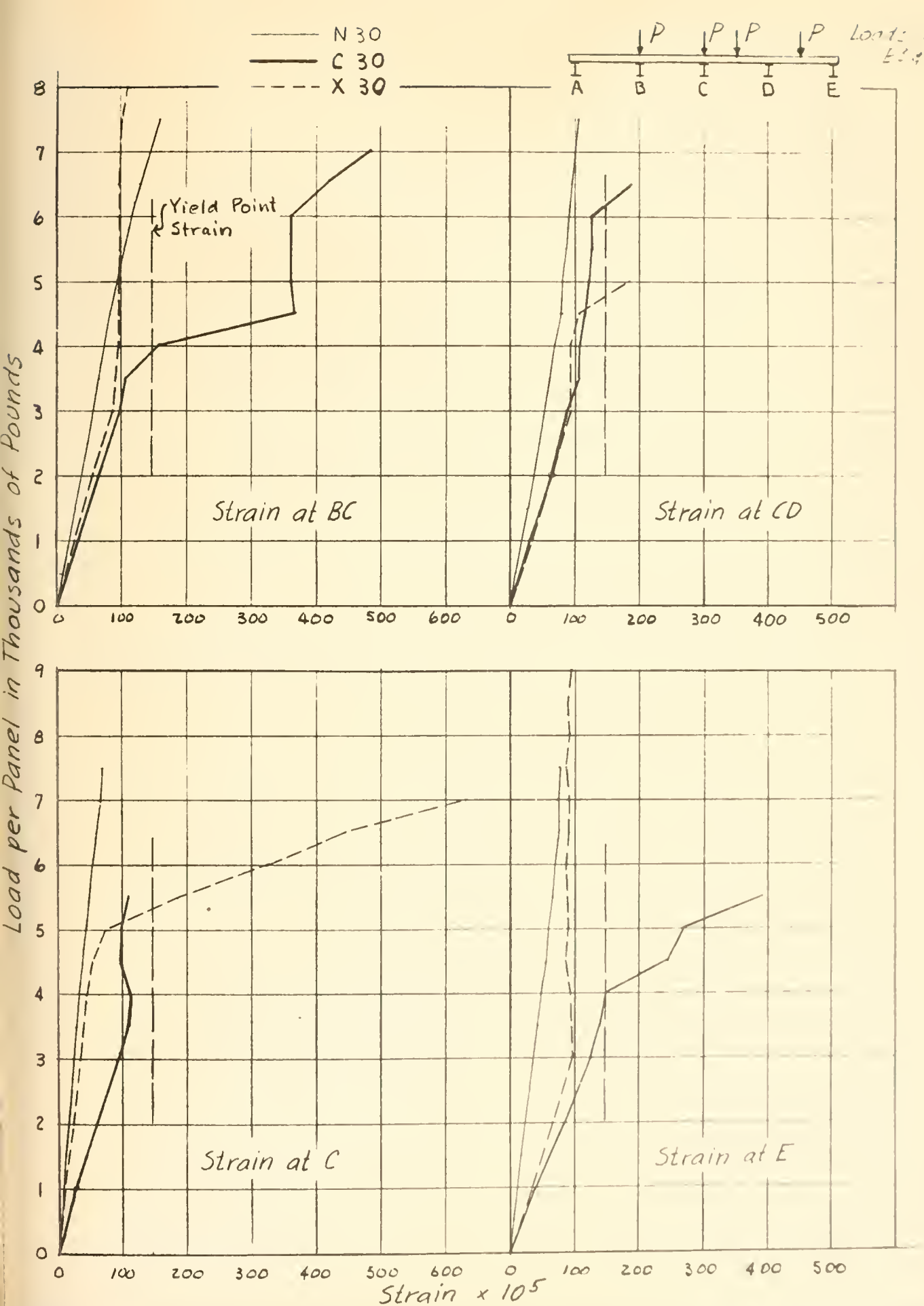

FIG. 36 YIELDING OF LONGITUDINAL SLAB REINFORCEMENT OVER

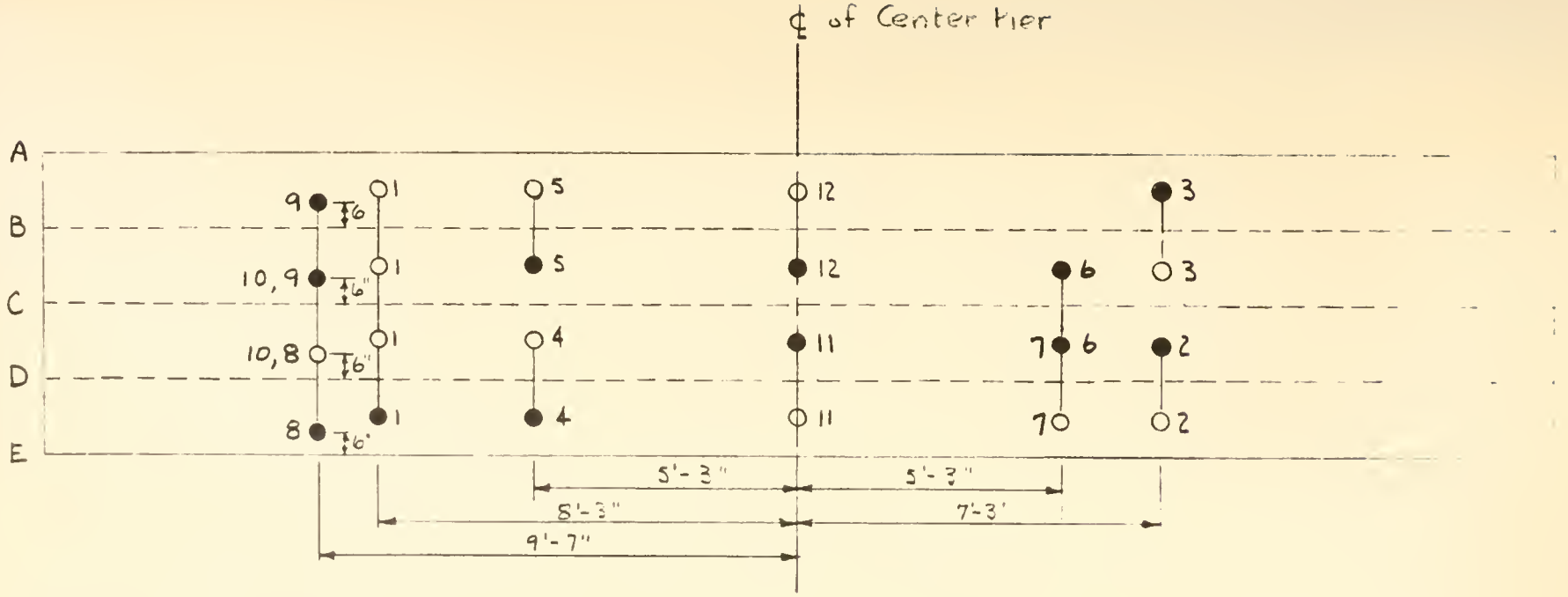

• Location of Punching

FIG. 37 LOCATION OF LOADS IN PUNCHING TESTS, BRIDGE C30

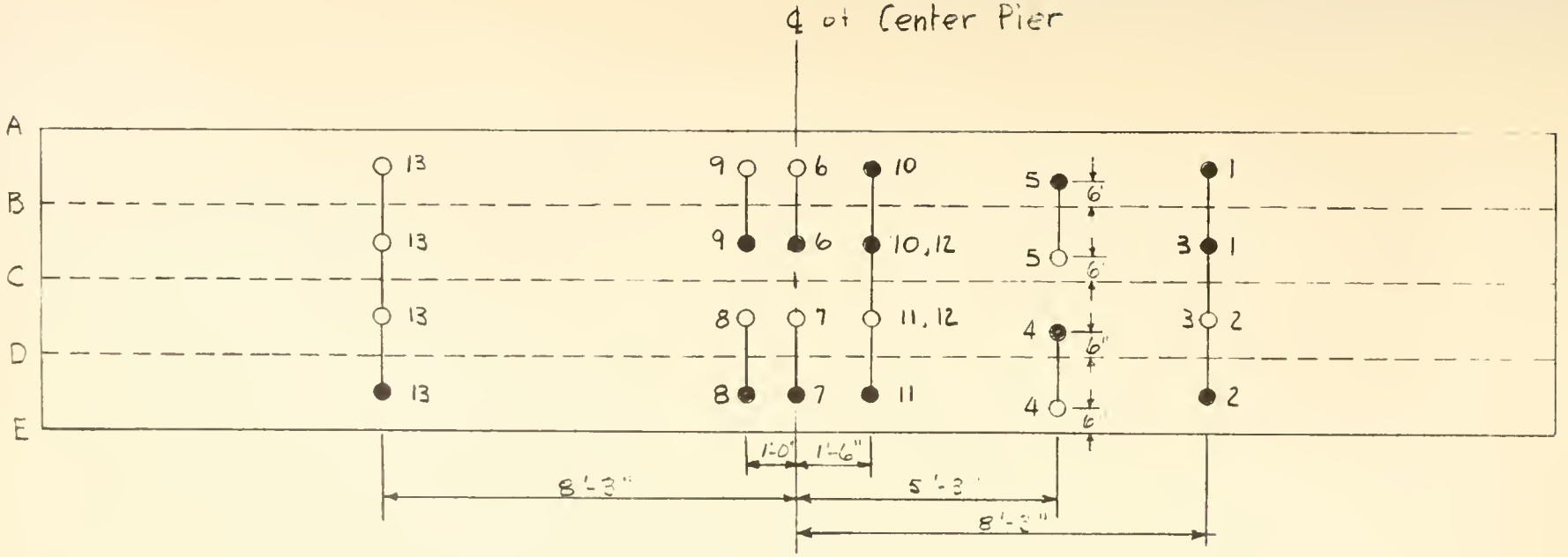

• Location of Punching

FIG. 38 LOCATION OF LOADS IN PUNCHING TESTS, BRIDGE X50

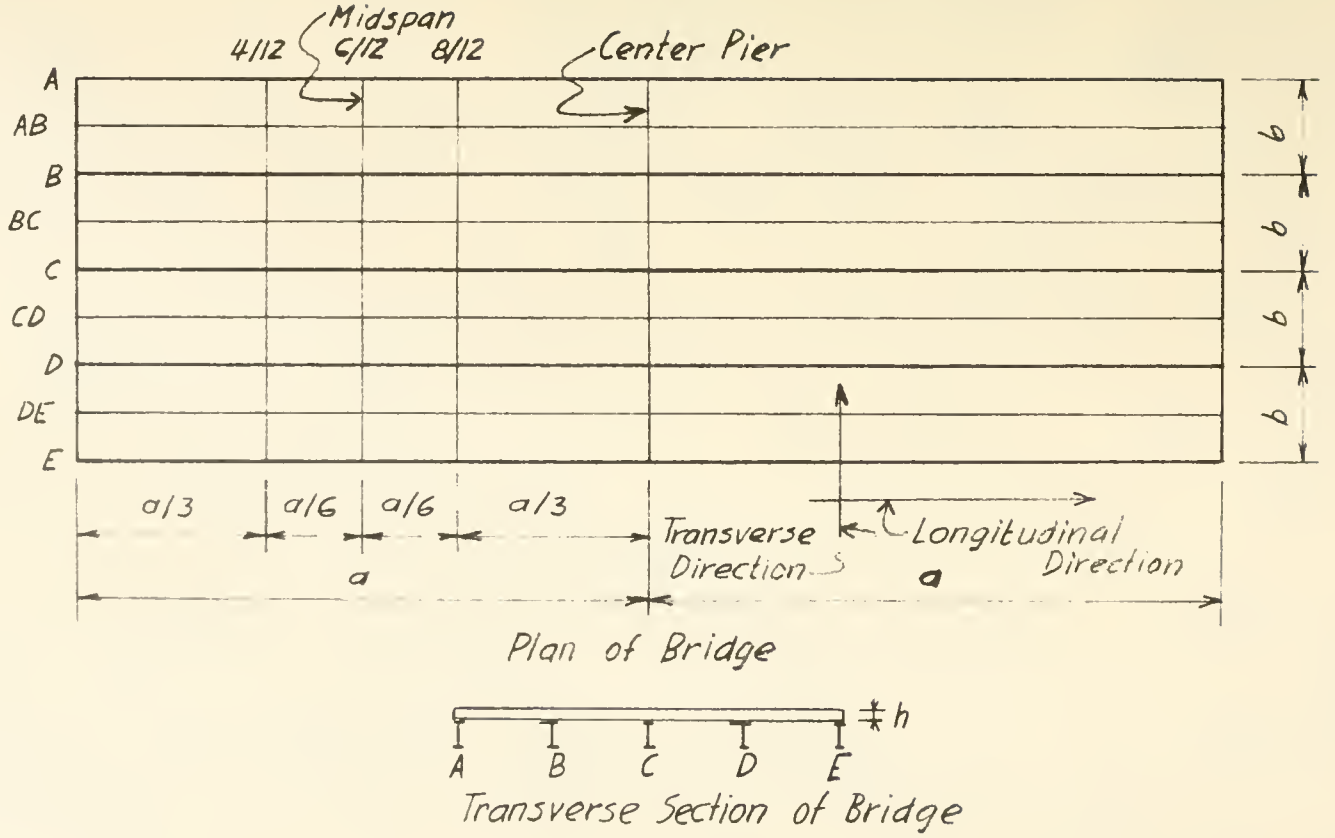

FIG. 39 OUTLINE OF CONTINUOUS BRIDGES FOR THEORETICAL ANALYSIS